The Role of the Histone Variant H2A.Z in Early *Xenopus laevis* Development

Karl David Brown

December 2007

A thesis submitted for the degree of Master of Philosophy

of the Australian National University

College of Medicine and Health Sciences Graduate Program

John Curtin School of Medical Research

Australian National University

Canberra, Australia

Statement

The research described in this thesis was solely and entirely conducted by the author unless acknowledgement is made in the text. It has not presented for any other degree.

Karl David Brown

December 2007

Acknowledgements

I would like to thank my supervisory panel for their support. Dr Patricia Ridgway was my primary supervisor whose guidance throughout this project was invaluable, likewise for Dr David Tremethick, leader of the Chromatin and Transcriptional Regulation group. Eldon Ball taught me the nuances of *in situ* hybridisation, and Sudha Rao provided valuable guidance relating to RNA-based techniques.

In addition to my panel, the wider scientific community at the ANU should be thanked. Among this community I would like to specifically thank: Danny Rangasamy and Torsten Juerlich for explaining the arcana of real-time PCR; Dave Hayward for showing me the minutiae of the molecular aspects of *in situ* hybridisation; and members of the Chromatin and Transcriptional regulation, and Gene Expression and Epigenomics Groups for their input and companionship over the period. Electrophoresis of sequencing reaction products and automated sequence data collection was performed by the staff of the Australian Cancer Research Foundation (ACRF) Biomolecular Resource Facility (BRF). The ANU and JCSMR provided generous scholarships and funding that made this work possible.

On a more personal note I would like to thank Jun Fan and Stephen Olms for taking a stray into their home.

I would like to thank my families for their support; my mother, father, my brother Nathan, Rose and Richard Bowman, Kylie, Damon, Sten, and Carolyn Jakobsen. Finally, my patient partner Elizabeth deserves special gratitude.

This document is dedicated to the memory of Dennis Woodhouse. He will remain an example to live up to.

Abstract

The genome of eukaryotes is packaged into the small volume of the nucleus in an organised manner. This structure of DNA and associated proteins is called chromatin. The basic unit of chromatin is the nucleosome; an octomer of core histone proteins and associated DNA. Other proteins such as linker histones can also associate with the DNA or the core histones. The modular structure of chromatin allows for structural variation with functional consequences including activation or repression of transcription. Alterations can include post-translational modifications to histones, remodelling by multi-protein complexes, DNA methylation, and non-allelic variants of the canonical histones. Changes to chromatin structure have an important impact on all DNA processing events.

This thesis investigated the histone variant H2A.Z, a variant of the canonical core histone H2A. H2A.Z is highly conserved and essential in a number of species suggesting it has a critical function. Preliminary work using the *Xenopus laevis* developmental model system had revealed that disruption of H2A.Z function resulted in defective embryo morphology consistent with disrupted gastrulation and mesoderm development (Ridgway et al., 2004a). This led to the following hypothesis: H2A.Z is important to gastrulation and mesodermal development in *X laevis* because it plays a developmental role.

Temporal and spatial expression patterns of *H2A.Z* mRNA demonstrated in this study are consistent with a role in mesoderm development. Peak *H2A.Z* mRNA expression levels occur during gastrulation. *H2A.Z* mRNA is enriched in the marginal zone of the late blastula, involuting tissue in the gastrula and in notochord (a mesodermal tissue) in tailbud embryos. Significantly, maternal *H2A.Z* mRNA is enriched asymmetrically in

dorsal cells of the early blastula before zygotic transcription, indicating that H2A.Z may play a role in determining polarity of the dorsal ventral axis.

Two important processes for development were examined in this thesis: cell fate and cell movement. Determination of mRNA levels and localisations for a selection of mesodermal marker genes indicates that cell fate programs progress normally in embryos where H2A.Z function is disrupted. However, the localisation of mesoderm derived cells is perturbed suggesting cell movement is perturbed. Taken together these studies suggest the H2A.Z histone variant has a specific role in regulating cell mobility during early *Xenopus laevis* development.

Publication arising in part from this research

Ridgway, P., **Brown, K.D.**, Rangasamy, D., Svensson, U. and Tremethick, D.J. (2004). Unique residues on the H2A.Z containing nucleosome surface are important for *Xenopus laevis* development. *J Biol Chem*, **279**, 43815-43820.

Table of contents

List of abbreviations

A. thaliana: *Arabidopsis thaliana*

Ab: antibody

Abs: Absorbance

Ac: acetylation

ACF: ATP-utilising chromatin-assembly and –remodelling factor

ACRF: Australian Cancer Research Foundation

ACT: Australian Capital Territory

AEEC: Animal Experimentation Ethic Committee

ANU: The Australian National University

Arp: Actin related protein

AQIS: Australian Quarantine Inspection Service

AS: anti-sense

ATP: adenosine triphosphate

BAF: BRG associated factor

BAP: Brahma associated protein

BB/BA: Benzyl-benzoate / benzyl alcohol

Bdf1: Bromo-domain factor one

bp: base pairs

BRF: Biomolecular Resource Facility

BRG: Brahma related gene

Brm: Brahma

C. elegans: *Caenorhabditis elegans*

CBP: CREB binding protein

cDNA: complementary DNA

CENP-A: centromere protein A

CHD: chromodomain helicase DNA-binding protein

CHRAC: chromatin-accessibility complex

Chz1: chaperone for H2A.Z-H2B dimers

CRE: Core enhancer region

Ct: cycles at threshold

CTP: cytosine triphosphate

C-terminal: carboxy-terminal of an amino acid chain

DEPC: diethyl pyrocarbonate

DIG: digoxigenin

DMSO: dimethyl sulfoxide

DNA: deoxynucleic acid

dNTP: deoxyribonucleotide triphosphate

D. melanogaster: *Drosophila melanogaster*

DOM: Domino

ds: double stranded

DSB: double strand break (in DNA)

Dsh: named for the null mutants effect on fly hair orientation (Wallingford et al., 2002; Wallingford et al., 2000).

E. coli: *Escherichia coli*

EDTA: ethylene diamine tetraacetic acid

EGFP: enhanced green fluorescent protein

EGTA: ethylene glycol tetraacetic acid

FGF: fibroblast growth factor

Fz: Frizzled

GAPDH: Glyceraldehyde 3-phosphate dehydrogenase

Gsc: Gooscoid

gDNA: genomic DNA

GTP: guanine triphosphate

hBRM: human Brahma

H. sapiens: *Homo sapiens*

H1: histone 1

H2A: histone 2A

H2A-Bbd: histone 2A Barr-body deficient

H2A.Zdn defect: The defect arising from the injection of mRNA encoding the dominant negatives H2A.ZNQ and H2A.ZCS into *Xenopus laevis* embryos at the two cell stage.

H2B: histone 2B

H3: histone 3

H4: histone 4

HAT: histone acetyltransferase

HDAC: histone deacetylase

HEPES: 4-(2-hydroxyethyl)-1-piperazineethanesulfonic acid

HP1: heterochromatin protein 1

HPRI: human placental RNase inhibitor

INCENP: inner centromere protein

INO80: complex named for the gene product ino80 first identified from a mutation causing inositol auxotrophy in yeast

ISWI: Imitation switch

K: lysine

kb: kilobase pairs

LB: Luria broth

LBA: Luria broth with ampicillin.

MBT: mid-blastula transition.

MBSH: modified Barth's saline with HEPES

me: methylation

MEMFA: MOPS, EDTA, $MgSO_4$, formaldehyde

Mi-2: human dermatomyositis-specific antigen recognised by patient Mitchell autoimmune antibodies 2

MMR: Marc's Modified Ringer's Solution

MOR: Moira

mRNA: messenger ribonucleic acid

myo-2: Myosin-2

N-terminal: amino-terminal

NHMRC: National Health and Medical Research Council

Nhp: non-histone protein

NQdn: H2A.ZNQ dominant negative mRNA injected embryos

nt: nucleotides

NTD: neural tube defect.

NTP: nucleotide triphosphate

NuRD: nucleosome-remodelling histone-deacetylation

NuRF: nucleosome remodelling factor

OD: optical density

p: probability value

PBAF: polybromo BRG associated factor

PBAP: polybromo Brahma associated protein

PBS: phosphate buffered saline

PBT: Phosphate buffered saline with 0.1% v/v Tween 20

PCR: polymerase chain reaction.

PEH: paired ends of helices

RbAp: retino-blastoma associated protein

RIPA: radio-immuno-precipitation assay (buffer)

RNA: Ribonucleic acid

RNAi: RNA interference

RSC: remodel structure of chromatin

RT: reverse transcription

Rvb: RuvB-like protein

S: serine

S. cerevisiae: Saccharomyces cerevisiae

SD: standard deviation

SEM: standard error of the mean

siRNA: short interfering RNA

Snf: sucrose non-fermenting

Spp.: species

ss: single stranded

Stbm: Stabismus

SUMO: small ubiquitin-like modifier

SWI/SNF: switching defective/sucrose non-fermenting

SWR1: SWI/SNF related protein

T: threonine

TAE: Tris-acetate-EDTA

TE: Tris-EDTA

Tip60: Tat interacting protein 60

Tm: melting temperature

TSA: trichostatin A

UTP: uracil triphosphate

UTR: untranslated region

UV: ultraviolet

Wnt: these genes are named for two members of the family, *wingless* of *D. melanogaster* (Nusslein-Volhard and Wieschaus, 1980) and *integrated* from vertebrates (Nusse and Varmus, 1982).

X. laevis: *Xenopus laevis*

Xbcan: *Xenopus* brevican

Xbra: *Xenopus* brachyury

XMyoD: *Xenopus* myogenic determinant

XVent2: *Xenopus* Ventral 2

1 Introduction

1.1 Chromatin structure

The eukaryotic cell stores a large amount of DNA in the small volume of the nucleus; the human genome is over a metre in length. This is achieved by packaging DNA into a structure called chromatin (Horn and Peterson, 2002; Vermaak and Wolffe, 1998). Variations in chromatin structure can influence almost all DNA-related cellular processes including transcription (Li et al., 2007), recombination, repair, and replication (Ehrenhofer-Murray, 2004). This thesis will investigate one alteration to chromatin, incorporation of variant histone H2A.Z, in the context of development.

1.1.1 Nucleosome assembly and structure

The basic unit of chromatin is the nucleosome. The principle components of the nucleosome are DNA and histones (Figure 1). Histones are small basic proteins that have a structured central region and unstructured tails (Luger et al., 1997). A histone's central region interacts with the other histones, DNA of the nucleosome (Felsenfeld and Groudine, 2003) and other non-histone proteins (Wolffe and Hayes, 1999). Early dialysis studies indicated the nucleosome consisted of a $(H3/H4)_2$ histone tetramer and two H2A/H2B histone heterodimers associated with a length of DNA (Eickbush and Moudrianakis, 1978; Ruiz-Carrillo et al., 1979). Nucleosome assembly *in vitro* at physiological ionic strength begins with formation of $(H3/H4)_2$ tetramers on the DNA followed by H2A/H2B heterodimers (Ruiz-Carrillo et al., 1979). However, *in vivo* nucleosome assembly is not spontaneous or unregulated. Histone chaperone proteins prevent random association of histones with DNA, and target histones to nucleosome

assembly complexes (Akey and Luger, 2003). The histones of the octomer are known as the core histones and are the principle protein components of chromatin (Figure 1) (Arents and Moudrianakis, 1993; Luger et al., 1997; Wolffe and Hayes, 1999). The four canonical core histones all have the histone fold consisting of two tandem helix-strand-helix motifs that enables hetero-dimerisation and combine to form DNA interaction sites (Arents et al., 1991; Arents and Moudrianakis, 1995; Baxevanis et al., 1995). The histone fold domains provide each histone dimer in the octomer with three DNA binding sites: two β bridge motifs and a single PEH (paired ends of helices) motif (Arents et al., 1991; Luger et al., 1997). The β bridges begin with two positively charged amino acids (Arents et al., 1991; Luger et al., 1997). Fourteen α helices per nucleosome have amino terminals in the path of DNA around the octomer that form hydrogen bonds with the DNA (Luger et al., 1997). In addition to these interactions within the path of DNA around the octomer, the histones' protruding tails are positively charged, thus tail-DNA charge interactions can alter the accessibility of negatively charged DNA (Arents et al., 1991; Arents and Moudrianakis, 1993; Luger et al., 1997). X-ray crystallography of the nucleosome demonstrated that almost two turns of DNA (approximately 147bp) wraps around the nucleosome core in the completed nucleosome (Figure 1) (Arents et al., 1991; Luger et al., 1997). The complete nucleosome is a flattened 'disc' (Figure 1) with the DNA wrapped around the outer edge (Arents et al., 1991; Luger et al., 1997).

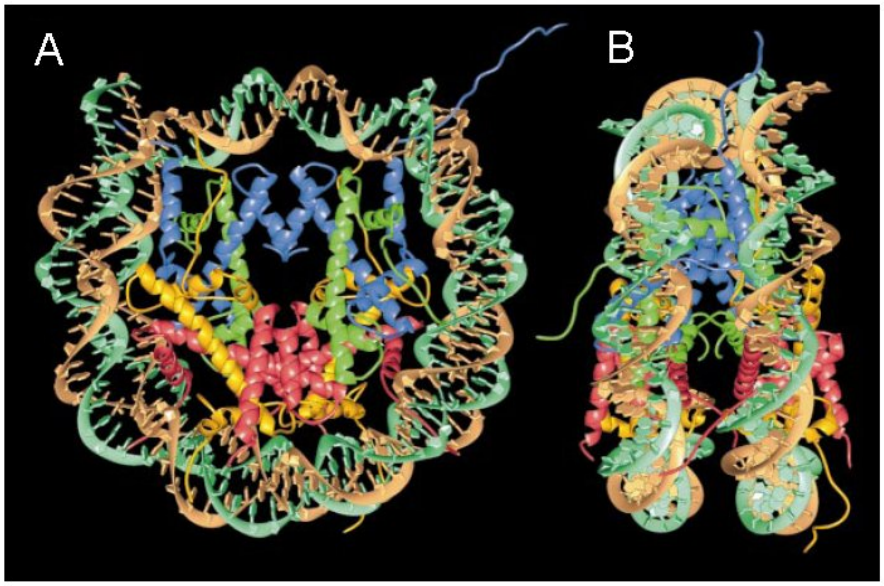

Figure 1 **Nucleosome core particle**. A) Octomer of histone proteins (yellow, H2A; red, H2B; blue, H3; green, H4) with 147bp of DNA (phosphodiester backbones in dark green and brown), view from above the DNA superhelix. B) As 'A' except the view is perpendicular to the DNA superhelix. (Adapted from (Luger et al., 1997)).

1.1.2 Higher order chromatin structures

The structure of chromatin is hierarchical (Figure 2). At the lowest level nucleosomes on DNA can be envisaged as 'beads on a string', though the DNA wraps around the nucleosome cores rather than passing through them (Arents et al., 1991; Luger et al., 1997). This structure is known as the 10nm fibre corresponding to the diameter of nucleosomes (Horn and Peterson, 2002; Wolffe and Hayes, 1999). Between each nucleosome a linker histone such as H1 can associate with the DNA (Doenecke et al., 1997; Horn and Peterson, 2002). Other nuclear proteins can also associate with either the DNA or the histones (refer to 1.1.3). For example transcription factors, proteins that bind to specific DNA sequences to regulate transcription, can function by altering chromatin structure such as promoting loops in 10nm fibres (Green, 2005; Hahn, 2004; Thomas and Chiang, 2006).

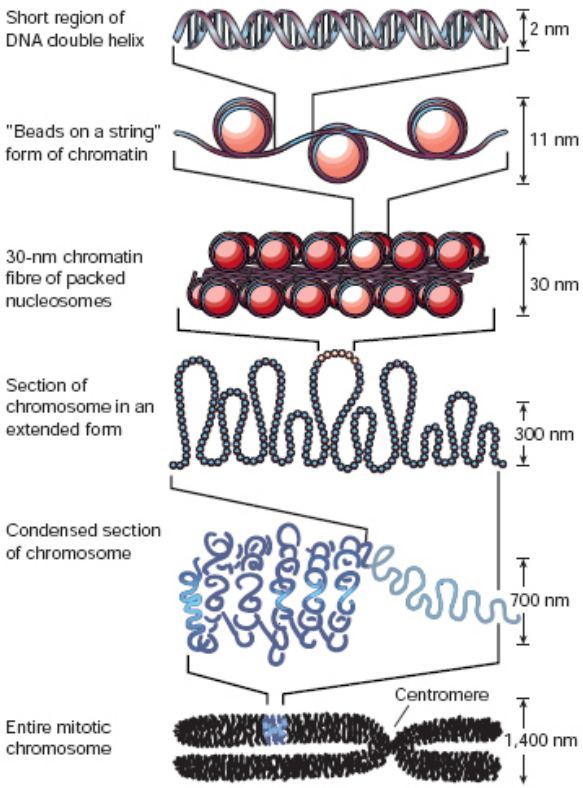

Figure 2 **Chromatin folding**. The first level of compaction is the association of DNA with nucleosomes to create the 10nm 'beads on a string structure'. This can condense into a 30nm diameter fibre. Further compaction of chromosomes is observed *in vivo,* 60-300nm diameter fibres are observed at interphase, these can be further compacted into fibres of around 700nm diameter and finally fully condensed mitotic chromosomes occur during mitosis and meiosis (Adapted from (Felsenfeld and Groudine, 2003)).

Interactions between nucleosomes and between nucleosomes and linker histones can compact the 10nm 'beads on a string' into higher order structures (Belmont and Bruce, 1994) (Figure 3). *In vitro* compaction of 10nm fibres first produces 30nm fibres, and 30nm fibres are also observed in fixed cells (Belmont and Bruce, 1994; Gordon et al., 2005). Interactions between H4 amino-terminal (N-terminal) tails and an H2A acidic patch domain on adjacent nucleosomes are required for 30nm fibre formation (Robinson and Rhodes, 2006). Currently, two models compete for the structure of the 30nm fibre (Figure 3). The solenoid model places nucleosomes into a simple helix (Finch and Klug, 1976; Robinson and Rhodes, 2006) (Figure 3). In the competing

'zigzag' model the 10nm fibre is twisted (-71.3^{o} rotation of adjacent nucleosomes) so nucleosomes alternate between two halves of a two start helix (Bednar et al., 1998; Dorigo et al., 2004; Schalch et al., 2005) (Figure 3). The zigzag model is supported by cross-linking studies on arrays of 12 nucleosomes (Dorigo et al., 2004) and a low resolution (9Å) crystal structure for an array of four nucleosomes condensed into a short 30nm fibre sufficient to determine the positions and orientations of nucleosomes (Schalch et al., 2005).

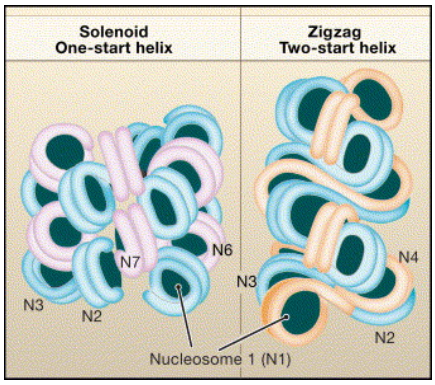

Figure 3 **Models of the 30nm Chromatin Fibre**: (Left) In the solenoid model proposed by Rhodes and colleagues, the fibre is an interdigitated one-start helix (Robinson and Rhodes, 2006). Alternative helical gyres are coloured blue and magenta. The linker DNA has not been modelled. (Right) In the zigzag model suggested by Richmond and colleagues, the fibre is a two-start helix with the linker DNA criss-crossing between the adjacent rows of nucleosomes(Dorigo et al., 2004). Alternative gyres are coloured blue and orange. Views have the fibre axis running vertically. Image courtesy of D. Rhodes, figure from (Tremethick, 2007).

At higher ionic strengths *in vitro* the 30nm fibres oligomerise to form thicker chromonema fibres (Gordon et al., 2005). Fibres 60-400nm in diameter are observed in fixed cells at interphase (Belmont and Bruce, 1994). During mitosis condensed chromatids (anaphase and telophase) have 400-600nm diameters (Gordon et al., 2005; Woodcock and Dimitrov, 2001) (Figure 2), however the exact structures and formation *in vivo* of fibres are unknown (Woodcock and Dimitrov, 2001).

In vivo chromatin domains can be classified by the degree of compaction as either euchromatin or heterochromatin (Grewal and Jia, 2007). Euchromatin is largely non-condensed chromatin such as predominates during interphase. Conversely,

heterochromatin continues to be condensed throughout interphase and provides regulated activation of some genes as well as repression (Grewal and Jia, 2007). Heterochromatin is further divided into two classes, constitutive and facultative heterochromatin (Sexton et al., 2007). Constitutive heterochromatin occurs at regions along the DNA that are in this condensed form in all cells of the organism. Constitutive heterochromatin forms on regions containing a high density of repetitive DNA sequences such as the satellite sequences found within the constitutive heterochromatin of the centromere. Facultative heterochromatin loci are differentially condensed during development in different cell types. Heterochromatin has traditionally been associated with transcriptional repression while euchromatin was associated with activation of transcription. This notion was supported by work in several systems including positional variegation and artificially inserting endogenously active genes within the telomeres in *D. melanogaster,* and mating-type loci in *S. cerevisiae* (Laurenson and Rine, 1992). However, for some genes heterochromatin formation is required for activation because heterochromatin has structural diversity allowing some genes within heterochromatin to be more accessible than others (Hahn, 2004).

Higher order chromatin structures beyond the degree of compaction of the 10nm fibres include well-known large scale chromatin structures such as the condensed chromosomes of mitosis. That individual chromosomes occupy specific domains within the nucleus has been known for some time (Heard and Bickmore, 2007). More recently it was discovered that chromatin from different chromosomes protrudes into the inter-chromosome domain and within this domain gene-poor chromatin regions are more centrally located (Heard and Bickmore, 2007; Misteli, 2007). Evidence has emerged for high order structural organisation such as large scale looping of chromatin into ‘transcription factories’ containing actively transcribed regions of different

chromosomes (Akhtar and Gasser, 2007; Sexton et al., 2007). Chromatin dynamically associates with the nuclear envelope with transcriptionally active chromatin predominantly attached to nuclear pores (Akhtar and Gasser, 2007). To summarise, chromatin structure is hierarchical, dynamic, and varies non-randomly across the genome and the cells of the organism (Misteli, 2007).

1.1.3 Alterations to chromatin structure

That the nucleosome's octomer core has subunits and contains sites for post-translational modification allows variations in chromatin structure influencing accessibility or affinity of chromatin components to each other or other proteins, such as the transcriptional machinery, chromatin remodellers, transcription factors, and enzymes responsible for histone post-translational modification, or methylation/demethylation of the DNA, thereby altering transcription (Fan et al., 2002; Kuo et al., 1998; Li et al., 1998; Nagy et al., 1997; Varga-Weisz et al., 1995; Whitehouse et al., 1999). Chromatin higher-order folding is dependent on interactions within and between nucleosomes, nucleosomes and linker histones, and the spacing of nucleosomes along the DNA. At the nucleosome level these interactions can be modified through chromatin remodelling machines, post-translational histone modifications, and incorporation of histone variants. For example, in the condensed structure of the centromere, H3 is replaced by centromere protein A (CENP-A) (Sullivan and Karpen, 2001; Sullivan, 2001). Short interfering RNAs (siRNAs) also have roles in targeting heterochromatin initiation sites, though at this point the mechanism remains unknown (Grewal and Jia, 2007). In reality several alterations to chromatin contribute to any functional state. For example in *X. laevis* histone acetylation by p300 and CREB binding protein (CBP) at promoters for some developmentally regulated genes, including *Siamois,* leads to decompaction and

recruitment of the TATA-binding protein (a transcription factor), and eventual recruitment of remodelling machinery for transcription (Hecht et al., 2000).

Recently, genes encoding proteins that remodel chromatin or post-translationally modify histones were found to have a large number of connections (hub genes) within genetic networks for developmental signalling genes in *C. elegans* (Lehner et al., 2006). These hub genes were experimentally confirmed to be key modulators of numerous biological processes, including developmental signalling, indicating the central role of chromatin (Lehner et al., 2006).

1.1.3.1 Chromatin remodelling machines

Chromatin remodelling machines are multi-protein complexes containing an ATPase subunit, ATP hydrolysis is necessary to mobilise otherwise stable nucleosomes (Bao and Shen, 2007; Bouazoune and Brehm, 2006; Mohrmann and Verrijzer, 2005). Chromatin remodelling outcomes include: separation of end-DNA from the nucleosome, sliding of histone octomers relative to the DNA, removal of histones as single proteins, dimers or octomers, and substitution of histone variants (Akey and Luger, 2003; Belotserkovskaya et al., 2003; Jin et al., 2005; Li et al., 2007). Nucleosomes can act as an obstacle to transcription, replication, and repair, or in some cases to improve transcription by positioning factors and promoting access to DNA (Ehrenhofer-Murray, 2004; Jin et al., 2005; Kireeva et al., 2002; Li et al., 2007). Yeast studies have shown DNA surrounding transcription start sites is globally depleted of nucleosomes; an outcome of remodelling machine action (Owen-Hughes and Engeholm, 2007). The actions of remodelling machines alter the accessibility of DNA to transcription factors, sites on histones for post translational modification, or other protein-protein interactions (Hirschhorn et al., 1992; Horn and Peterson, 2002). Other subunits within chromatin remodelling machines have functions including DNA

binding, complex assembly or stability, post translational modification, targeting of specific chromatin regions, or protein binding (Mohrmann and Verrijzer, 2005). Variation in remodelling machine subunit composition enables different complexes to remodel chromatin in ways appropriate to a range of biological functions at specific regions of the genome (Akey and Luger, 2003; Belotserkovskaya et al., 2003; Li et al., 2007; Saha et al., 2006).

There are five families of chromatin remodelers; SWI/SNF, ISWI, NuRD, INO80 and SWR1 (Driscoll et al., 2007; Felsenfeld and Groudine, 2003; Mueller et al., 1985; Nathan et al., 2006; Peterson and Laniel, 2004; Xu et al., 2005; Zhang et al., 2003) (Table 1, complex names are expanded in the List of Abbreviations). RNA and DNA polymerases are chromatin remodelling machines directly involved in transcription (Kireeva et al., 2002; Wolffe and Hayes, 1999). The remodelling complexes and their individual subunits are conserved. For example two SWI/SNF family members, *S. cerevisiae* SWI/SNF and *H. sapiens* PBAF, share multiple homologous subunits including SWI2/SNF2 and BRG1, SWI3 and BAF55, and SNF5 subunits (Table 1). Conservation of chromatin remodelling machinery indicates the importance of chromatin remodelling for an organism's survival. Interestingly, it has been shown that remodelling machines show stages and tissues specific enrichment during *X. laevis* development (Linder et al., 2004) and CHD4 has been demonstrated to have a developmental role in *X. laevis* (Linder et al., 2007). Other proteins associated with chromatin, such as those responsible for post translational modifications to histones, are also conserved (Kouzarides, 2007) indicating the broader importance of chromatin.

Remodelling complex family	Example remodelling complexes (*species*)	Known biological functions	Known subunits (equivalents)	References
SWI/SNF	SWI/SNF (*S. cerevisiae*)	PolII activation, elongation, double strand break (DSB) repair, gene activation and repression	SWI2/SNF2, SWP61/ARP7, SWP59/ARP9 SWI1/ADR6, SWI3, SWP73, SNF5, SWP82, SWP29/TFG3/TAF30/ANC1, SNF6, SNF11.	(Mohrmann and Verrijzer, 2005), (Mohrmann and Verrijzer, 2005)
	PBAF (*H. sapiens*)	Development, tumour suppressor, cell cycle	BRG1 (SWI2/SNF2, STH1), Polybromo/BAF180 (RSC1, RSC2, RSC4), BAF170 and BAF55 (SWI3), BAF57 (BAP111), BAF60A OR BAF60B (SWP73), BAF53 (BAP55), Actin, HSNF5/INI1 (SNF5)	(Mohrmann and Verrijzer, 2005; Pepin et al., 2007; Saha et al., 2006)
ISWI	CHRAC (*H. sapiens*)	Nucleosome assembly and spacing	SNF2H (ISWI, SNF2L, ISW2), WCRF180, CHRAC15, CHRAC17,	(Mohrmann and Verrijzer, 2005; Pepin et al., 2007; Saha et al., 2006)
	NuRF (*H. sapiens*)	Transcriptional activation	SNF2L (ISWI, ISW2) , BPTF, RBAP46, RBAP48	(Bao and Shen, 2007; Saha et al., 2006)
INO80	INO80 (*S. cerevisiae*)	DNA double strand break repair (recruited by phosphorylated H2A.X), PolII activation, gene specific regulation.	INO80, RVB1, RVB2, ARP4, ARP5, ARP8, Actin, NHP10, ANC1/TAF14, IES1 to 6,	(Bao and Shen, 2007; Saha et al., 2006)
	INO80 *(A. thaliana)*	Homologous recombination, gene transcription	INO80, RVB1, RVB2	(Bao and Shen, 2007; Saha et al., 2006; Wu et al., 2005)
SWR1	SWR1 (*S. cerevisiae*)	DNA double strand break repair, Htz1 deposition,	SWR1 (DOM-A, SRCAP, P400), ARP4, ARP6, SWC3, SWC4/EAF2/GOD1, SWC5/AOR1, SWC6/VPS71, SWC7, SWR2/VP372, YAF9, BDF1, Actin, RVB1, RVB2	(Bao and Shen, 2007; Bouazoune and Brehm, 2006; Saha et al., 2006)
	Tip60 (*D. melanogaster*)	DNA double strand break repair, H2A.Z deposition and acetylation	DOM-A (SWR1, SRCAP, P400),TIP60, PON, REP, MRG15, H2AV, TRA1, GAS41, ING3, E(PC), H2B	(Denslow and Wade, 2007; Saha et al., 2006)
NuRD/Mi-2/CHD	NuRD (*H. sapiens*)	Transcriptional repression and silencing, histone deacetylation, development	Mi-2, MBD2 OR 3, HDAC1, HDAC2, RBA P46, RBAP48, P66A OR P66B, MTA1, 2, OR 3 (MTA),	(Bouazoune and Brehm, 2006; Denslow and Wade, 2007)
	NuRD (*D. melanogaster*)	Transcriptional regulation, development	Mi-2, P55, RPD3 (HDAC1, HDAC2), MBD2 OR 3, MTA, P66/68	(Saha et al., 2006)

Table 1: **A selection of chromatin remodelling complexes**. The five known families of chromatin remodelling complexes with two example complexes from each family. Subunits are listed with items in parenthesis indicating equivalents (homologues or structurally similar proteins). A slash '/' indicates alternative names. The first subunit listed for each complex is the ATPase. Adapted from (Saha et al., 2006).

1.1.3.2 Post translational modification

Post translational histone modifications include phosphorylation (ph), ubiquitylation, ADP-ribosylation, methylation (me), SUMOylation, and acetylation (ac) of histone amino acid residues (Berger, 2007; Kouzarides, 2007). Proline isomerisation (Nelson et al., 2006) and deamination (arginine to citrulline conversion) can also occur (Cuthbert et al., 2004). Lysines (K) can be mono-, di- or tri-methylated (Me, Me2, Me3) (Kouzarides, 2007). Arginines (R) can be mono- or di-methylated (Kouzarides, 2007). Both canonical and variant histones can be modified (Kouzarides, 2007). Over 60 different residues on histones are known to harbour modifications (Kouzarides, 2007). Modifications thus far described are mostly in tail regions (Xu et al., 2005), however some residues within core domains can be modified, including H3 lysine 56 acetylation (H4K56ac) in *S. cerevisiae* and methylation of the equivalent residue (H4K59me) in mammals (Zhang et al., 2003). The number, sites, and types of post translational modification taken together provide a system with huge combinatorial power. These modifications are non-randomly distributed, most are reversible (no known enzyme can reverse arginine deamination or arginine methylation (Berger, 2007; Kouzarides, 2007)), and can alter chromatin's structural and functional properties providing a sophisticated regulatory system for the genome. Post translational modification function can be context dependent. Function can sometimes be determined directly by structure or indirectly by reading by 'adaptors', that are often components of remodelling machinery.

Post translation modification is required for *in vivo* chromatin assembly. Nucleosome assembly requires $(H3/H4)_2$ tetramers with particular post translational modifications (Sobel et al., 1995). Histone post translational modification can affect higher order chromatin structure, for example H4 acetylation at lysine 16 (H4K16ac) is an obstacle

to the 30nm fibres formation and higher order folding of these fibres (Shogren-Knaak et al., 2006). All core histone tail domains can shield the charge of DNA though they repress or potentiate oligomerisation of 30nm fibres into larger structures largely through other undefined interactions (Gordon et al., 2005; Wolffe and Hayes, 1999).

Post-translational modification can modify transcription directly, indirectly or both. Directly, by altering electrostatic charge or interactions between nucleosomes or histones and DNA, thus changing the accessibility of targets for DNA binding proteins (Becker, 2006; Peterson and Laniel, 2004). For example, histone hyperacetylation results in 10nm fibres decompaction providing access for transcription factors, one mechanism of this decompaction, alteration of the charge of the H4 N-terminal tail (free amino group terminal of an amino acid chain) by H4K16ac (acetylation neutralises the basic lysine) weakens interactions with the acidic patch of H2A on adjacent nucleosomes (Shogren-Knaak et al., 2006). An example of alteration to histone–DNA electrostatic interactions may be H3K56ac, since acetylation neutralises this residue's charge and fills most of the DNA-histone gap (Bernstein and Hake, 2006; Ehrenhofer-Murray, 2004; Shogren-Knaak et al., 2006). Post-translational modifications can act indirectly by altering/creating binding sites for chromatin binding proteins or complexes (Berger, 2007). For example H3K9me at promoter regions recruits HP1, promoting repressive heterochromatin formation (Ayyanathan et al., 2003) and H4K16ac prevents the action of the ACF remodelling complex (Shogren-Knaak et al., 2006).

Traditionally, particular post translational modifications at specific sites were correlated with either transcription or repression. More recently it has become apparent that some post translational modifications can recruit transcriptional activators and repressors. For example H3K9 methylation in mammals is restricted to promoter regions of inactive genes (Ayyanathan et al., 2003) and transcribed regions of active genes (Vakoc et al.,

2005), the mark is also enriched in pericentric heterochromatin where it is thought to promote silencing (Schotta et al., 2004). Variable function is due to the chromatin context, including variable protein-protein interaction sites, and cell type specific availability of associating proteins (Li et al., 2007; Peterson and Laniel, 2004). Context for post translational modifications can also be established by post translational modifications affecting each other, this can occur in several ways. Firstly, multiple modifications cannot occur on the same site so they are mutually exclusive, for example SUMOylation is repressive to transcription because it prevents acetylation or ubiquitylation of the modified residue (Nathan et al., 2006). Secondly, interference by adjacent modifications, for example binding of HP1 to H3K9me is blocked by H3S10ph (S: serine) (Fischle et al., 2005). Thirdly, alteration of an enzyme's recognition epitope reduces the enzyme's catalytic activity, for example isomerisation of H3P38 affects H3K36me by Set2 (Nelson et al., 2006). Also additional modifications enhance recognition of binding site by enzymes, for example the HAT GCN5 may recognise H3 better if H3S10 is phosphorylated (Lo et al., 2000). Finally, combinations of modifications on different tails can act together, for example H3K9me and H4K20me3 at pericentric heterochromatin (Li et al., 2007; Shogren-Knaak et al., 2006).

Post translational modifications	Sites	Selected functions/locations	References
Acetylated lysine	H2A(5,9,13), H2B(12,15,20), H3(9,12,14,18,59), H4(5,8,13,16)	H3K9: transcriptionally poised genes in embryonic stem cells. H3K9 and H3K14: active genes in human and mouse; mitotic chromosome condensation regulation. H3K12: DNA damage repair. H4K16: obstacle to 30nm fibre formation and higher order folding.	(Azuara et al., 2006; Bernstein et al., 2005; Driscoll et al., 2007; Fischle et al., 2005; Schotta et al., 2004; Shogren-Knaak et al., 2006; Xu et al., 2005; Zhang et al., 2003)
Phosphorylated serine/threonine	H3(3,10,28), H4(1)	H3T3: possible role in metaphase chromosome alignment. H3S10: mitotic chromosome condensation regulation. H4S1: DNA packaging during gametogenesis.	(Dai and Higgins, 2005; Fischle et al., 2005; Krishnamoorthy et al., 2006; Zhang et al., 2003)
Methylated arginine	H3(17,23), H4(3)	Multiple sites: transcriptional activation and targeting for deimination	(Wang et al., 2004)
Methylated lysine	H3(4,9,27,36,79), H3 (56 in yeast, 59 in mammals), H4(20)	H3K4: transcriptional elongation, transcriptionally 'poised' domains in embryonic stem cells, and remodelling complex binding at trimethylated transcription start sites. H3K9: repression and transcription through recruitment of different HP1 isoforms. H3K27: X-inactivation, transcriptionally 'poised' domains in embryonic stem cells, and transcriptional repression in somatic cells. H3K36: transcriptional activation when present in coding regions and prevents inappropriate transcriptional initiation within coding regions of active genes. H3K59: transcriptional silencing. H3K79: double strand break repair. H4K20: pericentric heterochromatin maintenance in metazoans, gene silencing, and DNA repair after ionizing radiation in yeast.	(Ayyanathan et al., 2003; Azuara et al., 2006; Bannister et al., 2005; Bernstein et al., 2005; Carrozza et al., 2005; de Napoles et al., 2004; Huyen et al., 2004; Sanders et al., 2004; Schotta et al., 2004; Shukla and Bhaumik, 2007; Vakoc et al., 2005; Wysocka et al., 2006; Zhang et al., 2003)
Ubiquitylated lysine	H2A(119), H2B(120 or 123 in *S. cerevisiae*)	H2AK119: transcriptional repression and X inactivation in metazoans. H2BK120: transcriptional elongation.	(de Napoles et al., 2004; Shukla and Bhaumik, 2007)
SUMOylated lysine	H2A(126), H2B(6 or 7)	Multiple sites: transcriptional repression	(Nathan et al., 2006)
Isomerised proline	H3(30,38)	Multiple sites: transcriptional activation and repression	(Nelson et al., 2006)
Deimination	H3 (2,8,17,26) H4 (3)	Multiple sites: transcriptional repression	(Cuthbert et al., 2004; Wang et al., 2004)

Table 2: **Post translational modifications to canonical histones**. For each modification the canonical histones modified (and amino acid numbers) are given as well as examples of functions and/or genomic locations affected. Adapted from (Peterson and Laniel, 2004).

1.1.3.3 DNA methylation

As well as histone post translational modification, the chromatin's DNA component can be chemically altered by methylation of cytosine (Doerfler, 1981; Wyatt, 1951), typically at CG dinucleotides or CNG trinucleotides (Doerfler, 1981; Grandjean et al., 2007), though some cytosine methylation is targeted to other sites (Grandjean et al., 2007). DNA methylation is generally associated with transcriptional repression (Doerfler, 1981; Naveh-Many and Cedar, 1981) and commonly occurs in repeats (Bestor, 2000; Doerfler, 1981; Roizes, 1976), transposons (Bestor, 2000; Walsh et al., 1998), and within genes (Bestor, 2000; Doerfler, 1981; Miller et al., 1978). DNA methylation is excluded from most promoter regions at CpG islands (Bestor, 2000; McClelland and Ivarie, 1982) further linking DNA methylation with transcriptional regulation.

1.1.3.4 Histone variants

The canonical histones make up the bulk of the histone content in all mitotic eukaryotic cells and are defined by several features: they have multiple gene copies in clustered cassettes in the genome, the genes contain introns, the non-polyadenylated transcripts are produced exclusively in S-phase, and the proteins are incorporated behind the replication fork during this period (Bernstein and Hake, 2006; Jin et al., 2005). Histone variants all have the histone fold though they need not have all the features of canonical histones listed above (Jin et al., 2005). Variants have different tails and can alter the octomer core structure, therefore variant incorporation can alter chromatin function by changing post translational modification sites, protein-protein interactions with remodellers or transcription factors, or by directly altering chromatin structure (eg. 10nm fibre compaction) and thereby DNA accessibility (Fan et al., 2002; Jin et al., 2005). These changes to function can be global, regional, or loci specific. Some examples: the variant $H1^{o}$ globally represses transcription in early *X. laevis*

development (Costanzi et al., 2000), CENP-A (an H3 variant) is required for centromere formation (Suto et al., 2000), while the variant H1b interacts with Msx1 to form a complex that binds the Core Enhancer Region (CER), an important regulatory DNA sequence for *MyoD* (Lee et al., 2004), to induce a repressive chromatin state (Bernstein and Hake, 2006).

Variant histones can replace H2A, H2B, H3, or linker histones but no H4 variants have been uncovered. Most known variants are of the H2A histone family (Costanzi et al., 2000). A selection from the numerous H2A variants known is given in Table 3. The most abundant H2A variants are H2A.Z and H2A.X (Costanzi et al., 2000). Studies in multiple organisms have found H2A.Z makes up approximately 10% of the H2A content (Jin et al., 2005; Kobor et al., 2004; Mizuguchi et al., 2004; Redon et al., 2002). The variant H2A.Z is the focus of this project.

H2A variant	**Function/expression.**	**Reference**
MacroH2A1.2	Concentrated on the inactive X of female mammals.	(Costanzi et al., 2000)
H2A.Bbd	Almost completely excluded from the inactive X chromosome in mammals.	(Chadwick and Willard, 2001)
H2AX	Phosphorylated at double strand breaks in mammals. Present in *X. laevis* oocytes.	(Paull et al., 2000; Rogakou et al., 1998)
H2AvD	*D. melanogaster* H2A.Z and has functional activities of both H2A.Z and H2AX.	(Madigan et al., 2002)
H2A.Z	Plays a structural role in centric chromatin and is associated with transcriptional regulation.	(Farris et al., 2005; Greaves et al., 2007; Thatcher and Gorovsky, 1994)

Table 3 **Selected H2A variants** adapted from (Bernstein and Hake, 2006).

1.2 The histone variant H2A.Z

1.2.1 Gene and transcript

The *H2A.Z* gene is highly conserved. Orthologs for *H2A.Z* have been found in many organisms including mammals (Hatch and Bonner, 1990), chicken (Harvey et al., 1983), trout (Nickel et al., 1987), *C. elegans* (Updike and Mango, 2006), sea urchin (Ernst et al., 1987), yeast (Carr et al., 1994), *tetrahymena* (Allis et al., 1986), and the slime mould *Physarum* (Mueller et al., 1985). In the human gene a 234bp proximal promoter

region has been defined containing six transcription factor binding sites; three CCAAT (sites for CCAAT box family transcription factors), two GC (GGGCGG binding sites for transcription factor Sp1), and a TATA box (Hatch and Bonner, 1996). In addition to this proximal promoter two more distal transcription factor binding sites exist between -234 to -361bp from the transcription start site (Hatch and Bonner, 1990). Some sites are conserved between species (Bernstein and Hake, 2006). In *X. laevis* the major H2A.Z transcript is ~869bp not including the poly-A tail (Iouzalen et al., 1996) with a ~381bp translated region (Iouzalen et al., 1996). *H2A.Z* transcription is not limited to S phase as with canonical core histones; a conclusion supported by the transcript's lack of the 3' stem loop structure found in S-phase transcribed histones (Hatch and Bonner, 1990). The transcribed region contains introns; four in human and chicken (Hatch and Bonner, 1990). Intron and exon lengths vary between species (Hatch and Bonner, 1990). In the human gene these introns are 276 to 438bp in size (Hatch and Bonner, 1990). The gene also contains a polyadenylation signal (Ernst et al., 1987; Hatch and Bonner, 1990; Iouzalen et al., 1996) and the transcript is polyadenylated in most species (Hatch and Bonner, 1990). In *X. laevis, H2A.Z* mRNA has polyadenylated and non-polyadenylated forms (Iouzalen et al., 1996), which is likely to affect mRNA stability and translation *in vivo* (Allende et al., 1974; Beilharz and Preiss, 2007).

1.2.2 Protein

When translated from the mRNA transcript described above, a 127aa, 14.1kDa protein is produced (Ernst et al., 1987; Iouzalen et al., 1996). The H2A.Z amino acid sequence is sufficiently conserved from canonical H2A (~57%) to replace the canonical histone within the nucleosome (the histone fold is conserved) and includes the 'H2A box' identifying it as a H2A variant (Jackson et al., 1996). H2A.Z's amino acid sequence is highly conserved, even in distantly related organisms such as humans and *S. pombe,* in

fact H2A.Z is more conserved than canonical H2A (Thatcher and Gorovsky, 1994). Despite small differences in codon usage, H2A.Z's protein sequence is 100% identical for rat, bovine, and human (Clarkson et al., 1999).

Any roles specific to H2A.Z must be linked to one or more differences from canonical H2A. Differences in protein sequence compared to canonical H2A include alterations to the core and tail regions (Harvey et al., 1983). The H2A.Z-containing nucleosome's crystal structure shows changes to the amino acid sequence alter nucleosome stability and surface features (Figure 4) (Suto et al., 2000). An acidic patch on the nucleosome surface is extended in H2A.Z by alterations in the C-terminal α-helix (Figure 4) (Suto et al., 2000). The acidic patch interacts with the H4 tail of adjacent nucleosomes (Fan et al., 2002). Consistent with the predicted H2A.Z-H4 inter-nucleosome interaction, *in vitro* H2A.Z facilitates 30nm fibre compaction (Fan et al., 2002). Changes to the L1 loop H2A-H2A interaction site favour incorporation of a second H2A.Z (Suto et al., 2000). A conserved histidine motif (HIH) within the core region bound a metal ion in crystal structure studies (Figure 4) (Suto et al., 2000). *In vivo* the HIH motif is likely to be a protein-protein interaction site (Suto et al., 2000). Three hydrogen bonds removed from the nucleosome interior results in less stable H2A-H3 interaction (Park et al., 2004). However, experimentally H2A.Z incorporation does not produce destabilisation, rather it produces greater H2A.Z/H2B-$(H3/H4)_2$ stability (Suto et al., 2000).

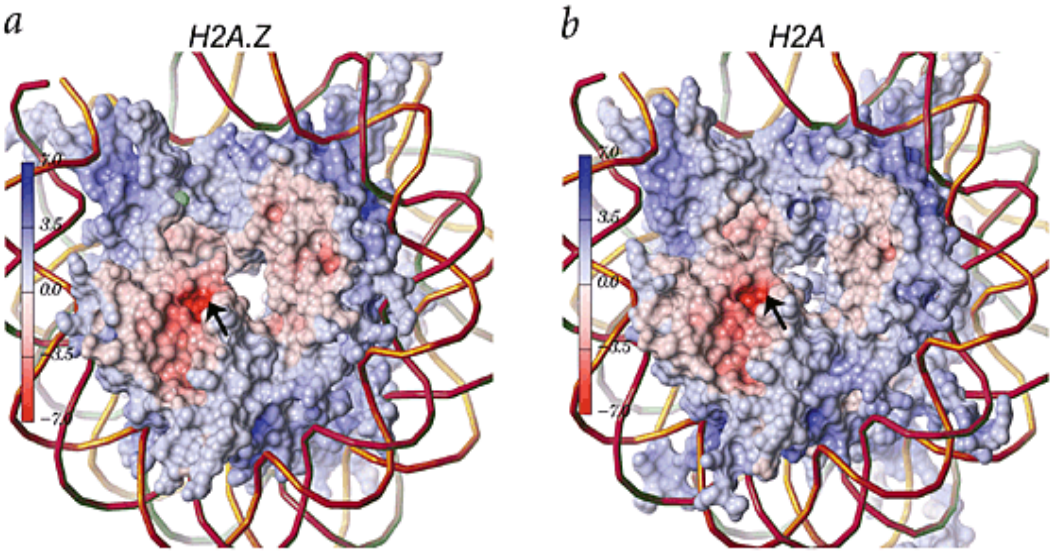

Figure 4 **H2A.Z incorporation alters nucleosome structure**. Comparison of nucleosomal surfaces of H2A.Z (*a*) and H2A (*b*) containing nucleosome cores at 2.6Å resolution. Electrostatic potentials at the accessible solvent surface (1.4Å, the radius of a water molecule, from the nucleosome surfaces) colour coded from +7.0 (deep violet) to -7.0 (deep red) kcal mol^{-1} e^{-1} have been mapped onto the nucleosomal surface (Getzoff et al., 1983). Molecular surfaces were modelled with MSMS (Sanner et al., 1996) using a 1.4Å spherical probe. The black arrow indicates the acidic patch (deep red region) on the nucleosome surface that in H2A.Z nucleosomes is extended compared to canonical nucleosomes. The coloured green area on '*a*' is the manganese ion bound to the HIH motif not present on the surface of canonical nucleosomes. Figure adapted from (Suto et al., 2000).

1.2.3 Incorporation of H2A.Z into chromatin

This section discusses H2A.Z incorporation into chromatin from the initial targeting and assembly into the nucleosome through to the consequences for higher order structure. Interestingly, *in vitro* H2A.Z incorporation inhibits 30nm fibre oligomerisation (Fan et al., 2002). H2A.Z is enriched in centric and pericentric heterochromatin, and binds INCENP (inner centromere protein), which is associated with pericentric heterochromatin (Carr et al., 1994; Greaves et al., 2007; Krogan et al., 2004; Rangasamy et al., 2003; Rangasamy et al., 2004). H2A.Z plays a structural role in centromeres which may explain why H2A.Z depletion leads to chromosome segregation defects and genome instability (Rangasamy et al., 2004). Clearly, H2A.Z assembly can lead to specialised structural chromatin domains.

H2A.Z incorporation is non-random (indicating the process is targeted) and occurs throughout the cell cycle (Leach et al., 2000; Raisner et al., 2005). Indeed H2A.Z incorporation requires chromatin remodelling machinery and chaperones distinct from canonical H2A (Luk et al., 2007; Ruhl et al., 2006; Wu et al., 2005). H2A.Z localisation is related to possible structural and functional roles, such as mitotic chromosome segregation (Rangasamy et al., 2004) and transcriptional regulation (Meneghini et al., 2003; Raisner et al., 2005; Santisteban et al., 2000). H2A.Z must therefore be targeted to specific chromosomal regions. Work done largely in yeast is now starting to produce a detailed picture of how H2A.Z is targeted to and incorporated into chromatin by an ATP-dependent chromatin remodelling machine (Jin et al., 2005). In yeast this complex is called SWR1 (named for the Swr1 ATPase subunit), in human SRCAP, and in *Drosophila melanogaster* (*D. melanogaster*) dTip60 (named for its Tip60 histone acetyl transferase subunit) (Jin et al., 2005; Krogan et al., 2003; Mizuguchi et al., 2004; Ruhl et al., 2006).

H2A.Z is assembled into nucleosomes flanking transcription initiation sites containing a 22bp DNA sequence within promoters (Raisner et al., 2005). However, exactly how H2A.Z and SWR1 are targeted to other heterochromatin regions remains unknown (Jin et al., 2005). It has been proposed that histone post translational marks allow a component of SWR1 to bind to nucleosomes, candidates include subunits Swc6 and Arp6, which are required to bind SWR1 to nucleosomes (Wu et al., 2005) and Bdf1 and 2 which bind acetylated H4 (Raisner et al., 2005) (see Table 1 section 1.1.3.1). This then recruits the other SWR1 complex subunits (Jin et al., 2005; Mizuguchi et al., 2004). SWR1 then facilitates the removal of the H2A/H2B dimer, though the precise mechanisms remains unknown (Luk et al., 2007). Note though that the 22bp DNA

sequence alone is not sufficient to recruit H2A.Z and therefore requires a second currently undescribed mechanism for H2A.Z recruitment (Raisner et al., 2005).

In yeast, the H2A.Z/H2B dimer is associated with a chaperone, Nap1 or the H2A.Z specific Chz1 (called HIRIP3 in metazoans), that binds to the Swc2 (YL-1 in metazoans) SWR1 component (Luk et al., 2007; Wu et al., 2005), then SWR1 exchanges H2A.Z/H2B into the nucleosome structure (Mizuguchi et al., 2004; Wu et al., 2005). Swc2 binds to the H2A.Z α-C-helix, which differs from the corresponding domain in core H2A, demonstrating that this is an H2A.Z specific interaction (Luk et al., 2007; Wu et al., 2005). Due to changes in the L1 loop that prevent canonical H2A and H2A.Z from co-existing in a nucleosome a second H2A.Z is incorporated into the nucleosome (Suto et al., 2000).

1.2.4 H2A.Z and transcription

H2A.Z is implicated in transcriptional regulation by its non-random distribution throughout different organisms' genomes, though localisation of H2A.Z offers conflicting indications of its role in transcription (Jin et al., 2005; Redon et al., 2002). In *Tetrahymena* H2A.Z is localised to the transcriptionally active macronucleus (Allis et al., 1986) while in yeast Htz (the H2A.Z homologue) has been associated with silencing and activation (Meneghini et al., 2003; Raisner et al., 2005; Santisteban et al., 2000). More specifically in yeast, Htz is enriched at particular DNA motifs associated with promoters, typically immediately downstream of transcription start sites (Albert et al., 2007; Raisner et al., 2005) and to euchromatin adjacent to silenced regions where it prevents the spread of silencing (Meneghini et al., 2003; Millar et al., 2006). The positioning of H2A.Z-containing nucleosomes on promoter DNA in yeast is more variable than in other genomic regions, suggesting that H2A.Z positioning nucleosomes may regulate the promoter regions' accessibility to non-histone proteins in this

organism (Albert et al., 2007). H2A.Z is also found in nucleosomes flanking the transcription start site within both active and inactive promoters (Raisner et al., 2005).

H2A.Z is associated with both transcriptionally repressive and active histone post translational modifications. In yeast Htz interacts genetically with the pathway for H3 lysine 4 methylation (H3 K4me) to produce more pronounced phenotypes than mutations in either alone (Ng et al., 2003). H3 K4 dimethylation (H3K4me2) correlates with genes poised for activation, while H3 K4 trimethylation (H3K4me3) is associated with recent transcription by polymerase II (Ng et al., 2003). Efficiency of H2A.Z incorporation flanking transcription start sites is increased by H3K4 methylation, H3K79 methylation, and H4K16 acetylation, marks associated with transcription, but these marks are not essential for H2A.Z incorporation (Raisner et al., 2005). H2A.Z is also less often SUMOylated than canonical H2A (Nathan et al., 2006). SUMOylation is a repressive post-translational modification (Nathan et al., 2006). H2A.ZK14ac is enriched at transcribed genes, while hypoacetylated H2A.Z is associated with repression (Millar et al., 2006).

H2A.Z localisation in several metazoan genomes offers similarly contradictory evidence. In *D. melanogaster* H2Av is more widely, though still non-randomly, spread over the genome (Leach et al., 2000) and is associated with silenced regions (Swaminathan et al., 2005). In mice H2A.Z is enriched in the compact gene-poor pericentric and centric heterochromatin (Greaves et al., 2007; Rangasamy et al., 2004). Potentially H2A.Z has a role in genome stability (Greaves et al., 2007; Rangasamy et al., 2004). Whether H2A.Z plays a role in transcriptional silencing at the centromere or has a purely structural role in this region remains an open question. Additionally, vertebrate H2A.Z distribution is not limited to the centromere. Evidence from mammalian cells indicates that, as with yeast, vertebrate H2A.Z is localised upstream of

genes and downstream of transcription start sites (Farris et al., 2005). In cells not expressing the gene *c-myc,* H2A.Z is present in both the promoter and transcribed regions, though depleted toward the transcribed region's 3' end. When transcription is induced H2A.Z is depleted from the transcribed region (Farris et al., 2005). In the housekeeping gene *GAPDH* (Glyceraldehyde 3-phosphate dehydrogenase), H2A.Z was present within the promoter not the transcribed region (Farris et al., 2005). As already noted, exactly how H2A.Z is targeted to specific genomic regions is unclear (see section 1.2.3).

Two mechanisms have been proposed for transcriptional modulation by H2A.Z. Firstly, that H2A.Z containing regions act as a barrier to the spread of silencing, the variant histone could be involved in the maintenance and/or establishment of boundary structures, into actively transcribed regions (Meneghini et al., 2003). Secondly, remodelling of H2A.Z-containing nucleosomes is required for transcription (Farris et al., 2005).

The second mechanism involves H2A.Z exchange for H2A. As already discussed, H2A.Z-containing nucleosomes are more stable *in vitro* than their canonical counterparts (Park et al., 2004) (see section 1.2.3), therefore exchange of H2A.Z for H2A and vice versa may alter the accessibility of DNA associated with the nucleosome. Initially, H2A.Z is incorporated into nucleosomes near promoters, then H2A.Z is removed from the nucleosome and transcription occurs, however the timing and detailed mechanisms remain unknown (Jin et al., 2005).

One possible model, suggested by Farris (2005), for H2A.Z's role in transcription is that H2A.Z incorporation is repressive and marks regions poised for transcription. With H2A.Z incorporation (see also 1.2.3), genes may be transcriptionally poised because H2A.Z favours 10nm fibre compaction into 30nm fibres, though not further compaction

(Park et al., 2004). Favouring the 30nm fibre may also contribute to establishing chromatin structures that prevent the spread of silencing. Within the transcribed region the presence of stable H2A.Z nucleosomes (Park et al., 2004) is thought to repress transcription (Farris et al., 2005). To extend this model, the variable positioning of H2A.Z nucleosomes within promoters (Albert et al., 2007) may modulate transcriptional regulation. As can be surmised from this model, our understanding of H2A.Z in transcriptional regulation has come a long way since the early studies that correlated H2A.Z with either repression or activation. However, we do not yet have complete understanding of the molecular mechanisms behind the models. How H2A.Z is targeted to particular genomic regions and the details of H2A.Z exchange for H2A upon transcription remain unclear.

1.3 Chromatin and transcriptional regulation during metazoan development

Chromatin has essential roles in the control of gene transcription throughout metazoan development. Often early embryonic transcription is globally repressed until after a specific developmental stage, such as the mid-blastula in *X. laevis* (see section 3.1.1.2). Histone variants, as well as other mechanisms that alter chromatin structure, have been implicated in the regulation of key developmental genes and global changes to transcription. For example, many transcription factors are either implicated in development, and/or have developmentally regulated expression (Latinkic and Smith, 1999; Saka et al., 2000; Tada et al., 1998; Tintignac et al., 2004; Veenstra et al., 2000). In metazoans distinct histone combinations are found in germ, undifferentiated embryonic, and different somatic cell types (Bouvet et al., 1994; Dimitrov et al., 1993). This section presents an overview of changes to chromatin throughout early development in *X. laevis*.

In *X. laevis* the first twelve divisions are synchronous, and proceed without transcription or gap phases (Graham, 1966; Newport and Kirschner, 1982). These 'cleavage divisions' are facilitated by large maternal stores of histone protein that contribute to a globally repressive chromatin structure (Prioleau et al., 1994). Germ cell DNA is highly methylated. Methylation at specific gene promoters decreases during the cleavage divisions eventually activating these genes thereby inducing the mid-blastula transition (Stancheva et al., 2002).

After the cleavage divisions, the mid-blastula transition (MBT) marks the beginning of zygotic transcription. Chromatin at the MBT has lost most of the maternal proteins including the maternal store of core histones. Titration out of these maternal histones by DNA replication contributes globally to less repressive chromatin structures immediately post MBT (Almouzni and Wolffe, 1995; Prioleau et al., 1994). Later transcriptionally permissive histone post-translational modifications that characterise pre-MBT blastomeres are replaced with modifications, such as H4 hyperacetylation that establish transcriptionally repressed domains (Kikyo and Wolffe, 2000). The importance of post translational modifications to development is dramatically demonstrated by experimental global histone hyperacetylation (such as by TSA treatment, (Stewart et al., 2006)), which prevents proper gastrulation in *X. laevis* by perturbing transcriptional regulation (Almouzni et al., 1994). With each cell division a decline in the chromatin's totipotent character occurs as new patterns of chromatin causing tissue specific expression are established (Kikyo and Wolffe, 2000). These alternations continue into gastrulation transforming totipotent into somatic cells (Kikyo and Wolffe, 2000).

Histone variant expression is often developmentally regulated (Aul and Oko, 2001; Iouzalen et al., 1996; Ohsumi and Katagiri, 1991). For example *X. laevis* oocytes have

large stores of the variant H2A.X that are titrated out as cell divisions proceed (Dimitrov et al., 1994; Ohsumi and Katagiri, 1991). Another example is B4, the dominant linker histone at the mid-blastula transition that is replaced by the end of gastrulation by H1 (Dimitrov et al., 1993). Moreover, histone variants have functional implications for development, for example H1b is required for regulation of *MyoD,* a key developmental gene (Lee et al., 2004).

1.4 H2A.Z is essential for metazoan development

Several lines of evidence suggest a developmental role for H2A.Z in metazoans. Firstly, knock-out experiments have shown H2A.Z is essential in organisms including fly and mouse (Faast et al., 2001; van Daal and Elgin, 1992), though not yeast (Carr et al., 1994; Jackson and Gorovsky, 2000), indicating that H2A.Z may have additional functions in more complex organisms. Secondly, H2A.Z expression is developmentally regulated in metazoans (Ernst et al., 1987; Harvey et al., 1983; Iouzalen et al., 1996; Rangasamy et al., 2003). Taken together, evidence suggests H2A.Z might regulate developmental transcription or have a more general function in chromosome segregation.

1.4.1 H2A.Z is targeted to a selection of foregut genes during *C. elegans* development

In *Caenorhabditis elegans* (*C. elegans*) H2A.Z and the remodelling complex SWR1 are recruited to a subset of foregut gene promoters *in vivo* when transcription is initiated (Updike and Mango, 2006). Only the tissue specific genes *Myosin-2 (myo-2)* and *R07B1.9* were identified within this subset (Updike and Mango, 2006). Reduction of H2A.Z levels by RNAi results in delayed expression of these genes, defects in pharyngeal and intestinal development (the organs were misshapen), and was eventually

lethal (Updike and Mango, 2006). This observation is consistent with the proposed 'poised' chromatin state of H2A.Z-containing nucleosomes (see section 1.2.4).

1.4.2 Essential regions of H2Av during fly development

In *D. melanogaster* the variant H2Av is within the H2A.Z family and is also phosphorylated at double strand DNA breaks, an H2A.X function in mammals (Paull et al., 2000) and of canonical H2A in yeasts (Madigan et al., 2002). Following the work that determined that H2Av was essential in *D. melanogaster* (van Daal and Elgin, 1992) rescue experiments identified protein regions important to fly development (Clarkson et al., 1999). A region including the C-terminal α-helix was found to be essential (region M6) and three regions resulting in partial rescue were also identified (Clarkson et al., 1999). These were: portions of the C-terminal (region M7); the N-terminal tail including important post-translational modification sites (M1); and a portion of the histone fold α2 helix (M4) (Clarkson et al., 1999). Regions M6 and M7 were essential for survival into adulthood (Clarkson et al., 1999) (Figure 5).

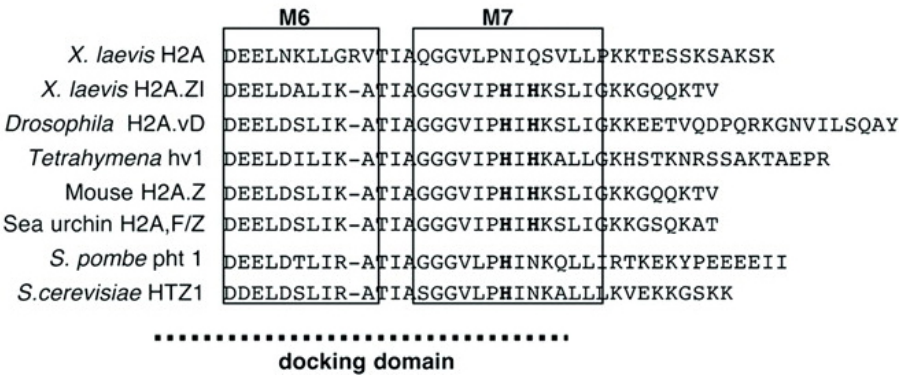

Figure 5 **A histidine motif in H2A.Z is conserved in metazoans**. Sequence comparison of H2A.Z protein from different species. The two histidine residues required for normal development are **bold**, the M6 and M7 essential domains for *D. melanogaster* development are boxed (Clarkson et al., 1999), and the docking domain is indicated with a dotted line. Sequences were from the following: *X. laevis* H2A and mouse H2A.Z (Suto et al., 2000), *X. laevis* H2A.Z1 (Iouzalen et al., 1996), *D. melanogaster* H2A.vD (Clarkson et al., 1999), *Tetrahymena* hv1 (White et al., 1988), sea urchin H2A.F/Z (Ernst et al., 1987), *S. pombe* pht1 (Carr et al., 1994), and *S. cerevisiae* HTZ1 (Jackson et al., 1996) (figure adapted from (Ridgway et al., 2004a))

The essential region M7 contained a conserved histidine motif (Rangasamy et al., 2003) (see section 1.2.3). Since H2A.Z's histidine motif is conserved in metazoans though not in yeast (Figure 5) and also conserved in *C. elegans* (swissprot: locus H2AV_CAEEL, accession Q27511.3)), this indicates that H2A.Z has acquired an additional function in metazoans (Suto et al., 2000). The histidine motif is likely to be a protein-protein interaction site *in vivo* (Suto et al., 2000) possibly with transcriptional consequences for the developmental regulation of genes (see section 1.2.4).

1.4.3 H2A.Z localisation in early mouse development

H2A.Z transcription and localisation are developmentally regulated in the mouse. Semi-quantitative RT-PCR from different parts of the early mouse blastocyst found that the inner cell mass was depleted of H2A.Z mRNA at least twelve-fold compared to trophoblast cells (Rangasamy et al., 2003). When cell differentiation begins in the mouse embryo H2A.Z is first localised to the pericentric heterochromatin in specific cells then is localised to other nuclear regions except the nucleolus (Rangasamy et al., 2003). In these studies, the M6 region was determined to be essential for INCENP binding (Rangasamy et al., 2003). However, M7 region containing the histidine motif was not necessary (Rangasamy et al., 2003). This indicates that H2A.Z's general structural role at the centromere (discussed in section 1.2.3) may be initiated in early mammalian zygotic cells and indicates that H2A.Z may have additional separate roles that rely on distinct features of the H2A.Z containing nucleosome surface.

H2A.Z expression is also developmentally regulated in mouse spermatogenesis. The protein and transcript levels that increase more than five- and two-fold respectively by pachytene are not detected in mature spermatozoa (Greaves et al., 2006). The timing of H2A.Z expression correlates with meiotic sex chromosome inactivation (Greaves et al., 2006). Post-mitotically H2A.Z replaces macroH2A maintaining the sex chromosomes

in transcriptionally silent facultative heterochromatin (Greaves et al., 2006). This demonstrates that H2A.Z can influence transcriptional activity in a developmentally regulated fashion during vertebrate differentiation. Taken together with H2A.Z's developmentally regulated expression in early mouse embryos these results indicate that low H2A.Z levels are a feature of undifferentiated cells. As differentiation proceeds H2A.Z expression increases and H2A.Z plays a role in establishing proper heterochromatin structures in the differentiated cells (Greaves et al., 2006).

1.4.4 H2A.Z is essential for correct mesoderm development in *X. laevis*

Studies in mice did not address whether H2A.Z has a specific role in transcriptional regulation in the early embryo distinct from its role in the centromere. To investigate H2A.Z's role during vertebrate development, *X. laevis* was used because it is a tractable vertebrate model for developmental studies (Sive et al., 2000).

1.4.5 Morphological observations indicate defective mesoderm formation

Reducing H2A.Z expression in *X. laevis* embryos by siRNA resulted in a developmental defect with the blastopore failing to close during gastrulation (Figure 6, B). Gastrulation is the stage of development when the three primary tissue types are established by extensive morphogenic shape changes. The defect induced by H2A.Z depletion is consistent with defective gastrulation and mesoderm formation (Smith et al., 1991). As embryos continue to develop, the dorsal surface of neurula and later stage embryos remains open resulting in a neural tube defect. By the tailbud stage the embryo is forming a head and tail bud, however the neural tube remains open and the trunk is shortened (Figure 6). Trunk elongation in normal development is due to notochord convergent extension; however, in the defective embryos the trunk is shortened. The

notochord is descended from the marginal zone involuting cells that form the third tissue layer, the mesoderm, through gastrulation. The defect observed is therefore consistent with defective progression of mesoderm formation at gastrulation, (the normal head development indicates that prechordal mesoderm and other non-mesodermal tissues are developing normally). Based on these observations we developed the hypothesis that the histone variant H2A.Z is important for gastrulation and mesodermal development (Ridgway et al., 2004a).

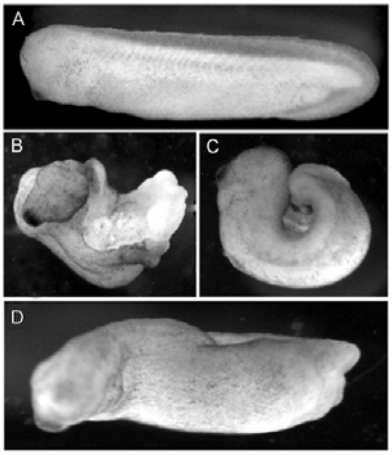

Figure 6 **Inhibition of H2A.Z by siRNA produces a gastrulation defect**. The blastopore fails to close and the trunk is shortened. Embryos shown are at stage 33/34; A untreated sibling, B siRNA injected embryo displaying the defect, C and D examples of rescue experiments where co-injection of *H2A.Z* mRNA has a dose dependent rescue effect on the *H2A.Z* RNAi indicating that defect is specific to H2A.Z (Ridgway et al., 2004a).

1.4.6 A histidine motif on the H2A.Z-containing nucleosome surface is important for vertebrate development

To determine the minimal region of H2A.Z required to maintain normal development in *X laevis* plasmids containing mutations in *H2A.Z* mRNA were created based on information from rescue experiments in *D. melanogaster* (Clarkson et al., 1999) and crystal structure studies (Suto et al., 2000). These included several encoding proteins with exchange of residues in surface features unique to H2A.Z containing nucleosomes (Figure 7); the extended acidic patch and HIH motif (see section 1.2.3) (Ridgway et al.,

2004a). The mRNAs produced *in vitro* from these plasmids were injected into two cell embryos where they overexpressed the encoded proteins. H2A.Z over-expression slowed development and acidic patch removal (H2A.ZNK) prevented this developmental delay (Figure 8) (Ridgway et al., 2004a). Therefore H2A.ZNK may mimic canonical H2A (Fan et al., 2002). Three C-terminal region mutations produce defect higher rates, H2A.ZCS, H2A.ZNH, and H2A.ZNQ. H2A.ZCS has the entire α-C helix swapped for that of canonical H2A. This region is the 'M6' region found to be essential in *D. melanogaster* (see 1.4.2). H2A.ZNH and H2A.ZNQ exchange one or both histidine residues of the histidine (HIH) motif respectively for the equivalent canonical H2A residue. *H2A.ZNH, H2A.ZNQ* or *H2A.ZCS* mRNA over expression resulted in an identical phenotype to that produced by *H2A.Z* siRNA depletion, indicating these proteins were acting as dominant negatives (Ridgway et al., 2004a). The defect arising from injection of mRNA encoding the dominant negative H2A.ZNQ will be referred to as the H2A.Zdn defect. Since disrupting even a single histidine residue of the motif causes the H2A.Zdn defect, we concluded that the histidine motif on the surface of H2A.Z-containing nucleosomes is important for proper development in *X. laevis* (Ridgway et al., 2004a).

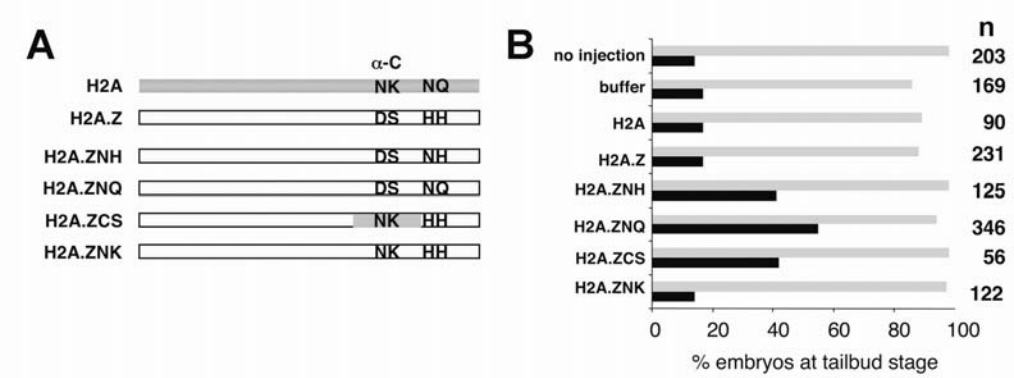

Figure 7 **Specific mutations in H2A.Z have a dominant negative effect** (A) Schematic of the proteins expressed by microinjected RNAs in *X. laevis* embryos. Grey indicates regions with the peptide sequence of canonical H2A. Letters indicate amino acid substitutions at two key motifs, the acidic patch (DS to NK) and the histidine motif (HH to NH or NQ). Position of the α-C helix is indicated. The plasmids to produce these RNAs are described in 02.1. (B) Percentage survival and defect rates for embryos expressing the various exogenous proteins. Percentage survival is given in grey. The percentage defective is given in black. The number of embryos for each is given to the right. Results are pooled from several experiments (Ridgway et al., 2004a).

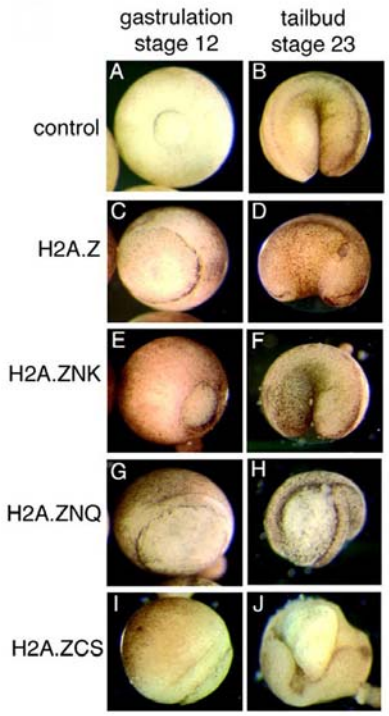

Figure 8 **Defective morphology of embryos over-expressing altered H2A.Z indicates a dominant negative effect**. Embryos at stage 12 and 23. A and B uninjected controls; C and D, *H2A.Z* RNA injected showing morphology consistent with delayed development; E and F *H2A.ZNK* RNA injected have normal development, G and H defective development in *H2A.ZNQ* RNA injected embryos; I and J *H2A.ZCS* RNA injection produces defective morphology. The morphology of embryos G-J has the same defects as embryos depleted in H2A.Z by siRNA. The defects seen in G-J and siRNA treated embryos are consistent with a disruption to proper mesoderm development (Ridgway et al., 2004a).

1.5 Scope of thesis

The histone variant H2A.Z is essential for embryonic survival in several organisms. RNAi and H2A.Z dominant negative experiments in *X. laevis* indicate that H2A.Z function is required for correct mesodermal development. Since it has been determined that H2A.Z's histidine motif is required for the histone's function in development this thesis project characterises H2A.Z's developmental function in the *X. laevis* model.

The dn H2A.ZNQ embryos were used as a model for loss of H2A.Z function. Several specific aims were formulated to test the hypothesis that H2A.Z is important for correct gastrulation and mesodermal formation in early *X. laevis* development.

1. To determine H2A.Z's spatial and temporal expression in early *X. laevis* embryos;
2. To determine whether H2A.Z plays a role in cell fate determination in mesodermal cell lineages;
3. To determine whether H2A.Z has a role in regulating cell movement during convergent extension of mesoderm tissue.

Spatial and temporal expression patterns were determined by *in situ* hybridisation and semi-quantitative RT-PCR methods, and these findings are described in Chapter 3. *H2A.Z* mRNA is present in the early blastula at low levels and is enriched on the prospective dorsal side. Later *H2A.Z* mRNA levels rise, peaking at gastrulation and are enriched in mesodermal tissues. These results show that *H2A.Z* has expression consistent with a role in regulating developmental expression of mesoderm genes. The second aim is addressed in Chapter 4, where I compared the levels of critical developmental genes in dnH2A.ZNQ embryos where H2A.Z function is perturbed to their normal siblings. Based on these findings, a role for H2A.Z in determining mesoderm cell fate was excluded. In Chapter 5, the final aim was addressed first by *in situ* hybridisation for localisation of mesodermal markers, then by RT real-time PCR of

a key gene known to control cell movement in both dnH2A.ZNQ embryos and normal siblings. The findings of these investigations are evidence that a critical cell motility process (convergent extension) is disrupted when H2A.Z function is perturbed, suggesting a role for H2A.Z in regulating the expression of genes required for convergent extension.

2 Materials and methods

2.1 Production of plasmids

Several plasmids for production of probes for *in situ* hybridisation (2.4) or for production of RNA for microinjection (2.3.2) were constructed from the RN3P vector (Zernicka-Goetz et al., 1996) as previously described (Ridgway et al., 2004a; Ridgway et al., 2004b; Zernicka-Goetz et al., 1996). This section (2) briefly describes plasmid production.

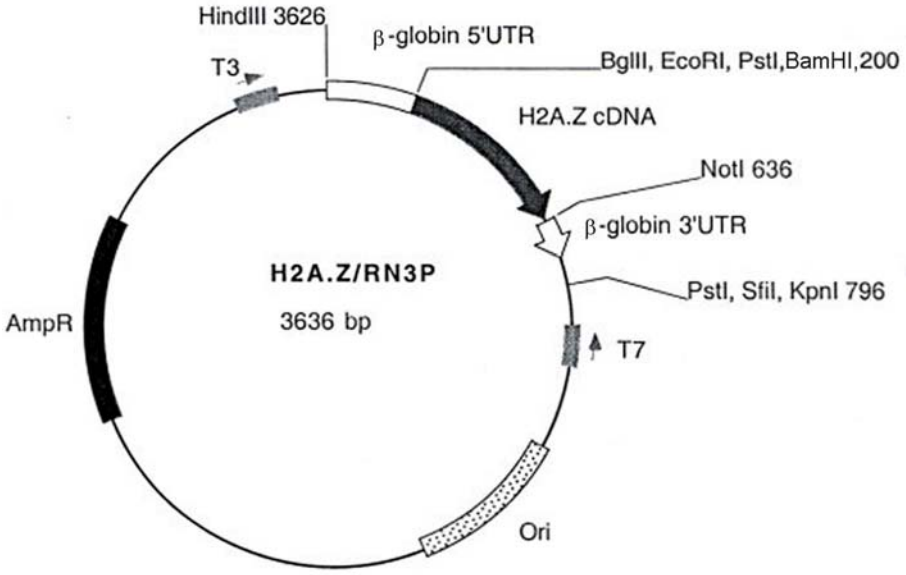

Figure 9 **H2A.Z/RN3P plasmid**. Example of the plasmid used for production of RNA for microinjection. AmpR: ampicillin resistance, Ori: origin of replication for amplification of plasmid within bacteria, T3: T3 RNA polymerase binding site (arrow indicates direction of transcription), T7: T7 RNA polymerase binding site (arrow indicates direction of transcription), β-globulin 5' UTR: β-globulin 5' untranslated region, β-globulin 3' UTR: β-globulin 3' untranslated region, HindIII, BglII, PstI, BamHI, NotI, SfiI, and KpnI: restriction enzyme binding sites, *H2A.Z* cDNA: transcribed insert (Ridgway et al., 2004b; Zernicka-Goetz et al., 1996).

The RN3P plasmid has several features pertinent to this project. The 5'-capping site and β-globin 5' and 3' untranslated region sequences confer greater translational efficiency

(Krieg and Melton, 1984). Finally, the plasmid offers numerous restriction sites for cloning including BamH1, Not1 and Kpn1 sites.

2.1.1 Plasmids constructed for production of mRNA for microinjection

RN3P plasmid and PCR produced inserts were digested by BamH1 and Not1 restriction enzymes (2.1.4.1) prior to ligation (2.1.4.2). The plasmids used for RNA production for microinjection were: RN3P-H2A.Z-EGFP, RN3P-H2A.ZNQ, RN3P-H2A, and RN3P-H2A.Z. Plasmids RN3P-H2A.ZNQ, RN3P-H2A, and RN3P-H2A.Z were sub-cloned from plasmids produced by D. Rangasamy (Ridgway et al., 2004a). RN3P-H2A.Z-EGFP plasmid was originally produced by P. Ridgway (Ridgway et al., 2004b).

2.1.2 Plasmids constructed for production of RNA probes for *in situ* hybridisation

RN3P plasmid and PCR produced inserts were digested by Kpn1 and BamH1 restriction enzymes (2.1.4.1) prior to ligation (2.1.4.2). Plasmids were designed as templates to produce anti-sense (AS) probes. Due to the location of the restriction digest sites used in creation of these plasmids, RNA probes for *in situ* hybridisation where neither 5'-capped nor contained the stabilizing β-globin 5' and 3' untranslated regions found in the RNAs for microinjection. The plasmids for probe production were: RN3P-H2A.ZAS, RN3P-XbraAS, RN3P-XMyoDAS, and RN3P-XbcanAS. All plasmid and insert sizes were confirmed by agarose gel electrophoresis (2.1.4.4) and restriction enzyme digestion (2.1.4.1). Inserted sequences for all plasmids were confirmed by DNA sequencing (2.1.4.6).

2.1.3 Polymerase chain reaction

Polymerase chain reactions (PCRs) were used to produce inserts for construction of plasmids and for semi-quantitative RT-PCR. PCRs used Platinum *Taq* Hi Fi (high

fidelity) polymerase (Invitrogen) as per the manufacturer's instructions except scaled to 20µl reaction size, and 1µl of dimethyl sulfoxide (DMSO) was included to prevent secondary structure formation in the RNAs. Reactions were performed on an iCycler thermocycler (BioRad). All oligonucleotide primers were from Proligo.

Primers for production of templates for reverse transcription (RT) to produce RNA probes for *in situ* hybridisation are given in Table 4. Lower case is used in the sequences to indicate flanking sequences added to original primer sequences to enable cloning and reverse transcription. The following PCR conditions were used for the production of all inserts: hold 1x 2min at 94°C, 25 cycles of 1min at 94°C, 2min at 55°C, 3min at 68°C, a final extension at 68°C for 10min, and then hold at 10°C.

Primer Set	**Sequences**	**Source**
XbraAS	XbraASF: 5' tttttt ggatcc gat gaa tca gta tg TAT ATC CAC CCA GAC TCA CCC 3' XbraASR: 5' tttccattt ggtacc GAT AGA GAG AGA GGT GCC CCG 3'	Modified from (Smith et al., 1991).
XMyoDAS	XMyoDASF: 5' tttttt ggatcc gat gaa tca gta tg AAC TGC TCC GAT GGC ATG ATG GAT TA 3' XMyoDASR: 5' tttccattt ggtacc ATT GCT GGG AGA AGG GAT GGT GAT TA 3'	Modified from (Hopwood et al., 1989).
XbcanAS	XbcanASF: 5' tttttt ggatcc gat gaa tca gta tg AAT CAG TAT GCC CCT GCT CTT TGA GAA CTG 3' XbcanASR 5' tttccattt ggtacc CAT TGG GGA TGC AGC TTG T 3'.	*Xbcan* primers were designed with Primer3 (Rozen and Skaletsky, 2000).

Table 4 **Oligonucleotide primers for constructing plasmid inserts for digoxigenin labelled RNA probe production for *in situ* hybridisation.** Lower case is used in the sequences to indicate flanking sequences added to original primer sequences to enable cloning and reverse transcription.

Primers for RT-PCR reactions are given in Table 5. Each reaction contained 2µl of cDNA produced from total RNA (2.5.2, 2.5.1). All PCR reactions in RT-PCR experiments included primers for the H4 internal control. All RT-PCR experiments included no reverse transcriptase (–RT) and no total RNA (–RNA) controls. PCR conditions used for all RT-PCR primers were as follows: 94°C for 2min; 34 cycles of 94°C for 30s, 58°C for 30s, and 68°C for 1min; then a final annealing step of 68°C for 15min before holding at 10°C until collection.

Primer set	Sequence	Source
H4	RTH4F: 5' CGG GAT AAC ATT CAG GGT ATC ACT 3' RTH4R: 5' ATC CAT GGC GGT AAC TGT CTT CCT 3'	(Gawantka et al., 1995; Niehrs et al., 1994)
Xbra	RTXBraF: 5' TAT ATC CAC CCA GAC TCA CCC 3' RTXBraR: 5' GAT AGA GAG AGA GGT GCC CCG 3'	(Smith et al., 1991)
XMyoD	RTXMyoDF: 5' AAC TGC TCC GAT GGC ATG ATG GAT TA 3' RTXMyoDR: 5' ATT GCT GGG AGA AGG GAT GGT GAT TA 3'	(Hopwood et al., 1989)
XVent2	RTXvent2F: 5' TGA GAC TTG GGC ACT GTC TG RTXvent2R: 5' CCT CTG TTG AAT GGC TTG CT	(Onichtchouk et al., 1996)
Gsc	RTGSCF: 5' AGG CAC AGG ACC ATC TTC ACC G 3' RTGSCR: 5' CAC TTT TAA CCT CTT CGT CCG C 3'	(Blumberg et al., 1991)
XH2A.Z	X385F: 5' ATG GCT GGA GGC AAG GCT GGC 3' X385R: 5' AGA CTG TTT TCT GTT GTC C 3'	(Ridgway et al., 2004a)

Table 5 **Oligonucleotide primers for RT-PCR**

2.1.4 Molecular cloning

2.1.4.1 Restriction Digests

Restriction digests were required to construct plasmids with the desired inserts. BamH1, Knp1 and Not1 (New England Biolabs) single digests, and BamH1/Not1 double digests were performed as per the manufacturer's instructions. Where DNA required BamH1 and Kpn1 digestion sequential digests were performed.

2.1.4.2 DNA Ligation

All ligations were performed with T4 DNA ligase (Invitrogen) as per the manufacturer's instructions. Briefly, purified and digested PCR product inserts and plasmid (1:5 ratio) were incubated in the supplied ligation buffer with 2.5U of T4 ligase at 16^{o}C for 12-16h.

2.1.4.3 Gel extraction for plasmid purification

Ligation products were checked for quality and quality of desired DNA and purified by agarose gel electrophoresis and agarose gel extraction using a QIAquick Gel Extraction Kit (Qiagen, catalogue number 28704).

2.1.4.4 Agarose gel electrophoresis

Agarose gel electrophoresis (Sambrook et al., 1989) was used to determine size of PCR, DNA ligation, plasmid amplification, and RT products. Briefly, electrophoresis used 1% agarose TAE gels electrophoresed at 90mV. Gels were stained with 1mgml^{-1} ethidium bromide (Sigma). DNA was visualised with short (most applications) or long (gel extraction) wavelength UV light.

2.1.4.5 Agarose gel extraction

DNA was excised from agarose gels with a scalpel blade and purified with a QIAquick Gel Extraction Kit (Qiagen catalogue number 28704) according to the manufacturer's instructions except that extracted DNA was eluted with Milli-pore purified water or DEPC (diethyl pyrocarbonate treated) water (Ambion).

2.1.4.6 DNA Sequencing

Sequencing reactions used the Big Dye Terminator mix (Applied Biosystems) and appropriate primers as per the manufacturer's instructions with the iCycler thermocycler (BioRad). DNA sequencing was performed with the ABI 3730 cycle sequencing system according to the manufacturer's instructions (Applied Biosystems). Electrophoresis of sequencing reaction products and automated sequence data collection was performed by the staff of the Australian Cancer Research Foundation (ACRF) Biomolecular Resource Facility (BRF).

2.1.4.7 Preparation of electrocompetent *E. coli* bacterial cells

Stock *E. coli* DH5α cells (in 10% glycerol) were streaked onto Luria Broth (LB) agar plates and incubated for 12-16h at 37^{o}C with agitation. A single colony was selected and used to inoculate 10ml LB. The culture was incubated for 12-16h at 37^{o}C. This starter culture was diluted 1:100 into 250ml of LB and incubated at 37^{o}C with 250rpm agitation until OD_{600} reached 0.5 to 1.0 Absorbance (Abs). Cultures were centrifuged at 2800g (6000rpm) and 4^{o}C for 15min in a Sorval RC5C centrifuge. The pellets were washed twice in 250ml of ice cold sterile MilliQ filtered water, centrifuged at 2800g

(Sorvall RC5C centrifuge with SLA 3000 rotor at 6000rpm) and 4^{o}C for 15min. The pellet was resuspended in 10% sterile glycerol (10ml), centrifuged at 6500g for 10min at 4^{o}C (SS34 rotor at 7000rpm) and the pellet resuspended in 1ml of 10% glycerol. 50µl aliquots were stored at -70^{o}C. Competency was determined by electroporation of a serial dilution of plasmid DNA.

2.1.4.8 Transformation of electrocompetent *E. coli* bacterial cells

Electrocompetent cells (50µl) were thawed on ice and mixed with supercoiled plasmid (1µg in 20µl water) and electroporated in the Gene Pulser II (Biorad) (capacitance 25µF, 2.5kV, Pulse Controller Plus set to Low Range 200 Ohms). The cells were transferred to 1ml LB for 1h at 37^{o}C before selection on LB ampicillin (100µgml^{-1}, Sigma) agar plates.

2.1.4.9 Plasmid amplification

Transformed E. coli were cultured in 5ml of LB ampicillin (100µgml^{-1}, Sigma) at 37^{o}C for 12-16h to produce a starter culture. This was used to inoculate 200ml LB ampicillin (100µgml^{-1}, Sigma) cultures grown at 37^{o}C for 12-16h. Purification of plasmids from bacterial cultures was achieved by either the QIAfilter Plasmid Mini Purification Kit (Qiagen catalogue number 12123) or QIAfilter Plasmid Maxi Purification Kit (Qiagen catalogue number 12262) as per the manufacturer's instructions. Plasmid DNA was stored in TE buffer (10mM Tris, pH 7.5, and EDTA pH 8.0) at -20^{o}C.

2.2 *In vitro* transcription

RNA for microinjection was prepared as previously described (Ridgway et al., 2004a; Zernicka-Goetz et al., 1996). Briefly, template plasmids for the production probe RNA were linearised by restriction digestion with Kpn1 (2.1.4.1). Linearised DNA templates were purified with the QIAquick PCR Purification Kit as per manufacturer's instructions with a final elution in 30µl of MilliQ water. Reverse transcription reactions

used T3 RNA polymerase (Fermentas) as per the manufacturer's instructions with DTT to prevent formation of RNA secondary structures, Human Placental RNase Inhibitor (HPRI) (Fermentas) as a precaution against degradation, and RNA cap analog (Ambion) (10mM) that adds a 5' cap structure to the RNA to ensure efficient translation after injection (Krieg and Melton, 1984). RT products were extracted with an equal volume of phenol/chloroform/isoamyl alcohol (Sambrook et al., 1989) and purified with Sephadex G-50 spin columns (Roche) to remove unincorporated nucleotides as per manufacturer's instructions. Concentration and quality of RNA was determined spectrographically (2.2.1) and by gel electrophoresis (2.1.4.4). RNA was stored in 3µl aliquots at -70^{o}C.

Production of digoxigenin labelled RNA probes for *in situ* hybridisation was conducted similarly with the following exceptions: 10mM DIG-NTP mix (with digoxigenin-11 UTP (Boehringer Mannheim) (1:10dilution of 100mM stock containing 10µl of 100mMof CTP, GTP, ATP, and 6.5µl of 10mM UTP and 3.5µl of 10mM of digoxigenin-11 UTP) replaced the standard NTP mix; and T7 RNA polymerase (Fermantas) was used instead of the T3 RNA polymerase. These changes produced digoxigenin labelled probes antisense to the endogenous mRNA targets.

2.2.1 Determination of nucleic acid concentration

Concentration of nucleic acids (DNA or RNA) in solution was determined by spectrophotometry utilising standard methods (Sambrook et al., 1989). Concentrations were calculated from optical density (OD) at 260nm. RNA quality was determined by 260/280 OD ratio (Sambrook et al., 1989).

2.3 *X. laevis* as a model animal

X. laevis has several advantages as a vertebrate system for developmental studies. Firstly, it is easy to maintain and handle. Egg laying can be induced by a simple hormone injection at any time of the year and eggs can be fertilised *in vitro* (Sive et al., 2000). The embryos produced can be monitored in a culture dish, are large in size and develop rapidly. Each developmental stage is well characterised and standard developmental tables were use to stage embryos throughout this project (Nieuwkoop and Faber, 1994). The chief disadvantages of the species are the long generation time and pseudo-tetraploidy (Sive et al., 2000). These will not impact on the techniques utilised within this project.

2.3.1 *In vitro* fertilization and culture of *X. laevis* embryos

X. laevis embryos were obtained from *in vitro* fertilisation of eggs and cultured according to standard protocols (Ridgway et al., 2004b; Sive et al., 2000). Briefly, Female *X. laevis* were injected in the dorsal lymph sac with 1000 IU in 300µl of chorionic gonadotrophin and left overnight. A male was sacrificed by cervical dislocation and the testes surgically removed and stored at 4^{o}C for up to 48 hours in OR2 media (Sive et al., 2000). Females were manually induced to lay eggs into a glass Petri dish and the eggs were fertilised with mashed testes for five minutes. Eggs were then covered with 0.1x MBSH (Modified Barth's Saline with HEPES (Sive et al., 2000)) and left to stand until cortical rotation was complete (approximately 30-40min). Jelly was then digested from the eggs by washing with 2% L-cysteine/HCl 0.1x MBSH pH7.8. Fertilised eggs were then rinsed at least four times with 0.1x MBSH before incubation in 0.1x Marc's Modified Ringer's solution (MMR (Sive et al., 2000)). Embryos were typically cultured at 18^{o}C and staged by the normal development tables (Nieuwkoop and Faber, 1994).

For TSA treatment embryos were cultured using standard techniques (2.3.1, (Sive et al., 2000)) with TSA (final concentration 5μM) added to the 0.1x MMR media as described previously (Almouzni et al., 1994; Xu et al., 2000). Media was changed daily and culture dishes wrapped in foil to avoid degradation of TSA by light.

2.3.2 mRNA microinjection

Microinjection of embryos was to a single blastomere at the two cell stage as described previously (Almouzni and Wolffe, 1995). Briefly, RNA for injection was produced by *in vitro* transcription (2.2), embryos in 1x MMR with 6% Ficoll (Sigma) were injected with 1ng of RNA in 9.2nl of injection buffer (15mM HEPES KOH (pH 7.6), 88mM NaCl) using the Nanoject injection system (Drummond) while viewing under the MZFL III microscope (Leica). After injection salt and Ficoll concentrations were progressively reduced to 0.1MMR over approximately 5 hours.

2.4 Whole mount *in situ* hybridisation

Embryos for *in situ* hybridisation were fixed in MEMFA (0.1 M MOPS (pH 7.4), 2mM EGTA, 1mM MgSO4, 3.7% formaldehyde) as described previously (Harland, 1991; Sive et al., 2000), except embryos were stored in ethanol rather than methanol. Whole mount *in situ* hybridisation was performed as described previously (Hayward et al., 2001), except without xylene for removal of lipids and hydrolysis of probes was unnecessary due to the short length (≤400nt) of the probes (Sive et al., 2000). Embryos were collected and immediately fixed in MEMFA before dehydration in an ethanol series and stored in ethanol at -20^{o}C. Embryos stored in ethanol were rehydrated by serial 2-5min washes with 75%, 50% and 25% ethanol PBT (phosphate buffered saline with 0.1% v/v Tween 20) and finally PBT. Embryos were then permeablised with radio-immuno-precipitation assay buffer (RIPA) (Rosen and Beddington, 1993) overnight at

4°C, rinsed with PBS then PBT and transferred to 1 part PBT: 1 part hybridisation buffer for 10min. After final equalisation with hybridisation buffer at 57°C, probes were hybridised at 57°C for at least 48 hours. Embryos were then rinsed, washed several times (30 min, overnight, then for 20min) at 57°C in hybridisation wash. Embryos were equalised to PBT then washed in PBT. Hybridised embryos were then incubated with anti-digoxygenin Fab fragments (Roche) (1:1600) in PBT for 4h at room temperature before washing in PBT. Following this wash they were rinsed with Tris 0.1M pH 9.5 then in alkaline phosphatase buffer. For detection 5-Bromo-4-chloro-3-indolyl-phosphate/nitro blue tetrazolium (Sigma) or BM Purple (Roche) was used as the colour substrate. Embryos were dehydrated in a series of glycerol solutions of increasing concentration and stored in 70% glycerol. Alternately, embryos were dehydrated in a series of ethanol solutions of increasing concentration and transferred to 1:2 benzyl benzoate, benzyl alcohol (BB: BA). A MZFL III microscope with IM50 software (Leica) was used for image capture.

2.5 Gene expression analysis

2.5.1 Total RNA extraction from whole embryos

RNA extraction for RT-PCR and RT real-time PCR was conducted as follows. For each sample, ten embryos were collected and immediately homogenised by pipetting in 150µl of RNALater (Ambion) and transferred to 4°C. Samples where extracted in 1500µl of Trizol (Invitrogen), as per the manufacturer's instructions, except that a volume of Trizol ten times that of the RNALater was used as recommended (Ambion). The extracted RNA was isopropanol precipitated (Sambrook et al., 1989) and redissolved in DEPC water (Ambion). Samples were treated with TURBO DNase (Ambion) according to manufacturer's instructions to remove any genomic DNA

(gDNA) contamination. DEPC treated water (Ambion) was used throughout and standard precautions to prevent RNase contamination including using fresh bench cover, regularly changing gloves and use of RNase Zap RNase inhibitor (Ambion) were taken. RNA quality and concentration were assessed by standard gel electrophoresis (2.1.4.4) and spectrographic methods (2.2.1). 3µl aliquots were frozen in liquid nitrogen and stored at -70^{o}C.

2.5.2 Reverse transcription

Reverse transcription (RT) for RT-PCR and RT real-time PCR was performed using the by Super Script III enzyme system (Invitrogen) was as per the manufacturer's protocols, with anchored oligo $d(T)_{15}$ (3.5µM final concentration) (Sigma) as primers and 1µg of total RNA template in a 20µl reaction. cDNAs were stored at -20^{o}C.

2.5.3 Densitometry of PCR products

To perform densitometry, 10ul of PCR products were subjected to standard agarose gel electrophoresis (1% agarose, 90V, 85 min) with ethidium bromide staining, except that samples were loaded with Orange G loading dye (Becker et al., 1996). Low Mass DNA ladder (Invitrogen) was also included in each gel. Imaging was by the Gene Genius bio imaging system (Syngene). Quantification was performed with the GeneTools program (Syngene) using manual band selection, automatic background correction, and calibrated against the DNA low mass ladder (Invitrogen). The resulting data was normalised against matching *H4* internal standards to produce results in units relative to *H4* mRNA levels and normalised to a reference sample.

2.5.3.1 Calibration of RT-PCR

To ensure the amount of product obtained from the RT-PCR was proportional to the concentration of mRNA in the total RNA original sample two calibration experiments were carried out for each primer pair. In the first experiment samples were collected

after different numbers of cycles and densitometry performed (2.5.3). From these results a number of cycles from those within the linear portion of the curves for all primers (34 cycles) was chosen. To ensure that the amount of PCR product from the selected number of cycles was proportional to the concentration of mRNA a serial dilution experiment was performed for each primer pair and densitometry performed.

2.5.4 RT real-time PCR

2.5.4.1 Real-time PCR conditions and primers

Primers for RT real-time PCR given in Table 6 were designed with Primer3 (Rozen and Skaletsky, 2000), selecting primers with product lengths of 100-250bp, melting temperature (Tm) ~60^{o}C, 40-50% GC content, and primer lengths under 22nt. All primers were manufactured by Proligo.

Primer Set	Sequences
H4	RLTH4F 5'ATA ACA TCC AGG GCA TCA CC 3' RLTH4R 5' ATC CGT ACA GAG TGC GTC CT 3'
H2A.Z	RLTH2A.ZF 5' CTG GCA AAG ATA CCG GAA AA 3' RLTH2A.ZR 5' TTC CAG CCA ATT CAA GAA CC 3'
Gsc	RLTGscF 5' CGA AGA GCA AAA TGG AGG AG 3' RLTGscR 5' GCA TCC AGC TAT CCC AAT GT 3'
Xbra	RLTXbraF 5' GAG CAT GGA GCA CAA ACA GA 3' RLTXbraR 5' CAA TTC AGG CCC AGG AAA TA 3'
MyoD	RLTMyoDF 5' GCT GGT TGC TGA ATT TCC AT 3' RLTMyoDR 5' TCA ACA CAA CAT TGG CAG GT 3'
Dsh	RLTDshF 5' ATT TAT TGC TGC CCC TTC CT 3' RLTDshR 5' GGT GGG CTT CCC ATT CTT AT 3'

Table 6: **Oligonucleotide primers for RT-PCR**

RNA extraction and cDNA production were as previously described (sections 2.5.1 and 2.5.2). Reactions used SYBR Green JumpStart *Taq* ReadyMix (Sigma-Aldrich) according to the manufacturer's instructions adjusted for 20µl reaction volumes. Every experiment included an –RT sample for each primer set as a negative control and sample matched reactions with H4 primers. All reactions were performed in triplicate. Templates were cDNA produced from 1µg of total RNA. Experiments were conducted in the ABI PRISM 7700 Sequence Detection System (Perkin Elmer/Applied

Biosystems) using the software supplied with the instrument. Reaction conditions were 40 cycles of: 95°C for 15 seconds, 60°C for 15 seconds, and 95°C for 15 seconds. Dissociation curves were examined after each run to ensure unexpected products from contaminants were not present.

2.5.4.2 Analysis of real-time PCR data

Analysis of real-time PCR data was based on methods described in the ABI PRISM 7700 Sequence Detection System Instrument Manual (Perkin Elmer/Applied Biosystems). Real-time PCR produces results in cycles at threshold (Ct) which is the number of cycles at which the level of fluorescence reaches an arbitrary threshold. Baseline fluorescence (the mean fluorescence over a set range of cycles before product amplification is judged to have reached a detectable range) is subtracted from all results. For the first experiment for each primer set the start of the range of cycles for the calculation of baseline was set at three (default) and the end of this range at cycles equal to the lowest Ct in the experiment minus two (using the default threshold calculated by the ABI PRISM 7700 Sequence Detection System). The start and stop numbers of cycles for calculation of baseline and the threshold level was recorded for each primer pair and used in subsequent experiments. Data was exported to Excel (Microsoft) for further analysis.

In summary, further analysis of the data (adapted from (Applied_Biosystems, 2004)) was as follows: All reactions were in triplicate. If the Ct's from a triplicate were more than 0.6 cycles apart data from that triplicate was discarded. The mean Ct from each of the remaining triplicates was calculated. Relative expression compared to *H4* expression was calculated for each sample ($2^{(Ct-CtH4)}$). This result was divided by the fold expression compared to *H4* of a reference sample (i.e. $(2^{(Ct-CtH4)})_{test}/(2^{(Ct-CtH4)})_{ref.}$).

Final results are therefore arbitrary units relative to a reference sample and *H4* expression.

2.5.5 Statistical Analysis

The probability (p), determined by a two tailed Student's t-test, was used to determine whether treatment groups were significantly different (Student, 1908). P is the likelihood that two samples are actually taken from the same population. Therefore, the lower the p value, the more likely that the difference in means is significant. Generally, in the biological sciences, p values of 0.05 or less are considered to be sufficiently unlikely to be due to chance and thus reflect a real difference between the two groups.

2.6 Regulatory Considerations

All protocols involving recombinant DNA were in accordance with the regulations of the Genetic Manipulation Advisory Committee and the Australian National University Council and had the approval of those authorities.

Importation and subsequent laboratory work involving *X. laevis* was in accordance with and approved by the Australian Quarantine Inspection Service (AQIS) (facility numbers: A0049 and A1265, transfer approval number 2006/006) and performed by licensed individuals. Protocols utilising *X. laevis* also had the approval of Animal Experimentation Ethics Committee (AEEC) (approval number J.MB.29.06) of the ANU and conformed to the ACT Animal Welfare Act (1992) and the NHMRC Australian Code of Practice for the Care and Use of Animals for Scientific Purposes.

3 Temporal and spatial expression of *H2A.Z* mRNA during early *X. laevis* development

3.1 Introduction

While it is well established that H2A.Z is essential for metazoan development (Clarkson et al., 1999) (as discussed in section 1.4), determining the function of H2A.Z during development requires further investigation. Disrupting H2A.Z function in *C. elegans* prevents proper digestive tract development (Updike and Mango, 2006) (discussed in section 1.4.1). In *D. melanogaster* mutations in the region of H2Av containing the histidine motif (named region M7 in Clarkson's 1999 publication) is 'partially' lethal (Ridgway et al., 2004a) (see section 1.4.2). A proportion of embryos survive until the pupal stage, however 81% did not eclose indicating that development is defective during or prior to pupation (Clarkson et al., 1999). However, the defects in the M7 rescued *D. melanogaster* were not fully characterised in that investigation. Given this evidence, and considering that the histidine motif is highly conserved (discussed in section 1.4.6), we hypothesised that the histidine motif of H2A.Z has a conserved developmental function (Ridgway et al., 2004a). An important process in the life of the early vertebrate embryo is gastrulation. Therefore, this study was focused on the potential role of H2A.Z in gastrulation. In this chapter our objective was to determine if the spatial and temporal expression of H2A.Z correlated with gastrulation and formation of mesodermal tissues.

3.1.1 Overview of *X. laevis* development to gastrulation

In this section an overview of early development in *X. laevis* is presented as background to investigations of the role H2A.Z during this period.

3.1.1.1 Early cleavage divisions

In *X. laevis* the first twelve divisions are fast, synchronous, proceed without transcription or gap phases (Graham, 1966; Newport and Kirschner, 1982) and are reliant on maternal protein stores (Earnshaw et al., 1980; Prioleau et al., 1994). These are termed cleavage divisions (Prioleau et al., 1994). There is no cell motility during this period (Newport and Kirschner, 1982). During these divisions cytoplasmic bridges connect sister blastomeres enabling some cytoplasm to be exchanged (Dale and Slack, 1987a). Embryos of 16-64 cells are sometimes called morula even though recent observations have determined a minute blastocoel is present following the first cell division. Following these first twelve divisions the mid-blastula transition (MBT) is reached after which the cell cycle and transcriptional activity of the blastomeres becomes progressively more somatic.

3.1.1.2 Mid-blastula transition

The mid-blastula transition (MBT) occurs at stage 8 on the standard developmental tables and marks the beginning of zygotic transcription (Newport and Kirschner, 1982) (see section 1.3), the introduction of the G1 phase to the cell cycle (Newport and Kirschner, 1982), desynchronised cell cycles (Bachvarova and Davidson, 1966), and the first instances of cell motility (Dale and Slack, 1987a). Asynchronous divisions produce an outer layer of cells and ‘deep’ cells beneath.

Enabled by the patterns of determinants laid down shortly after fertilisation (Miller et al., 1999; Weaver et al., 2003), further cell fate determinations and chromatin remodelling occur in the blastula during this period (Chalmers, 2003; Prioleau et al.,

1994). For example, by late blastula the deep cells are receptive to neuronal development signals while the superficial cells are unresponsive (Chalmers, 2003). Correlated with these changes is a transition from totipotency to pluripotency (Kikyo and Wolffe, 2000).

3.1.1.3 Gastrulation and mesoderm formation

Shortly after the MBT (stage 10) the process of gastrulation begins with the formation of the blastopore lip (Dale and Slack, 1987a) (Gerhart and Keller, 1986; Winklbauer, 1990). During gastrulation processes that determine cell fate and movement in the blastula continue to be refined. At the dorsal side the blastopore lip forms and the edge of the blastopore spreads from this point to encircle the vegetal pole. A portion of the marginal zone of the embryo involutes through this pore to create a third layer of tissue, the mesoderm. Concurrently, the pore constricts until the ectoderm covers the entire surface of the embryo (Dale and Slack, 1987a). Meanwhile, the mesoderm within the embryo (endomesoderm) continues to differentiate. The first cells to involute form the prechordal mesoderm and migrate to form head mesodermal tissues (Winklbauer, 1990). Cells that involute after this become chordamesoderm that forms the notochord and other dorsal structures (Gerhart and Keller, 1986; Winklbauer, 1990). From stage 10.5 cells of notochord fate undergo convergent extension to lengthen the embryo along the anterior-posterior (A-P) axis (Keller et al., 1992). These processes of cell fate determination and cell movement must proceed correctly if normal development is to occur.

3.1.2 Expression and localisation of *H2A.Z* mRNA in early *X. laevis* development

Histone variants often have developmentally regulated expression (see 1.3). Levels of H2A.Z transcripts have previously been shown to rise sharply in the ‘gastrula’

compared to the 'blastula' (Iouzalen et al., 1996), however, exact developmental stages were not specified. The initial description of H2A.Z in *X. laevis* failed to detect *H2A.Z* mRNA before gastrulation (Iouzalen et al., 1996). In light of results from the mouse zygote (Rangasamy et al., 2003) (see section 1.4.3) it seemed likely that low levels of H2A.Z expression should be found in the early zygote, prompting investigation of pre- and post MBT blastulae. My objective was to temporally measure the precise level of the *H2A.Z* transcripts to extend and clarify the earlier result.

3.1.3 Experimental approach

To investigate the hypothesis 'hypothesis that H2A.Z is important for correct gastrulation and mesodermal formation in early *X. laevis* development' I sought to determine whether changes in H2A.Z expression level and localisation in normal embryos correlates with important developmental events. Semi-quantitative RT-PCR and real-time PCR provided quantitative evidence of the levels of *H2A.Z* mRNA in whole embryos at different stages of development. As well as quantitative changes to H2A.Z there might also be accumulation of endogenous H2A.Z in specific tissues where it has specific function(s). Therefore, localisation of *H2A.Z* mRNA within the embryos was determined by *in-situ* hybridisation.

The developmental stages chosen for investigation represent key periods in early development that are disrupted in the dominant-negative treated embryos. Stages 5 and 9 flank the mid-blastula transition. Stages 10 and 12 follow the progress of the embryo through gastrulation. Stages 20 and 33/34 were chosen as a representative of later stage embryos when the H2A.Zdn defect is very apparent and development of the notochord elongates the trunk. If my hypothesis is correct then endogenous H2A.Z would most likely be enriched in involuting and mesodermal tissues during gastrulation (developmental stages 9 to 13) and possibly in later mesodermal tissues. Determining

temporal and spatial distribution of *H2A.Z* mRNA during these developmental stages was the first step in testing the hypothesis.

3.2 Results

3.2.1 *H2A.Z* mRNA levels in the early embryo

For semi-quantitative RT-PCR the amount of PCR product should be proportional to the amount of target mRNA. To ensure this was the case serial dilutions were performed. The result of the serial dilution experiment for H2A.Z is given as an example (Figure 10). This figure clearly shows that the amount of PCR product is proportional to the amount of total mRNA in the sample.

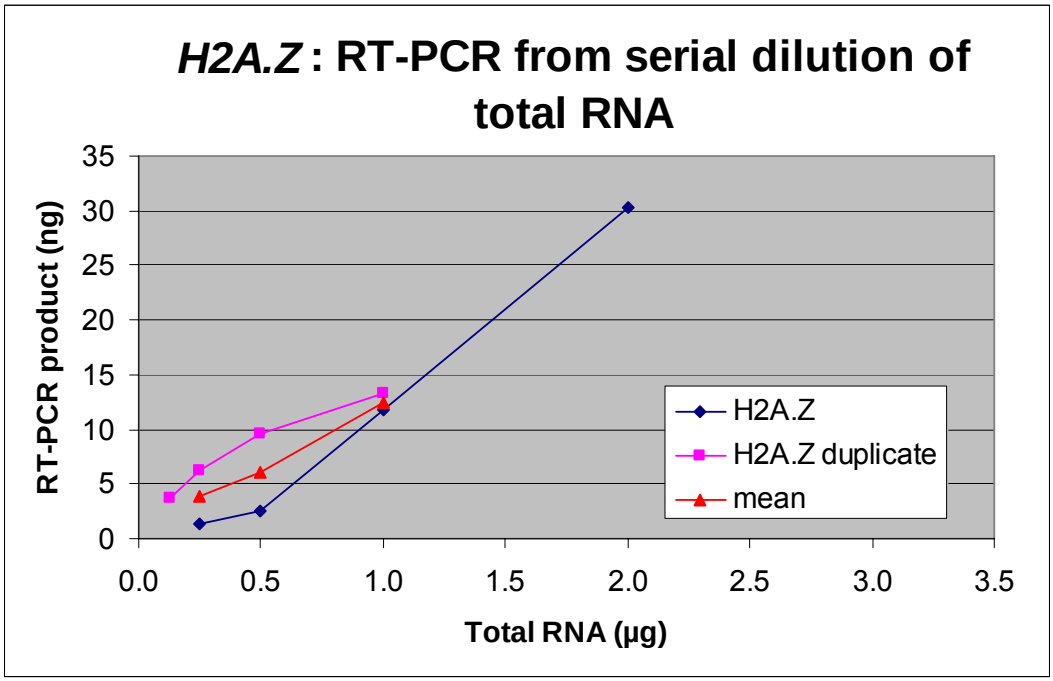

Figure 10 ***H2A.Z* serial dilution**. A serial dilution of total RNA was performed and RT-PCR performed at a number of cycles (34) within the linear range. Mass of PCR product (ng) was determined by densitometry (2.5.3). Dilution is given in fold concentration compared to the amount of mRNA used in later experiments (1µg RNA from 10 embryos). Duplicate experiments and mean (red) are shown.

These initial experiments used semi-quantitative RT-PCR to investigate the levels of *H2A.Z* mRNA expression during early development. Figure 11 shows a typical gel from

these experiments. Two different concentrations of a Low Mass DNA ladder were used as indicators of band sizes and as standards for quantitation. A –RNA control demonstrates that the reagents were free of contamination and a –RT control demonstrates that the samples are free of genomic DNA. A serial dilution of a stage 12 sample demonstrates that linear amplification from different concentrations of template is occurring. This gel has *H2A.Z* (385bp) and *H4* (188bp) PCR products amplified from cDNA derived from embryos of stages 5, 8, 10, 12 and 20. H4 was used as an internal standard as *H4* mRNA levels are stable throughout this period of development (see Figure 13, section 3.2.2), and are a commonly used standard in *X. laevis* work that investigates mRNA levels of genes during early development (Aybar et al., 2003; Onichtchouk et al., 1996; Panitz et al., 1998). It can be seen from Figure 11 that *H2A.Z* mRNA is present at all the developmental stages investigated.

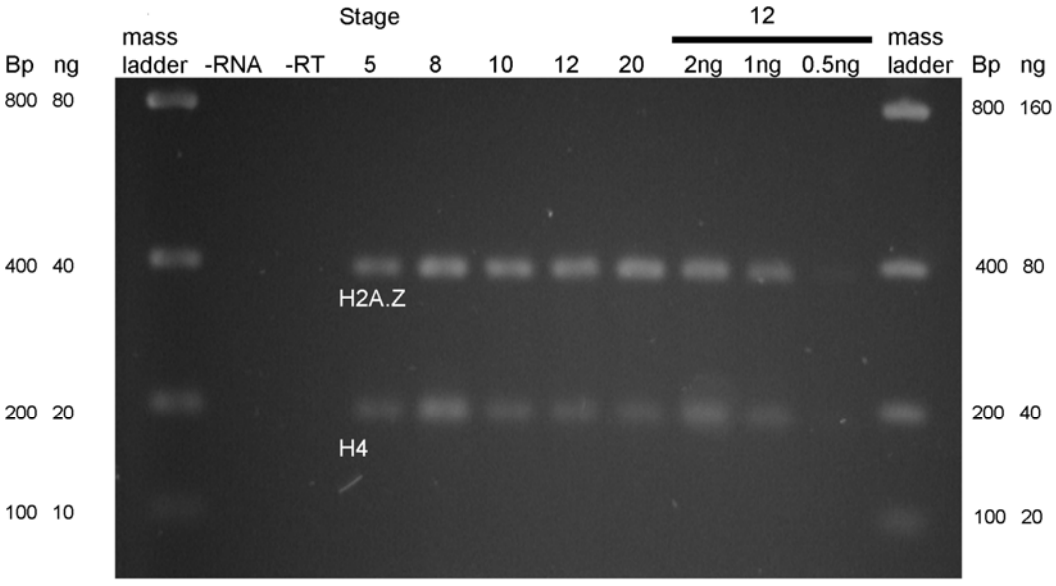

Figure 11 ***H2A.Z* RT-PCR gel example**. Numbers above the lanes indicate developmental stage. The upper band is the amplicon from *H2A.Z* and the lower from the *H4*. The DNA mass ladder has known amounts of DNA in each band as indicated. During densitometry the automatic background feature of the GeneQuant software compensates for the variable background in different region of the gel. A serial dilution of a stage 12 sample is illustrated at right.

Densitometry was performed on the gels; the results are given as Figure 12. This figure gives the mean expression of *H2A.Z* relative to endogenous *H4* at developmental stages 5, 8, 9, 10, 12, 14, 16 and 20. Where the number of samples in a given stage is sufficient to allow calculation, error bars are given for standard error of the mean (SEM). *H2A.Z* mRNA is at its lowest level at stage 5, after this a moving mean line of best fit trend line shows that levels rise sharply to the onset of gastrulation (stage 10) and remains above pre-gastrulation levels though to the tailbud stage. The detection of *H2A.Z* mRNA here was supported by later *in-situ* hybridisation results (see 3.2.3). In summary *H2A.Z* mRNA was shown to be present at every stage of development investigated and levels rose sharply before gastrulation.

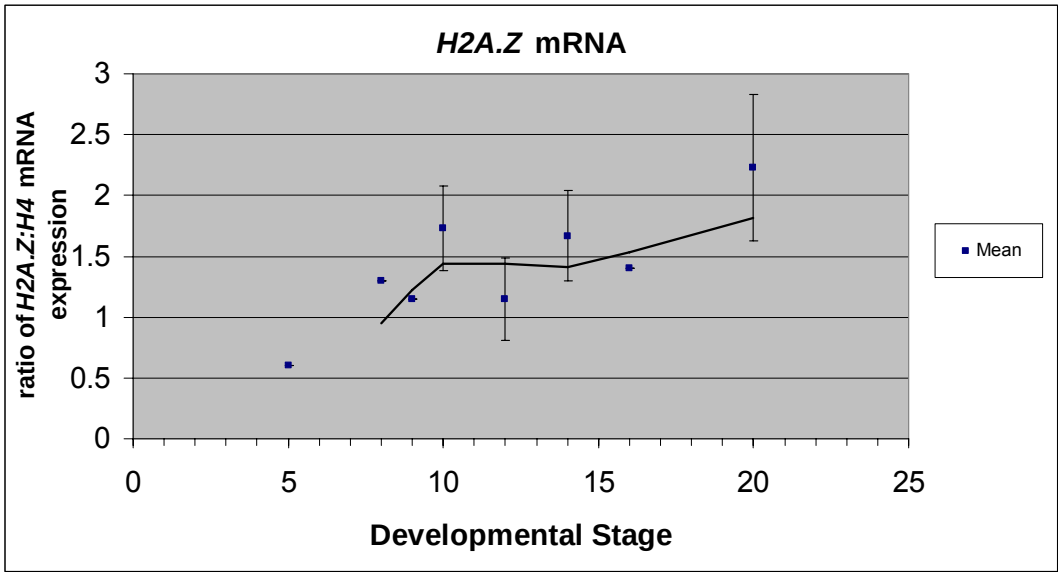

Figure 12 **Endogenous *H2A.Z* mRNA expression**. X axis units are relative to result from 1µg stage 10 wild type total RNA with *H2A.Z* normalised to an *H4* internal control as discussed in 2.5.3.1. Blue squares indicate the mean. Where applicable error bars are given as standard error of the mean. Black line is a moving mean line of best fit. Number of repetitions was three for stages 5, 9, 10, and 14; four repetitions for stages12 and 20. Stages 5 and 19 have no error bars as these stages had only two repeats each. Stages 8 and 16 have no error bars as these where single samples.

The results of these experiments are generally consistent with previous work in the literature. Stage 5 is during the early cleavage divisions before the initiation of zygotic transcription therefore mRNA detected at this stage must be of maternal origin (Prioleau

et al., 1994). After the MBT (stage 8) transcript levels in the whole embryo were higher, most likely indicating zygotic transcription of *H2A.Z* mRNA (Iouzalen et al., 1996). The previous investigation of *H2A.Z* mRNA expression in early *X. laevis* embryos failed to detect *H2A.Z* mRNA in morula (stages 4-6) and blastula (stages 7-8) embryos by northern blot, concluding that maternal stores were exhausted in the zygote (Iouzalen et al., 1996). The reason for this discrepancy may be the higher sensitivity of the PCR-based methods used here. It is significant to note that this is the first report of *H2A.Z* mRNA in the pre-MBT *X. laevis* embryo. This may reflect the requirement for low levels of H2A.Z to maintain its structural role in chromosome segregation. These results also detected low levels of mRNA during the cleavage stages, supporting the suggestion that maternal stores are becoming depleted (Bachvarova and Davidson, 1966). The increase in *H2A.Z* mRNA at the MBT matches the timing of activation of transcription in mesoderm and endoderm (Iouzalen et al., 1996). This supports a role for H2A.Z in either or both of these tissues. In summary, *H2A.Z* mRNA is detected at low levels in the early blastula consistent with depletion of maternal stores (Bachvarova and Davidson, 1966) then rises after the MBT consistent with the onset of zygotic transcription in the endoderm and mesoderm (Bachvarova and Davidson, 1966; Iouzalen et al., 1996).

The error bars indicate that there was a great amount of variability in the measurements of *H2A.Z* mRNA levels obtained using RT-PCR. This variability prompted the change to a different technique leaving the number of data points for some stages of development investigated by RT-PCR very small. Having determined that *H2A.Z* mRNA rises sharply at gastrulation I proceeded to confirm this result with a more precise technique.

3.2.2 Determining *H2A.Z* mRNA levels by RT real-time PCR

After the repeat experiments using the semi-quantitative RT-PCR for *H2A.Z* (3.2.1 above) and other developmentally important genes (see section 4.2.1.2) showed a great deal of variability in the data a more precise method was sought, and RT real-time PCR was chosen (Klein, 2002). RT real-time PCR is a sensitive technique for determining the level of specific mRNAs within samples.

3.2.2.1 Real-time PCR optimisation

Before RT real-time PCR could be used to determine the levels of *H2A.Z* mRNA at selected stages of development the technique needed to be optimised for this system. The first step in optimisation was to determine if the selected internal standard gene was suitable. The canonical histone *H4* is commonly used as an internal control in RT-PCR and real-time PCR analysis of early development in *X. laevis* (Aybar et al., 2003; Onichtchouk et al., 1996; Yokotal et al., 1995). To confirm that *H4* is a suitable control under the conditions of our protocol, Ct values across the investigated developmental stages were compared (Figure 13). An explanation of Ct values can be found in chapter 2 (2.5.4.2). There was little variation found in *H4* mRNA levels between the stages investigated (Stages 9, 10, 12 and 20, Figure 14) and between individual stages and the combined data from all stages (far right, Figure 14). Therefore *H4* was determined to be an appropriate gene to use as an internal control for the stages of development investigated.

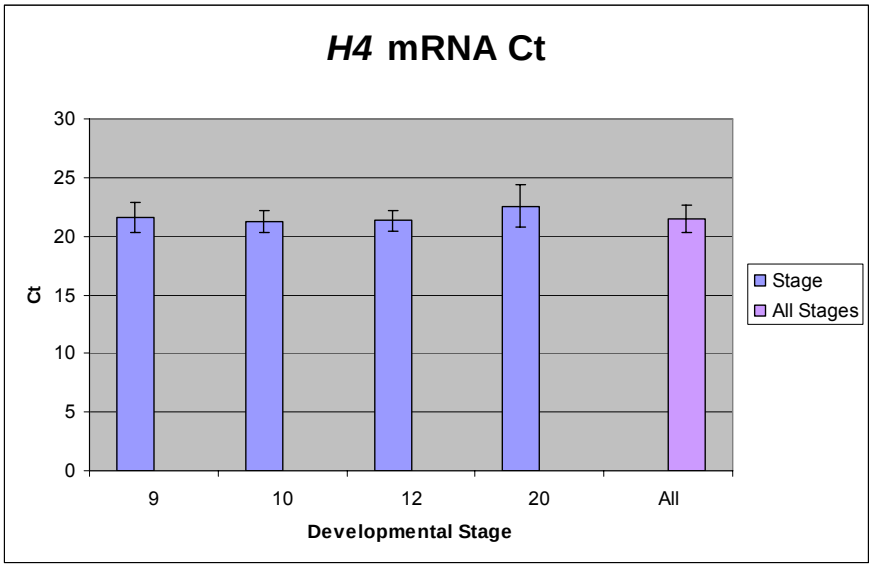

Figure 13 ***H4* is an appropriate internal control**. Error bars show standard deviations. 'All' is the mean of all the individual data points for H4 at all stages from all experiments.

As a positive control for the RT real-time PCR analysis, *MyoD* mRNA levels in trichostatin A (TSA) treated embryos were compared to untreated embryos (Figure 14). It has been shown previously that TSA treatment greatly represses *MyoD* mRNA transcription after gastrulation (Steinbach et al., 2000).

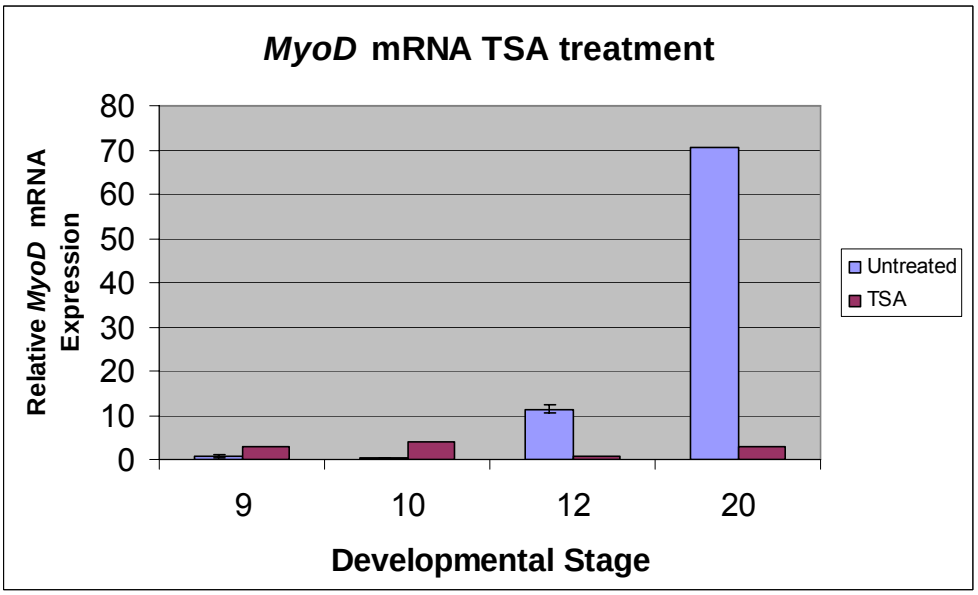

Figure 14 **TSA treatment represses *MyoD* expression**. Untreated results for stage 9, 10 and 12, n = 3, 4, and 8 respectively, All others n=1. Where applicable error bars from the mean indicate SEM. Data is given as expression relative to *H4* and a reference sample at stage 9 as described in 2.5.4.2.

As expected, *MyoD* mRNA levels in TSA treated embryos are greatly reduced compared to untreated controls (Figure 14). This preliminary experiment indicates that the real-time PCR technique was effective and that experiments to determine endogenous *H2A.Z* mRNA levels could proceed.

3.2.2.2 Endogenous *H2A.Z* mRNA levels peak at gastrulation.

Having optimised the RT real-time PCR technique, the level of endogenous *H2A.Z* mRNA at selected stages of development was determined. Embryo stages were selected to investigate *H2A.Z* mRNA levels during gastrulation and to confirm the elevated levels in neurula stage embryos. Stage 9 represents embryos just prior to gastrulation. Stage 10 represents the onset of gastrulation, and stage 12 the late gastrula after the peak seen in the RT-PCR data. Stage 20 is a post-gastrula stage that RT-PCR results indicated may also have elevated *H2A.Z* mRNA levels (see Figure 12).

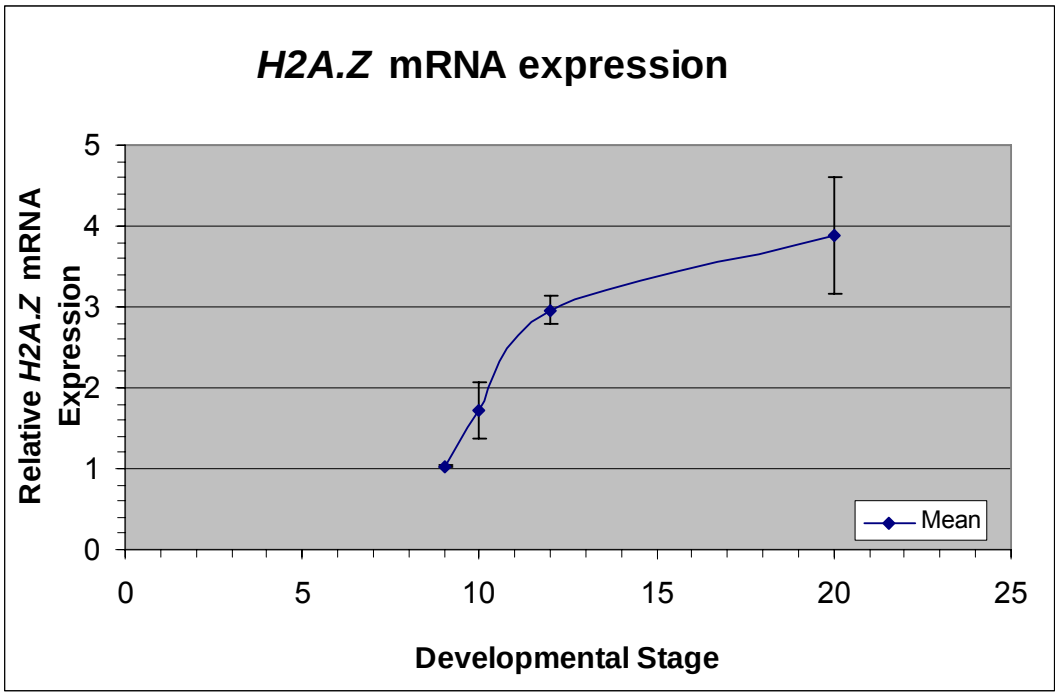

Figure 15 ***H2A.Z* mRNA levels rise at gastrulation** Filled blue squares indicate the means. Error bars from the mean indicate SEM. Data is given as expression relative to H4 and a reference sample at stage 9 as described in 2.5.4.2. Results for stages 9 and 20 are from three repetitions while results for stages 10 and 12 are from three repetitions.

The real-time PCR (Figure 15), like the RT-PCR, indicates a sharp rise in *H2A.Z* mRNA at the onset of gastrulation. Unlike the previous experiments, here *H2A.Z* mRNA continues to rise at stage 12. These results also confirm that *H2A.Z* mRNA is at higher than pre-gastrulation levels in late neurula (stage 20) embryos.

3.2.3 *H2A.Z* mRNA localisation during development

3.2.3.1 *H2A.Z* mRNA is enriched in a subset of blastomeres at stage 5

As already noted, in the mouse H2A.Z levels rise when differentiation begins (Rangasamy et al., 2003). Mouse H2A.Z is enriched in differentiated cells relative to the inner cell mass (Rangasamy et al., 2003). This raises the question of whether in the frog H2A.Z is found in all cells, differentiated cells, or only cells of particular lineages. Since previous northern blot analysis failed to detect *H2A.Z* transcripts in the pre-MBT blastula (Iouzalen et al., 1996), localisation of mRNA during these early stages remained unknown. For this reason I performed *in situ* hybridisation for *H2A.Z* mRNA on pre-MBT blastulas.

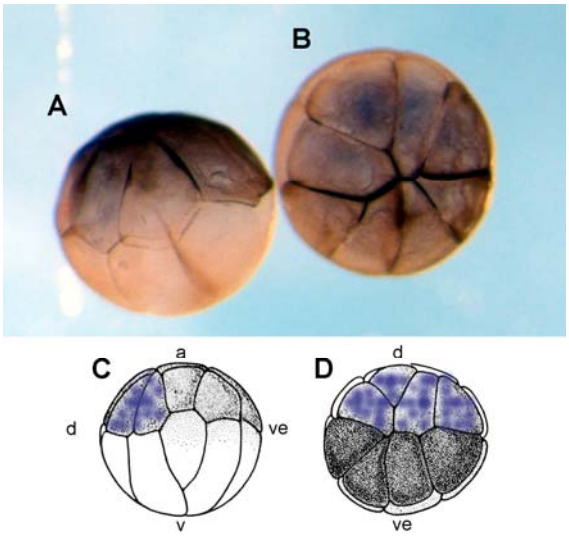

Figure 16 ***H2A.Z* mRNA is enriched in dorsal animal blastomeres at stage 5**. (A) *H2A.Z* mRNA detected by BM Purple stain (deep blue) is confined to animal and not vegetal cells. Stain is confined to left most animal blastomeres only. (B) Stain is limited to dorsal blastomeres only. (C, D) diagrams of A and B respectively. v = vegetal, a = animal, d = dorsal and ve = ventral. Stained blastomeres are coloured blue. Staging and drawings for diagrams from (Nieuwkoop and Faber, 1994).

A surprising finding was the asymmetric enrichment of *H2A.Z* mRNA in the dorsal blastomeres of the stage 5 embryo (Figure 16). Blastomeres are identified as dorsal by the slightly lighter endogenous pigmentation (Nieuwkoop and Faber, 1994). As discussed previously (3.1.1.1) there is no zygotic transcription at this stage therefore, this RNA must be of maternal origin. Since the enrichment and asymmetric localisation cannot be due to preferential transcription within these cells, the mRNA must preferentially locate to the dorsal region very early in development. This result confirms the detection of *H2A.Z* mRNA in whole embryos at stage 5 by RT-PCR (Figure 11). Simultaneous application of this technique to other genes with different patterns of expression acted as a control for non-specific expression (shown in section 4.2.2).

3.3 *H2A.Z* mRNA is enriched in the marginal zone and some mesodermal tissues.

Having determined that maternal *H2A.Z* mRNA is enriched in dorsal blastomeres pre-MBT, knowing that a dominant negative of H2A.Z causes a mesodermal defect, and having confirmed that *H2A.Z* mRNA levels rise sharply at gastrulation, I next determined whether H2A.Z is enriched in mesodermal or dorsal tissues at later stages. I applied *in situ* hybridisation to embryos just prior to, and during gastrulation (stages 9, 10, and 12) to determine whether *H2A.Z* mRNA is enriched in mesoderm and prospective mesoderm. I also investigated two later stages (stages 20 and 33/34) to determine whether there was enrichment of *H2A.Z* mRNA in later dorsal and/or mesodermal tissues.

In situ hybridisation was limited to providing spatial information only. Variability in the time required for the stain development in individual embryos makes comparison of the degree to which embryos are stained not quantitative. The spatial data provided by this

technique, however, compliments the quantitative information measured by RT real-time PCR.

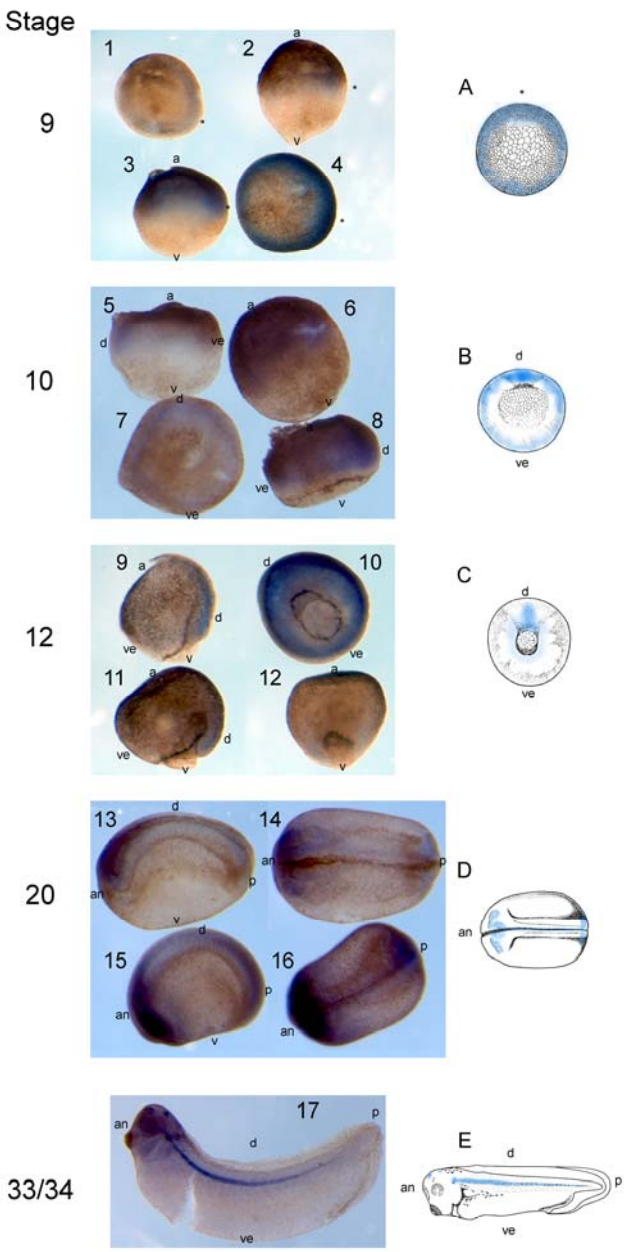

Figure 17 **Endogenous *H2A.Z* mRNA is enriched in the marginal zone and some mesodermal tissues.** Orientation of the embryos and diagrams is indicated a = animal pole, v = vegetal pole, d = dorsal, ve = ventral, an = anterior, and p = posterior. * in stage 9 embryos indicates the probable dorsal side. Given that stain is present in the dorsal region of stage 10 embryos, the region with stronger stain in stage 9 embryos is likely to be the dorsal side. Individual embryos are numbered. *In situ* hybridisation stains *H2A.Z* mRNA containing tissue a deep blue/purple. Areas stained in the embryos are coloured blue on the diagrams A-E. Diagrams A, B, C illustrate stages 9, 10 and 12 respectively from a vegetal viewpoint. D: dorsal view of at stage 20. E: lateral view at stage 33/34. All diagrams adapted from standard tables (Nieuwkoop and Faber, 1994). Stage 9: embryo 1, vegetal view stain is seen through the vegetal endoderm made transparent by BB/BA clearing; 2, lateral view; 3, lateral view; 4, animal view stain is seen through the intervening tissues made transparent by BB/BA clearing (see methods 2.4). Stain was allowed to further develop in embryos 3 and 4 than in embryos 1 and 2. Stage 10: embryo 5, lateral view; 6, ventral view (area of stain to right is on dorsal side made visible by the puncture to blastocoel required by the protocol); 7, vegetal view; 8, lateral view with dark pigment of blastopore pore lip especially visible. Stage 12: embryos 9 and 11, lateral view stain is concentrated in the dorsal midline and is visible due to transparency of intervening tissues; 10, view through animal pole with internal structures visible. In embryo 10 stain was allowed to develop further than in other embryos in this figure to allow tissues only lightly stained in other embryos to be clearly marked. Embryo 12: ventral view with focus adjusted to show lateral marginal zone tissues are lightly stained. Stage 20: embryos 13 and 15 lateral view, 14 and 16 dorsal views. Stage 33/34: embryo 17 lateral view.

In situ hybridisation showed that *H2A.Z* mRNA was localised to specific tissues during early development. Before gastrulation (stage 9, Figure 17, embryos 1-4) *H2A.Z* mRNA is enriched in a band corresponding to the marginal zone of the embryo. The stain is darker and thicker in one quadrant which, on the basis of observations at later stages, is thought to be the dorsal side. When gastrulation begins (stage 10, Figure 17, embryos 5-8) the pattern of *H2A.Z* mRNA staining remains similar, though the dorsal portion of the marginal zone is more stained relative to the rest of the marginal zone. As gastrulation progresses (stage 12) the concentrated area of stain extends into the chordamesoderm (Figure 17, embryos 9-12) due to convergence of marginal zone cells fated to become this tissue during gastrulation (Gerhart and Keller, 1986; Winklbauer, 1990). The identification of the stained tissue in the gastrulae is supported by the distribution of stain to tissues of chordamesodermal origin in tailbud embryos (Figure 17, embryos 13-16). At stage 20 the notochord is stained as are portions of the prospective eye and the mesencephalon (Figure 17, embryos 13-16). In the final stage investigated (33/34) the notochord, otic vesicles, and portions of the mid- and hindbrain stained for *H2A.Z* mRNA (Figure 17, embryo 17). The localisation of endogenous H2A.Z to mesodermal and pre-mesodermal tissues supports the suggestion from the morphological observations of H2A.Zdn defective embryos, that H2A.Z may have a role in mesoderm formation.

3.4 Discussion

This chapter has examined the localisation and expression level of *H2A.Z* mRNA in the early *X. laevis* embryo through gastrulation and tailbud stages. The spatial and temporal distribution of endogenous *H2A.Z* mRNA was determined by *in situ* hybridisation, RT-

PCR, and RT real-time PCR. These results demonstrated that *H2A.Z* mRNA is enriched in a particular lineage of cells and *H2A.Z* mRNA levels are developmentally regulated.

H2A.Z transcripts were detected for the first time in the early blastula (stage 5). A large pool of maternal mRNAs for other histones including canonical core histones and blastula specific variant linker histones exists in mature oocytes and early blastula (Dimitrov et al., 1993) so the existence of maternal *H2A.Z* mRNA is not unprecedented. A previous study failed to detect *H2A.Z* mRNA at this early stage, concluding that maternal *H2A.Z* transcripts were depleted by the time an oocyte was mature and that *H2A.Z* mRNA was not present again until zygotic transcripts were produced after the MBT (Iouzalen et al., 1996). This discrepancy can be explained by the use here of more sensitive PCR-based methods rather than northern blotting. At later stages when *H2A.Z* mRNA levels are higher, the RT-PCR and RT real-time PCR results presented here are in good agreement with this earlier study.

At the early blastula stage transcripts were enriched in dorsal animal blastomeres. This is the first time that a histone variant has been shown to be localised to specific cells of a vertebrate morula (early blastula of *X. laevis*). In mouse early *H2A.Z* mRNA expression is detected by RT-PCR in the differentiated trophoectoderm, not the stem cells of the inner cell mass indicating that *H2A.Z* mRNA expression increases with differentiation in eutherians also (Rangasamy et al., 2003). It seems likely that, as shown here for *X. laevis,* very low levels of maternal *H2A.Z* mRNA in the undifferentiated inner cell mass of the mouse await detection by more sensitive methods (such as RT real-time PCR) (see also 1.4.3). The presence of *H2A.Z* mRNA before the onset of zygotic transcription must be due to maternal stores originating in the oocyte before fertilisation. Therefore *H2A.Z* has not been preferentially transcribed within these early blastomeres, instead *H2A.Z* mRNA must have been moved to its current

location after fertilisation determined the future dorsal ventral axis (Gerhart et al., 1989; Kikkawa et al., 1996; Vincent et al., 1986). It is known that after fertilisation the cortical cytoplasm rotates around 30^{o} from the sperm entry point relative to deeper cytoplasm (Gerhart et al., 1989; Kikkawa et al., 1996; Rowning et al., 1997), thus establishing the previously radially symmetrical cytoplasm into distinct dorsal-ventral (D-V) symmetry. This cortical rotation is thought to align microtubules along which organelles containing dorsalising determinants are transported up to 90^{o} from the vegetal pole (Miller et al., 1999; Weaver et al., 2003). For example the protein dishevelled (Dsh) is initially located at the radial pole of the oocyte, then on fertilisation this protein is displaced by cortical rotation to the prospective dorsal region of the cytoplasm (Dale and Slack, 1987a). It is likely that the same process concentrates pre-existing maternal *H2A.Z* mRNA into the region of the cytoplasm of the fertilised oocyte fated to become dorsal blastomeres. Alternatively, cytoplasmic bridges exist between early blastomeres allowing the transport of material between cells even after cell division has begun (Dale and Slack, 1987a). In summary, maternal *H2A.Z* mRNA is present at low levels in the early blastula and is localised to dorsal animal blastomeres.

After the MBT the levels of *H2A.Z* transcripts at least double compared to the levels in the early blastula. A rise in mRNA levels after the MBT also occurs for canonical histones and other variants, the exception being some H1 variants (Dimitrov et al., 1993). Localisation of *H2A.Z* transcripts post-MBT is concentrated in the cells of the marginal zone especially in the dorsal portion of this region. These cells are a subset of the descendants of the dorsal blastomeres of stage 5 embryos (Dale and Slack, 1987a). Little is known about the tissue localisation of canonical and variant histones in the early *X. laevis* embryo, though canonical histones are assumed to be present in all tissues (Turner et al., 1988). Taken together these results indicate that maternal *H2A.Z*

mRNA is present in a subset of blastomeres before the MBT, and on initiation of zygotic transcription some of the descendants of these cells transcribe *H2A.Z*. This raises the possibility that H2A.Z is an enhancer or marker for its own transcription. As already discussed the presence of H2A.Z is likely to poise genes for transcription (see section 1.2.4). This could be due H2A.Z protein incorporated into the chromatin of its own regulatory regions. Alternatively, H2A.Z protein could be being incorporated into regulatory regions of genes that are part of a pathway controlling H2A.Z expression. In summary the patterns of localisation and levels of *H2A.Z* mRNA expression in the blastula before and after MBT have opened up important avenues for future investigation of H2A.Z's role in autoregulation and regulation of expression of other zygotic genes.

H2A.Z mRNA expression overlaps with that of genes for mesoderm fate and cell movement. For example the spatial expression of *H2A.Z* mRNA in the late blastula (stage 8) matches that of *Xbra,* a pan-mesodermal marker at this stage and an important protein for mesodermal cell fate determinations (Conlon et al., 1996; Smith et al., 1991). By stage 12 the more limited enrichment of *H2A.Z* more resembles *Gsc,* which like *H2A.Z* also has peak expression during gastrulation (Niehrs et al., 1994). Gsc is an important protein for mesodermal cell fate determinations (Laurent et al., 1997; Niehrs et al., 1994). In neurula and tailbud embryos *H2A.Z* mRNA is enriched in the notochord, a mesodermal tissue undergoing convergent extension. A variety of developmental gene products are enriched in this tissue including *Xbra* and *Xbcan* (Latinkic and Smith, 1999; Sander et al., 2001). Co-localisation of H2A.Z mRNA enrichment to mesodermal tissues indicates H2A.Z function may be important for proper differentiation of these tissues.

A fate map for the blastomeres at stage 6 has been constructed (Figure 18) (Bauer et al., 1994). Although no blastomere's descendants deterministically follow exactly the same fate in every embryo, high proportions of them make up the bulk of specific tissues in later-stage embryos. Therefore the probable descendants of a blastomere in any particular embryo can be determined. The localisation of H2A.Z may follow the descendant tissues of the marginal zone and these blastomeres.

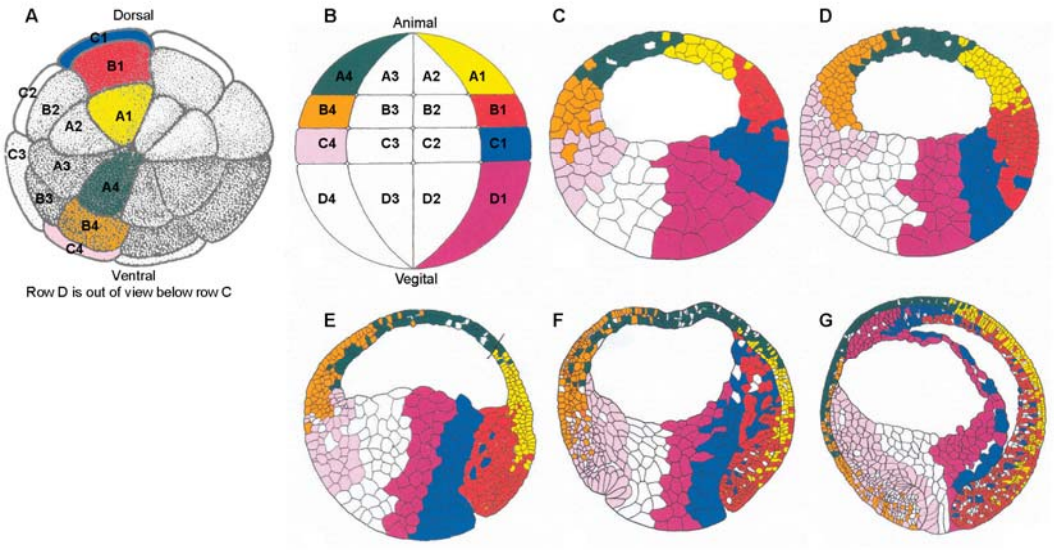

Figure 18 **Locations of cells derived from midline blastomeres of the stage 6 blastula**. (A) Nomenclature of blastomeres in the stage 6 embryo as per Nakamura and Kishiyama 1971 (reviewed Bauer et al. 1994) superimposed on the standard staging diagram for stage 6 animal view (Bauer et al., 1994). (B) Nomenclature of blastomeres in the stage 6 embryo (Kageura, 1997). (B-G) Lateral view dorsal to the right adapted from Bauer et al. 1994. (C-D) Summary diagrams illustrating the locations of the clones derived from the midline blastomeres of the stage 6 embryo. (C) Stage 8, (D) Stage 9, (E) Stage 10, (F) stage 11, (G) Stage 12.5.

In situ hybridisation enables us to determine whether localisation of *H2A.Z* mRNA enrichment is following the descendants of the blastomeres enriched for *H2A.Z* at stage 5. In the late blastula and early gastrula *H2A.Z* transcripts are localised to the marginal zone and appear to be more abundant and extend further animally on the dorsal side. The marginal zone tissues are descended from the row C blastomeres (third from the animal pole Figure 18), and the distribution of H2A.Z to the dorsal portion may derive from the B1 blastomere. Dorsal row C and B1 blastomeres are descendants of the dorsal

blastomeres enriched in *H2A.Z* mRNA at stage 5 (Figure 16). Together with blastomere D1, cortical cytoplasm from these blastomeres (C1 and B1) is able to induce a secondary axis, including mesodermal tissues when transplanted (Gerhart and Keller, 1986). However, more animally located blastomeres descended from the dorsal blastomeres, enriched in *H2A.Z* mRNA at stage 5, are not enriched in *H2A.Z* mRNA. As gastrulation progresses *H2A.Z* mRNA levels remain high (Figure 12 and Figure 15) and become concentrated in the prospective chordamesoderm on the dorsal side of the embryo. This is consistent with the convergence of marginal zone tissues toward the dorsal side during gastrulation (Gerhart and Keller, 1986). As gastrulation proceeds the chordamesoderm eventually involutes and develops into the dorsal structures of the embryo (Dale and Slack, 1987a). To follow the tissue specific expression of *H2A.Z* mRNA as the embryo develops two later stages of development were investigated, stages 20 and 33/34. Stage 20 is a late neurula/early tailbud stage. At this stage H2A.Z is enriched in the notochord, tailbud, eyes and mesencephalon (see Figure 17 embryo 17). These tissues are all at least partially descended from the mesoderm, which in turn is descended primarily from a few dorsal blastomeres of the 36 cell (stage 6) embryo (Figure 18 blastomeres B1, C1, and C2) (Iouzalen et al., 1996).

The pattern of H2A.Z expression determined by *in situ* hybridisation was previously interpreted as ubiquitous expression. The unstained regions were interpreted as difficult to stain yolky regions of the embryo. These yolky regions were also less stained in *in situ hybridisations* detecting the ubiquitously expressed canonical *H2A* (Iouzalen et al., 1996). From the Iouzalen et al. figure (reproduced as Figure 19 below) the stain for *H2A.Z* is overdeveloped and concentrated in the head, tailbud and in a line along the dorsal axis that could be the notochord. Another interpretation, drawn from the results presented here, is that the stain for *H2A.Z* is not lighter because reagents failed to

penetrate the yolky tissues but rather *H2A.Z* mRNA is more highly localised to specific tissues. Under this interpretation of their figure the result would be consistent with my own findings.

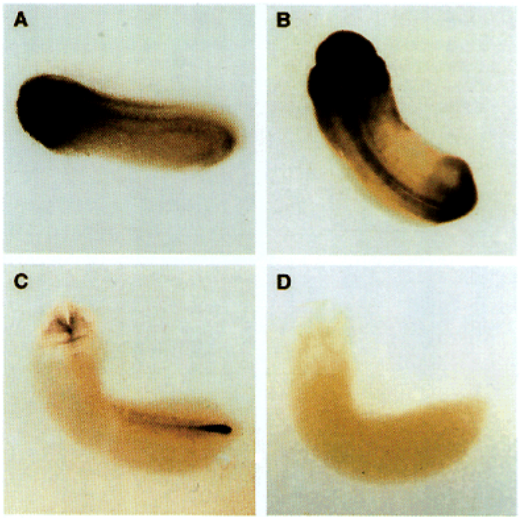

Figure 19 **Spatial expression pattern of *H2A.Z* and *H2A* mRNA in stage 25/26 *X. laevis* embryos**. Whole mount *in situ* hybridisation was used. (A) *H2A*, (B) *H2A.Z*, and (C) *Chordin* probe hybridisation signals are shown. (D) No hybridisation signal was detected in an embryo probed with a sense probe. Figure from Iouzalen et al. 1996.

A large scale *in situ* hybridisation study of randomly picked clones identified one clone as H2A.Z (Gawantka et al., 1998) (Figure 20). A single *in situ* hybridisation image of a stage 30 embryo hybridized to *H2A.Z* mRNA showed ubiquitous staining. Only the cement gland was completely unstained, though this may be because cement gland is refractory to stain. The protocol for this work used simultaneous development of stain of multiple 'baskets' each investigating a different gene in many embryos preventing careful monitoring of individual embryos, therefore I believe that the image is of an over-stained embryo. Despite this the notochord clearly shows enrichment of stain in Figure 20 consistent with my *in situ* staining pattern. My experiments have made significant improvements to understanding of *H2A.Z's* tissue specific expression in the *X. laevis* embryo highlighting the importance of extending and refining the results of large scale screening projects and initial characterisations.

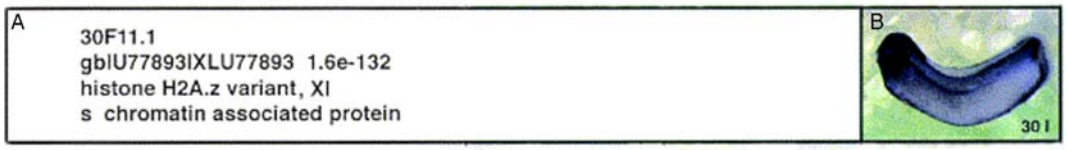

Figure 20 **Whole mount *in situ* hybridisation, sequence similarity and functional classification of a cDNA clone**. One of 273 partially sequenced cDNAs representing unique differentially expressed genes. (A) cDNA number within the study; accession number of best hit; *P*-value; name of best hit is *H2A.Z*; XI, a known *X. laevis* gene; s, structural gene; functional classification. The *P*-value is the probability provided by the BLAST programme and calculated using Karlin-Altschul statistics that the sequence similarity is due to randomness. (B) *in situ* hybridisation of stage 30 embryo, lateral view. Figure adapted from Gawantka 1998.

By stage 33/34 *H2A.Z* mRNA remains enriched in the notochord, though is not detected in the tailbud. In the head, *H2A.Z* mRNA levels are enriched in the otic vesical as well as portions of the mid- and hindbrain. Interestingly, a large scale screening of gene expression patterns identified a 'chromatin synexpression group' that included canonical H3 that was detected by in situ hybridisation in most tissues but depleted in cement gland, notochord and anterior somites (Gawantka et al., 1998). That H2A.Z is enriched differently to the other chromatin related proteins and canonical H3 further implies a specific developmental function for H2A.Z. The fate map of the 32 cell blastula shows that at stage 28-30 the otic vesicle is descended from A2, A3, B2, B3, and C3 blastomeres. Of these blastomeres the A2 and B2 are in the dorsal hemisphere of the embryo that was observed to be stained for *H2A.Z* mRNA at stage 5. The portions of the brain enriched in stage 33/34 embryos are descended from the mesencephalon which was enriched for *H2A.Z* mRNA at stage 20 (Gawantka et al., 1998). All of these tissues contain cells descended from the dorsal blastomeres of the stage 6 blastula (Dale and Slack, 1987a). It could be that *H2A.Z* expression is enriched in dorsal blastomeres, then as development proceeds is selectively and progressively repressed remaining in only a subset of descendent tissues where it is still required.

Both the temporal and spatial expression of *H2A.Z* mRNA is consistent with a role in gastrulation and mesodermal development. Localisation of *H2A.Z* mRNA follows

specific lineages of cells from the blastula through gastrulation and on into later stages of development. These findings lead to the hypothesis that H2A.Z regulates developmental gene expression patterns that determine and maintain specific dorsal cell fates. In the next chapter the mRNA level and localisation of selected genes important for proper cell fate determination, and markers of specific tissues were investigated in normal and dominant-negative *H2A.Z* mRNA injected embryos to determine whether H2A.Z has a role in regulating cell fate.

4 H2A.Z and cell fate in mesodermal lineages

4.1 Introduction

Developmental gene expression pathways are now being integrated with information from classical fate maps (Altmann et al., 2000; Vize, 2003). The early development of tissues in *X. laevis* has been characterised in great detail (Nieuwkoop and Faber, 1994) including cell fate determinants and cell movements in the blastula and gastrula stages (Bauer et al., 1994; Dale and Slack, 1987a) (see section 3.4, Figure 18). Perturbing developmental gene expression pathways can affect cell fate and/or movement resulting in defective morphology (Dosch et al., 1997; Gloy et al., 2002; Hopwood et al., 1992; Kurth et al., 2005; Lerchner et al., 2000; Onichtchouk et al., 1996; Smith, 2001; Tada et al., 1998; Tada and Smith, 2000; Wallingford and Harland, 2001). For example, if the down-stream Xbra target *Bix1* is overexpressed then *X. laevis* embryos develop lacking head and dorsal structures (Smith, 2001; Tada et al., 1998). We propose that the H2A.Zdn defect seen when H2A.Z function is perturbed (see section 1.4.5) results from disruption of gene expression pathways controlling cell fate and/or movement. In chapter 5 the possibility that H2A.Z plays a role in regulation of cell movement is investigated. Here I investigate the possibility that H2A.Z is involved in cell fate/determination.

As discussed in section 1.1.3 there are numerous ways in which chromatin structure can be altered to regulate transcription. There are many examples of alterations to chromatin structure during development, including incorporation of some histone variants, shown to have transcriptional consequences for developmentally important genes (see section 1.3), including the requirement for the B4 variant linker histone for mesodermal

competence (Steinbach et al., 1997). The work presented here and by others (discussed in section 1.4) demonstrates that the expression of the histone variant H2A.Z is developmentally regulated and that its function is essential for metazoan development. Having established that H2A.Z is important for proper mesoderm development and is enriched primarily in mesodermal tissue, we hypothesised that H2A.Z is involved in mesodermal cell fate determination because it is a component of a particular chromatin structure(s) necessary for proper regulation of key mesodermal genes. Previous investigations of the function of H2A.Z in several organisms support this idea, with evidence that the histone variant has a role in the regulation of transcription (Allis et al., 1980; Allis et al., 1986; Dhillon and Kamakaka, 2000; Donahue et al., 1986; Larochelle and Gaudreau, 2003; Santisteban et al., 2000; Stargell et al., 1993). Early differentiation of notochord, a mesodermal tissue, is reliant on the FoxA2 transcription factor, an orthologue of pha-4 (Ang and Rossant, 1994), which is necessary for targeting H2A.Z to the promoter of the mesodermal gene *Myosin heavy chain 2* (*myo-2)* in *C. elegans* (Updike and Mango, 2006) (see section 1.4.1). In vertebrates, H2A.Z could have a role in the early differentiation events in the embryo that set the stage for mesoderm formation at gastrulation. Alternatively, H2A.Z could have a role at gastrulation when mesoderm is established. This chapter investigates whether H2A.Z has a role in determining mesodermal cell fate in early *X. laevis* embryos.

4.1.1 A possible role for H2A.Z in the blastula

Since maternal *H2A.Z* transcripts are present before the MBT, H2A.Z may play a role in the development of the blastula. *In situ* hybridisation of endogenous *H2A.Z* in this study has shown that *H2A.Z* mRNA is enriched in stage 5 dorsal blastomeres (see Figure 16, section 3.2.3.1) consistent with H2A.Z having a role in dorsal cell fate specification, perhaps by being required for chromatin structures necessary for regulation of

transcription of specific early developmental genes. Notably, the dorsal tier B blastomeres that are daughter cells of the blastomeres enriched for *H2A.Z* mRNA at stage 5 (section 3.3, Figure 16) are within the Nieuwkoop Centre (Gimlich and Gerhart, 1984). The Nieuwkoop Centre induces formation of the Spemann's Organiser that in turn induces gastrulation and mesoderm formation (Gimlich and Gerhart, 1984). As part of the Nieuwkoop Centre the blastomeres contain maternal β-catenin and other dorsal determinants (Gimlich and Gerhart, 1984). H2A.Z with these other dorsal determinants may be important to establishing the dorsal-ventral axis and thus set the stage for gastrulation. This would explain why when H2A.Z function is perturbed gastrulation is disrupted and the H2A.Zdn defect becomes visible only after the onset of gastrulation.

4.1.2 A possible role for H2A.Z in the gastrula

Alternatively, H2A.Z may be important at gastrulation. I have already shown that *H2A.Z* mRNA levels rise sharply during gastrulation (see section 3.2.2.2) and that *H2A.Z* mRNA is enriched in the marginal zone and mesodermal tissues during gastrulation (section 3.3). In summary, H2A.Z is expressed in the right time and place to affect mesodermal cell fate decisions during gastrulation. Furthermore, when H2A.Z function is perturbed the H2A.Zdn defect becomes visible shortly after gastrulation (see 1.4.5). Gastrulation is a period when many cell fate determinations are being made and the anterior-posterior axis established, prior to gastrulation the prospective mesoderm of the blastula is differentiated only as dorsal or ventral (Agius et al., 2000; Dale and Slack, 1987b; Wylie et al., 1996), therefore H2A.Z may be important for proper cell fate determination during gastrulation. Disruption of the anterior-posterior axis would be consistent with the shortened trunks and improper mesoderm formation (Kieker and Niehrs, 2001) of the H2A.Zdn defect, possibly resulting from disruption of Wnt and/or chordin pathways.

4.1.3 Marker genes for mesoderm

Genes with mRNA or protein expression temporally and spatially limited to particular tissues can act as molecular markers for cells of those tissues (Dosch et al., 1997; Hopwood et al., 1992; Kurth et al., 2005; Lerchner et al., 2000). If disruption of H2A.Z affects cell fate then marker genes for particular tissues will have altered expression. Several genes are characteristic markers of mesodermal tissue including *Gooscoid* (*Gsc*), *Xenopus Brachyury (Xbra), Xenopus* myogenic determinant (*XMyoD*), and *Xenopus Ventral 2 (XVent2)* (Figure 21). A discussion of these genes as markers follows.

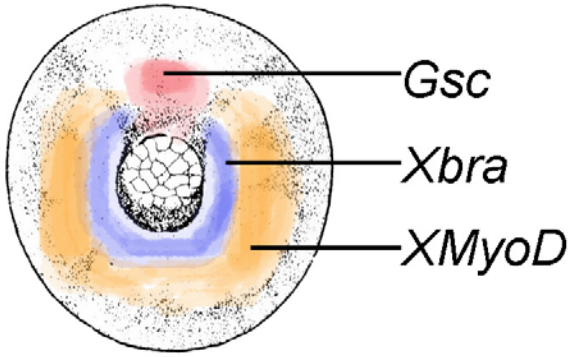

Figure 21: **Spatial distribution of mesodermal marker gene expression in the stage 12 gastrula.** Red: *Gsc* mRNA is present in the endomesoderm that eventually becomes head mesoderm. Actual expression of *Gsc* is weak at this stage. Violet: *Xbra* mRNA is expressed in involuting tissue that becomes chordamesoderm and later notochord. Orange: *XMyoD* mRNA levels are strongest in paraxial mesoderm with more ventral/lateral fates such as somites. *XVent2* mRNA spatial distribution (not shown) resembles that of *XMyoD* mRNA except it becomes restricted to the tailbud in later stages(Dosch et al., 1997; Gawantka et al., 1998). Modified from original diagram for stage 12 from standard tables (Nieuwkoop and Faber, 1994).

At the onset of gastrulation *Gooscoid* (*Gsc*) mRNA transcription, stimulated by the Wnt pathway via the transcription factor Siamois (Brannon et al., 1997; Fan and Sokol, 1997), begins in the Spemann's organiser (dorsal lip of the forming blastopore) (see Figure 21) (Niehrs et al., 1994). *Gsc* is an early response to Wnt signalling, and is not maternally transcribed. An eight-fold gradient of *Gsc* expression patterns the organiser and, directly or indirectly, other mesodermal tissues (Niehrs et al., 1994). Later *Gsc* is transcribed in the endomesoderm (see Figure 21), then head mesoderm (Niehrs et al.,

1994); tissues primarily descended from blastomere B1 of the stage 6 embryo (see Figure 18, section 3.4). Gsc is a transcriptional repressor that acts directly on another important gene for mesodermal fate determination *Brachyury (Xbra)* (Artinger et al., 1997; Latinkic and Smith, 1999).

Xbra mRNA is found throughout the marginal zone in the late blastula. Early *Xbra* expression specifies mesodermal cell fate (Conlon et al., 1996; Cunliffe and Smith, 1992; Cunliffe and Smith, 1994; Kispert et al., 1995; Latinkic et al., 1997). On gastrulation, *Xbra* transcription is inhibited in the endomesoderm and *Xbra* mRNA expression remains strong in the prospective notochord and thus is later restricted to the notochord (see Figure 21) (Artinger et al., 1997; Gont et al., 1993; Herrmann et al., 1990; Latinkic and Smith, 1999; Latinkic et al., 1997; Panitz et al., 1998; Smith et al., 1991; Xu et al., 2000). Xbra can induce its own expression in dorsal tissues through intermediates including fibroblast growth factor (FGF) (Conlon et al., 1996; Panitz et al., 1998; Tada et al., 1997). Xbra is a transcription factor important for the concentration-dependant mesodermal patterning (O'Reilly et al., 1995) required for proper dorsal and anterior-lateral mesoderm development (Conlon et al., 1996; Kispert et al., 1995).

XMyoD (abbreviation for *Xenopus* myogenic determinant) is another commonly used mesodermal marker gene (Dosch et al., 1997; Rupp and Weintraub, 1991; Steinbach et al., 1998). After the MBT Wnt signalling induces ubiquitous low level *XMyoD* expression before auto-activated tissue specific (muscle precursor) expression begins (Rupp and Weintraub, 1991; Steinbach et al., 1998) in two lateral regions of the later gastrula (see Figure 21). In the gastrula XMyoD is one of the transcription factors that specifies lateral mesoderm fate (Dale and Slack, 1987a; Dosch et al., 1997), and later becomes prominent in the somites (Dosch et al., 1997). Interestingly, MyoD levels are

reduced when histones are globally hyperacetylated (Figure 14) and acetylation of H3 and H4 may have a role in H2A.Z incorporation into chromatin (see 1.2.3).

Finally, *Xvent2* is another gene expressed in lateral mesoderm of the blastula, it has the same expression pattern as *XMyoD* during gastrulation, then later becomes restricted to the tailbud (Dosch et al., 1997; Gawantka et al., 1998).

In summary, *Gsc, Xbra, XMyoD,* and *Xvent2* mRNA expression can be used for identification of mesoderm tissue by RT real-time and spatial localisation by *in situ* hybridisation.

4.1.4 Experimental approach

If H2A.Z has a role in determining cell fate then disrupting that function would perturb cell fate decisions, leading to improper expression of cell fate marker genes. The H2A.Zdn defect would therefore be due to perturbation of correct cell fate determination. This idea can be tested by determining the expression levels and localisation of mRNA from selected marker genes in defective embryos, and comparing them to normal embryos. In this chapter we perturbed H2A.Z function by injecting RNA expressing a dominant negative protein (H2A.ZNQ) (see 1.4.6 and 1.4.5) to monitor changes to marker gene expression associated with the HIH motif of H2A.Z (see section 1.4.4). These injected embryos will be referred to as NQdn embryos or, if advanced enough to show the H2A.Zdn defect (stage 10+), H2A.Zdn embryos. Mesoderm marker genes (discussed in 4.1.3) were chosen because: A) the morphology of the H2A.Zdn defect (the blastopore fails to close, trunks are shortened, and heads develop normally) indicates that specific mesodermal lineages (such as the chordamesoderm) may be affected; B) many mesodermal marker genes are up-regulated during gastrulation when endogenous H2A.Z is most highly expressed.

To determine whether mesoderm cell fate was being disrupted, H2A.Zdn defect embryos were compared to normal control embryos, *H2A.Z* mRNA, and *H2A* mRNA injected embryos by measuring the mRNA expression from the selected marker genes. A *H2A* mRNA injection control was used to control for the general repressive affect of overexpressed histones (Wolffe and Hayes, 1999). *H2A.Z* mRNA injected embryos controlled for effects caused by over-expression of this specific variant. Quantification was by semi-quantitative RT-PCR, and RT real-time PCR (the reasons for this change of technique are discussed in 3.2.1). As well as abnormal expression levels of mesodermal genes, mesodermal genes may be expressed in inappropriate locations, with or without detectable changes to the levels of mRNA transcripts in the whole embryos. To investigate this possibility the spatial distribution of *XMyoD* and *Xbra* mRNA was determined by *in situ* hybridisation, as these transcripts are molecular markers for the dorsal and dorsal-lateral mesodermal tissues most likely to be affected when H2A.Z function is perturbed based on the morphology of the H2A.Zdn defect.

4.2 Results

4.2.1 Effect of perturbing H2A.Z function on the expression levels of mesodermal marker genes

4.2.1.1 Optimisation of microinjection

To determine whether the injected mRNAs were translated I used a H2A.Z-EGFP fusion protein to visually monitor, by microscopy, the expression of microinjected mRNA (Figure 22). EGFP fusion proteins have been widely used as markers in *X. laevis* (Ridgway et al., 2004a; Sive et al., 2000). The H2A.Z-EGFP image (Figure 22) demonstrates that protein was translated from introduced *H2A.Z-EGFP* mRNA. The localisation of H2A.Z-EGFP protein was consistent with earlier experiments, diffuse before the MBT and then localised to the nucleus (Ridgway et al., 2004a). This

experiment confirmed that proteins were translated from microinjected mRNA, indicating that these techniques of *in vitro* mRNA production and microinjection were successful. Therefore microinjection of mRNA encoding H2A.Z, H2A and H2A.ZNQ could proceed. Injection of these mRNAs produced morphologies consistent with earlier work in this laboratory (discussed in 1.4.5, (Ridgway et al., 2004a)). Note that defect levels were never 100% due to the low amounts of RNA used to prevent non-specific defects and that use of small amounts of RNA is typical of studies employing this technique (Nakano et al., 2000; Sive et al., 2000; Tada et al., 1997). Although only a single blastomere is injected the effects are bilateral because cytoplasmic connections exist between the blastomeres at this stage allowing passage of the injected mRNA (Newport and Kirschner, 1982). As I was now able to produce H2A.Zdn defect embryos for study I proceeded to determine the mRNA levels and localisation of marker genes for mesodermal cell fate.

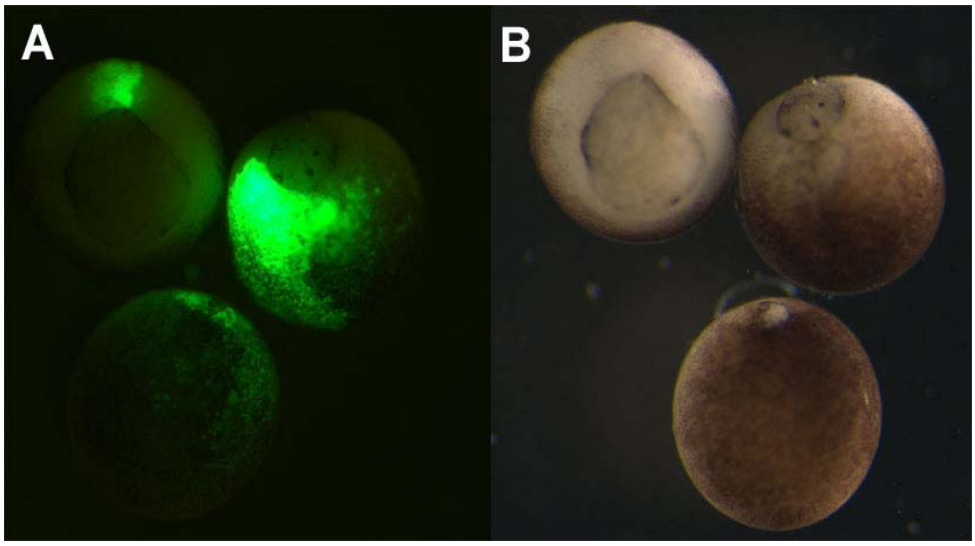

Figure 22 **Microinjected *H2A.Z-EGFP* mRNA is translated into protein**. Embryos were injected with 1ng of *H2A.Z-EGFP* mRNA at the two cell stage. (A) Embryos stages 11 to 12 seen under fluorescence with a Leica GFPII filter set. Strongest signal is on the injected side though expression of H2A.Z-EGFP is widespread in the embryos. (B) The same embryos under transmitted light.

4.2.1.2 mRNA levels of mesodermal marker genes are unaffected when H2A.Z function is perturbed

I investigated both the levels and localisation of mRNA from selected marker genes for mesodermal cell fate. Section 4.2.2 describes the localisation and this section deals with the mRNA levels of these genes. Two methods were used to determine mRNA levels of selected genes in the embryos, semi-quantitative RT-PCR and RT real-time PCR. First I will describe the results from semi-quantitative RT-PCR analysis then the results from real-time PCR.

To ensure that the mass of PCR product was proportional to the template cDNA, and therefore to the mRNA for the investigated gene in the sample, the RT-PCRs were run for a number of identical aliquots from the same sample and PCR product was retrieved at various numbers of cycles. After quantitation (as described in 2.5.3.1) a sigmoidal curve was produced for each primer set. Figure 23 is the curve for products from the *Gsc* primers from identical aliquots of a stage 12 sample. This figure illustrates the sigmoidal curve common to all of these experiments. A number of cycles within the linear region was selected for use with further reactions for each primer set (see section 2.5.3.1).

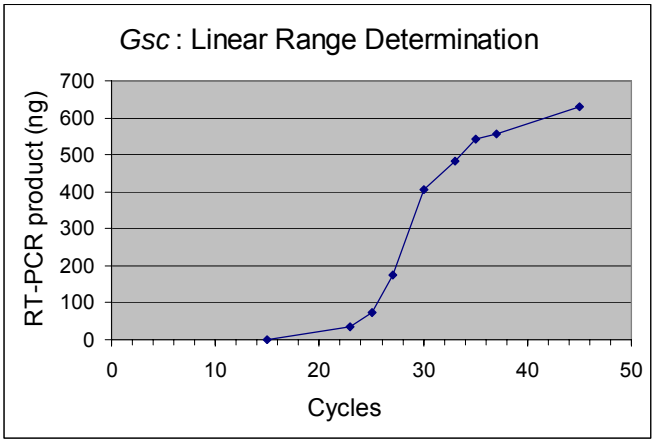

Figure 23: **Determining the range of cycle giving a linear increase in product from an RT-PCR reaction**. Uninjected embryos were collected at stage 12 (late gastrula) then analysed by RT-PCR with primer sets for *Gsc, MyoD, Xbra, XVent2*, and *H4*. *Gsc* primer amplification results shown as an example. Samples were collected after various numbers of cycles and the amount of PCR product determined.

RT-PCR gels determined that the genes investigated, *Gsc, Xbra, Xvent2* and *XMyoD*, were present in NQdn embryos at the same stages as in uninjected control embryos (Figure 24). Typical results from RT-PCR analysis are shown (Figure 24). In this figure –RT is a sample where the extracted total RNA was processed without reverse transcriptase. The –RT panels demonstrate that the total RNA was free of gDNA contamination (Figure 24). H4 was used as an internal standard (loading control).

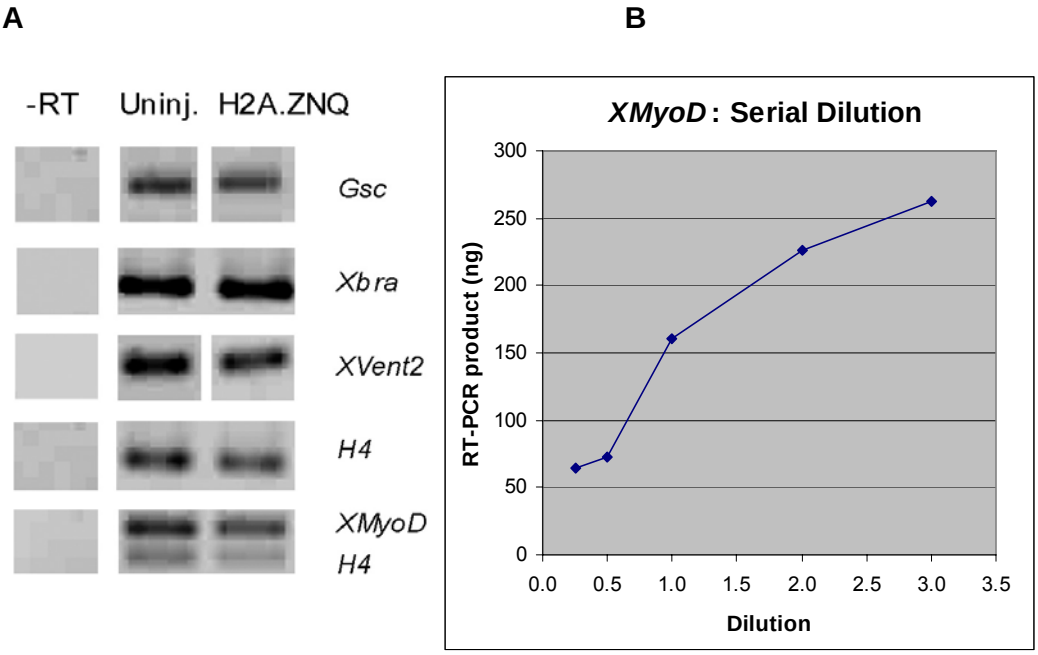

Figure 24 **Expression of mesodermal cell fate genes when H2A.Z function is perturbed**. A: Embryos injected with H2A.ZNQ or H2A.Z were collected at stage 12 (late gastrula) then analysed by RT-PCR with primer sets for *Gsc, MyoD, Xbra, XVent2*, and *H4*. Uninjected embryos and a sample that had not been reverse transcribed were included in every experiment. Each experiment has been repeated 3-5 times. B: An example of a serial dilution used to confirm that the RT-PCR products were proportional to the concentration of template in the sample. Uninjected embryos were collected at stage 12 (late gastrula). After RT the cDNA was serially diluted then analysed by RT-PCR with primer sets for *Gsc, MyoD, Xbra, XVent2*, and *H4. XMyoD* primer amplification results shown.

The mRNA levels of the selected marker genes were then determined for NQdn and uninjected control embryos. Mean results are given and where sufficient data was obtained standard error of the mean (SEM) (shown by error bars) and p values (given within the text) were calculated (2.5.5).

The mRNA levels of *Gsc* were analysed through gastrulation when Gsc mRNA was expected to be most highly expressed (Niehrs et al., 1994) (stage 9, 10, 12) as well as in a later tailbud stage when *Gsc* mRNA levels were expected to be lower (Niehrs et al., 1994) to ensure the technique was responding to changes in RNA levels within the samples (Figure 25). A single sibling set of uninjected embryos were also analysed for *Gsc* mRNA levels at neurulation, stage 14. The tailbud stage samples (stage 20) would also determine if there was anomalous *Gsc* mRNA levels in the dominant negative injected embryos compared to H2A.Zdn siblings at a stage of development after gastrulation. *Gsc* mRNA levels were highest at the first stage investigated (stage 9) in both the NQdn and the uninjected embryos (Figure 25). At this stage the mean values for both treatments appeared to be almost identical (expression relative to *H4*: uninjected 2.0, injected 2.1) however this technique was abandoned before sufficient replicates were generated for the calculation of p values at this stage. After stage 9 these results indicate a decline in *Gsc* mRNA. *Gsc* mRNA was only weakly detected at stage 20 in both treatments and in one uninjected sibling set was not detected (NQdn 0.5 n = 1; uninjected mean 0.4, n = 5) (Figure 25). The mean values for the uninjected and injected differed most at stage 12 (NQdn 1.4 n = 3; uninjected mean 0.6, n = 4) (Figure 25) however this difference was not significant (p=0.31). The results did detect changes in expression levels during cell development. However, these results do not provide any indication that *Gsc* mRNA expression is affected by perturbation of H2A.Z function at the stages investigated, including during gastrulation. This conclusion was somewhat surprising, given the morphology of H2A.Zdn embryos (see 1.4.5) indicate a defect in mesoderm development and *Gsc* is a key gene for mesoderm cell fate during gastrulation (discussed in 4.1.3). Two possible explanations come to mind. Firstly, that cell fate is not affected, an idea explored in chapter 5. Secondly, that changes to gene

expression affecting cell fate are occurring downstream or sideways of *Gsc* in the gene expression pathways for cell fate. This possibility could be examined by investigating further marker genes for mesodermal cell fate.

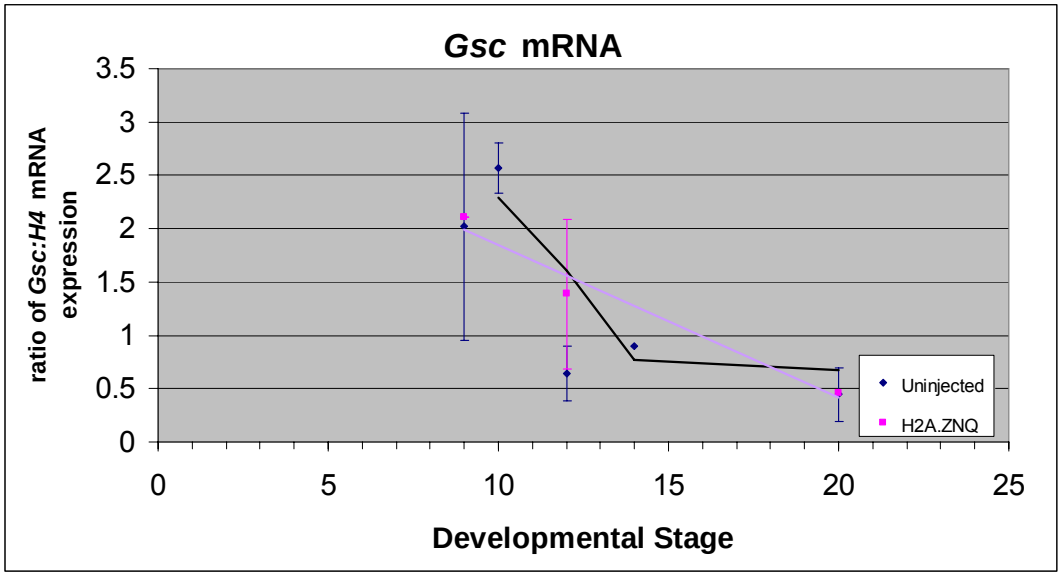

Figure 25 **Levels of *Gsc* mRNA after disruption of H2A.Z function**. Embryos were injected with mRNA encoding a dominant negative H2A.Z (H2A.ZNQ) or left uninjected, sibling sets pooled, and analysed by RT-PCR. Y axis units are relative to result from 1µg stage 10 wild type total RNA with *Gsc* normalised to a *H4* internal control as discussed in 2.5.3.1. Mean results given. Where applicable SEM is given as error bars. For uninjected sibling sets at stages 9 and 10 n = 2, and at stage 12 n = 4. For H2A.ZNQ mRNA injected sibling sets at stage 12 n = 3. For all other results n = 1. The black line is a moving mean line of best fit for the uninjected results. The mauve line is a moving mean line of best fit for the H2A.ZNQ injected results.

One downstream target of *Gsc* is *Xbra.* If H2A.Z's developmental function is downstream of *Gsc* then *Xbra* mRNA levels may be affected. Previous studies have shown that when Xbra function is disrupted gastrulation is late, the blastopore fails to close, and later shortened trunks result (Conlon et al., 1996). The similarity of this phenotype to the H2A.Zdn defect (see 1.4.5) may have indicated reduced *Xbra* mRNA levels in these defective embryos at some point in early development. If Xbra mRNA levels were affected then this would indicate that H2A.Z's normal developmental role directly or indirectly influences *Xbra* mRNA expression. To answer these questions the *Xbra* mRNA levels relative to H4 for uninjected and H2A.Zdn defect embryos were determined by semi-quantitative RT-PCR and are given in Figure 26. The stages used

were 9, 10, 12 14, 16 and 20, selected for when *Xbra* mRNA expression is present in normal embryos and to investigate both gastrulation and later developmental changes that may result. *Xbra* mRNA was detected in all the developmental stages and treatments investigated. *Xbra* mRNA expression peaked at the onset of gastrulation (stage 10, relative expression 2.22) in the control embryos and just prior to gastrulation (stage 9, relative expression 2.50) in a single NQdn sample. This may be because in practice stage 9 and stage 10 embryos are collected only a small time apart. Despite matched uninjected siblings the NQdn embryos in the stage 9 sample here may have been entering stage 10, however due to the delay in initiating gastrulation were indistinguishable from embryos at stage 9. That this single NQdn stage 9 sample might not be representative is supported by the similarity in *Xbra* mRNA expression levels between the two treatments at stages 12 (relative expressions: uninjected 1.85, NQdn 1.70, $p = 0.74$) and 20 (relative expressions: uninjected 1.65, NQdn 1.70, insufficient data to calculate a p value). After peaking, *Xbra* mRNA expression levels in both samples declines over the further stages investigated. These results do not support a reduction in *Xbra* mRNA expression at any stage nor a change in *Xbra* mRNA expression levels at most stages. The only indication that changes to *Xbra* mRNA expression may be related to the morphology of defective embryos was a single data point indicating a possible early peak in *Xbra* mRNA levels. Further investigation was needed to confirm this result and was conducted using a more precise technique; RT real-time (see Figure 28). If the expression or function of *Gsc*, *Xbra*, or other key cell fate genes was perturbed this would be expected to effect the expressions of mRNAs downstream in the developmental genes expression programs. I investigated one such gene *XMyoD* by RT real-time PCR (see Figure 29).

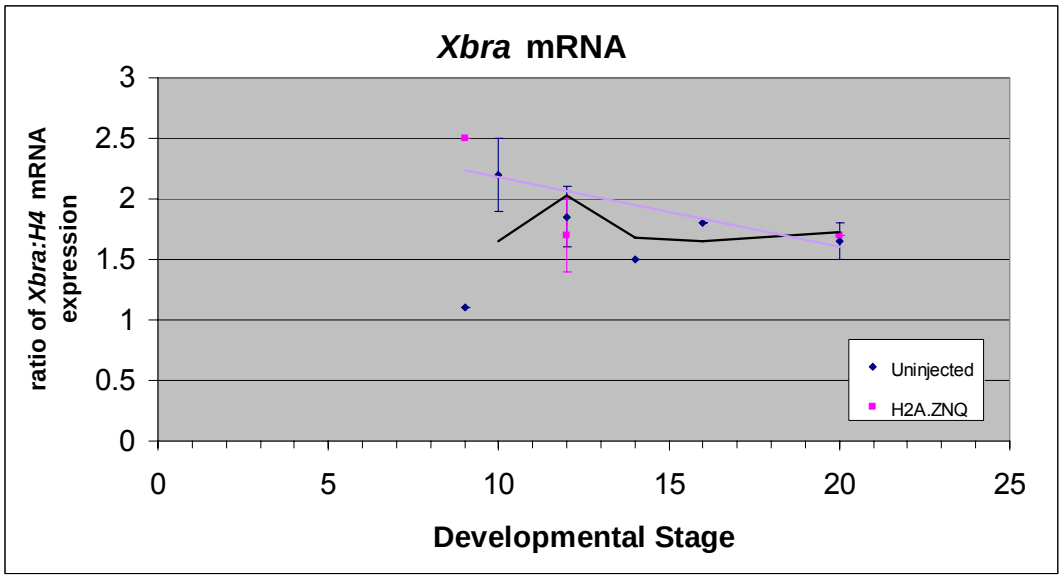

Figure 26 **Levels of *Xbra* mRNA after disruption of H2A.Z function**. Embryos were injected with mRNA encoding a dominant negative H2A.Z (H2A.ZNQ) or left uninjected, sibling sets pooled, and analysed by RT-PCR. Y axis units are relative to result from 1µg stage 10 wild type total RNA with *Xbra* normalised to a *H4* internal control as discussed in 2.5.3.1. Mean results given. Where applicable SEM is given as error bars. For uninjected sibling sets at stages 10 and 12 n = 2. For H2A.ZNQ mRNA injected sibling sets at stage 12 n = 2. For all other results n = 1. The black line is a moving mean line of best fit for the uninjected results. The mauve line is a moving mean line of best fit for the H2A.ZNQ injected results.

As can be seen from the SEM (error bars Figure 25 and Figure 26) the data for a given stage and treatment combination can be variable, for example for stage 12 *Xbra* mean relative expression is 1.85 and the SEM is 0.25. This indicates that any differences between the injected and NQdn embryos may not be significant. To determine if this was the case p values comparing the data for relative expression of each marker gene mRNA in NQdn with that from uninjected embryos were calculated at stage 12 where there were sufficient data points. For *Gsc* mRNA relative expression level data p = 0.31 and for *Xbra* mRNA p = 0.74. P values of 0.05 or lower were considered significant. To exclude the possibility that the inability to detect any significant difference in marker gene mRNA expression levels and the variability in the data was due to limitations in the precision of the semi-quantitative RT-PCR technique, further experiments to quantifying levels of marker genes when H2A.Z function was perturbed utilised the more precise RT real-time PCR method. Experiments using the semi-quantitative RT-

PCR method were discontinued. The RT real-time technique had already proven to be effective for determining endogenous *H2A.Z* mRNA levels (see 3.2.2.2, Figure 15).

The relative expression of mRNA from the genes *Gsc, Xbra* and *XMyoD* was determined for uninjected embryos, and those injected with RNA encoding H2A, H2A.Z or the dominant negative H2A.ZNQ by RT real-time PCR. All RT real-time experiments included –RT and –RNA controls. Results are relative to a selected stage 9 uninjected reference sample, all marker gene mRNAs were expected to be present at a low level at this stage. Stages 9, 10 and 12 were analysed by RT real-time PCR to confirm that there were no changes in the mRNA expression levels of the selected cell fate marker genes during gastrulation when the defect is first detected in embryos with perturbed H2A.Z function (see 1.4.5). To determine if any of the differences in mRNA expression levels between the two treatments were significant, p values for the various treatments compared to controls of the same stage were calculated, these are given separately to the expression level results (Table 7).

Firstly, we examined the mRNA levels of a key mesodermal determinant *Gsc* at three stages of development: 9, 10, and 12 (Figure 27). In uninjected embryos *Gsc* mRNA was detected at all three developmental stages investigated with the mean relative expression highest at stage 10 (Figure 27). *Gsc* mRNA was detected at all stages in all treatments. In all treatments mean *Gsc* mRNA levels were higher at stage 12, for example at stage 9 in uninjected embryos mean relative *Gsc* mRNA level is 0.45, at stage 10, 0.61, then reduced to 0.44 by stage 12. These results in the uninjected embryos *Gsc* mRNA (Figure 27) agree closely with previous studies where *Gsc* mRNA was detected by Northern blot at stage 8.5, peaked at stage 10.5 and was reduced by stage 13 (Blumberg et al., 1991; Panitz et al., 1998). The data is also supported by the findings of the semi-quantitative RT-PCR analysis of mRNA levels for this gene (see Figure 25).

Mean mRNA levels in all of the mRNA injected embryos were lower than uninjected embryos at the same stage with one exception, the *H2A.Z* mRNA injected embryos at stage 10 (Figure 27). The largest differences between the uninjected and the injected embryos was at stage 9 where the mean *Gsc* mRNA levels in the uninjected embryos were more than two-fold higher than all of the results for injected embryos at that stage (Figure 27). With such small differences in *Gsc* mRNA levels between the uninjected and mRNA injected and large variation between individual samples, determination of p values were necessary before concluding whether *Gsc* mRNA levels were perturbed or not in any of the treatments (see Table 7).

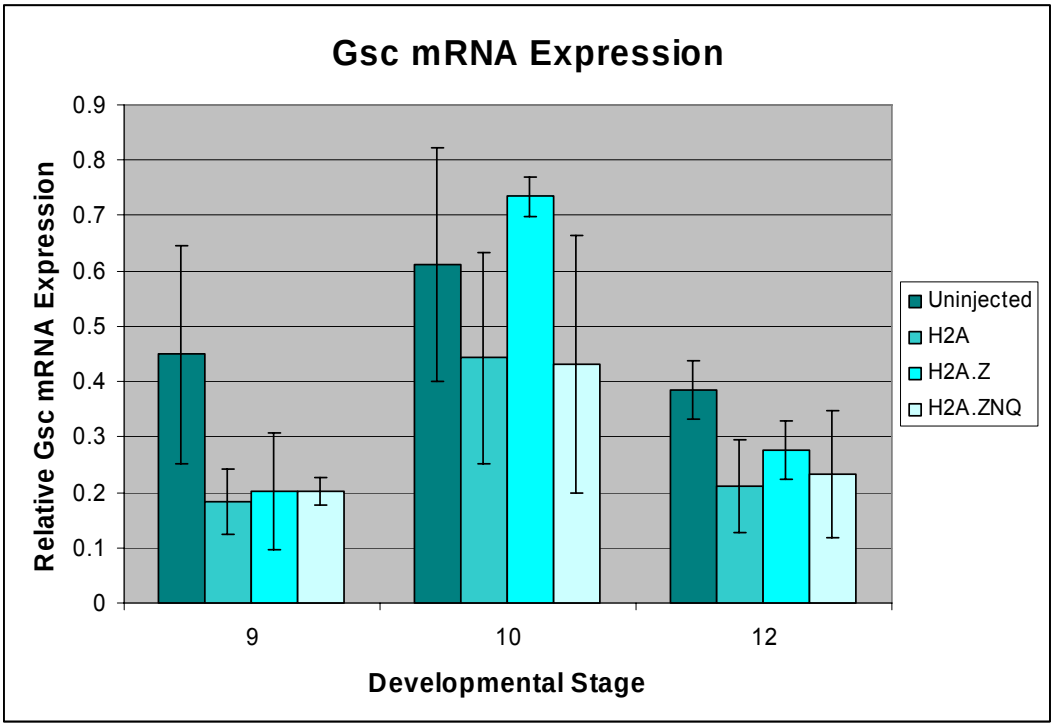

Figure 27 **Levels of *Gsc* mRNA when H2A.Z function is perturbed**. Embryos were injected with mRNA encoding H2A, H2A.Z or a dominant negative H2A.Z (H2A.ZNQ). Histograms are means of results from pooled sibling sets. Error bars indicate SEM. For uninjected sibling sets stages 9 and 10, and H2A.ZNQ mRNA injected sibling sets stages 9 and 10 n = 4. For all other results n = 3. Data is given as expression relative to *H4* and a reference sample at stage 9 as described in 2.5.4.2.

The next gene I investigated was *Xbra,* another important marker for mesodermal cell fate in gastrula stage embryos (see 4.1.3). *Xbra* mRNA was detected in all samples and stages analysed (Figure 28). No result is given for *H2A* mRNA injected embryos at stage 9 because no sample cDNA remained for this experiment. For similar reasons, only a single sample of *H2A* mRNA injected embryos at stage 10 was analysed by real-time RT-PCR for relative *Xbra* mRNA level. In all treatments mean relative *Xbra* mRNA was highest in stage 12 embryos and uninjected embryos had higher mean relative mRNA levels than injected embryos at all stages with the exception of NQdn embryos at stage 12 uninjected embryos *Xbra* mRNA mean relative level 4.02, compared to 4.23 for NQdn). The uninjected embryos mean relative *Xbra* mRNA level was always less than three-fold more than any injected embryo result at the same stage (largest fold difference 2.70 for uninjected over *H2A.Z* mRNA injected embryos at stage 9). These results support the trends seen in the semi-quantitative RT-PCR which detected *Xbra* mRNA at all three developmental stages investigated (stages 9, 10, and 12) in uninjected and NQdn embryos, and the mean relative expression was higher at stage 12 than stages 9 and 10 in both set of samples (Figure 26). Other researchers have detected *Xbra* mRNA RT-PCR first at stage 9.5, with maximal expression at stage 11.5 (Eimon and Harland, 2002; Panitz et al., 1998). As with *Gsc* the difference between uninjected and NQdn embryos was not significant ($p=0.20$ at stage 12). There was no evidence that expression of *Xbra,* an important mesodermal marker downstream of *Gsc,* was affected when H2A.Z's developmental function was perturbed. The *Xbra* results do not support a role for H2A.Z in cell fate before and during gastrulation. Next I looked further downstream in cell fate by investigating expression of *XMyoD*.

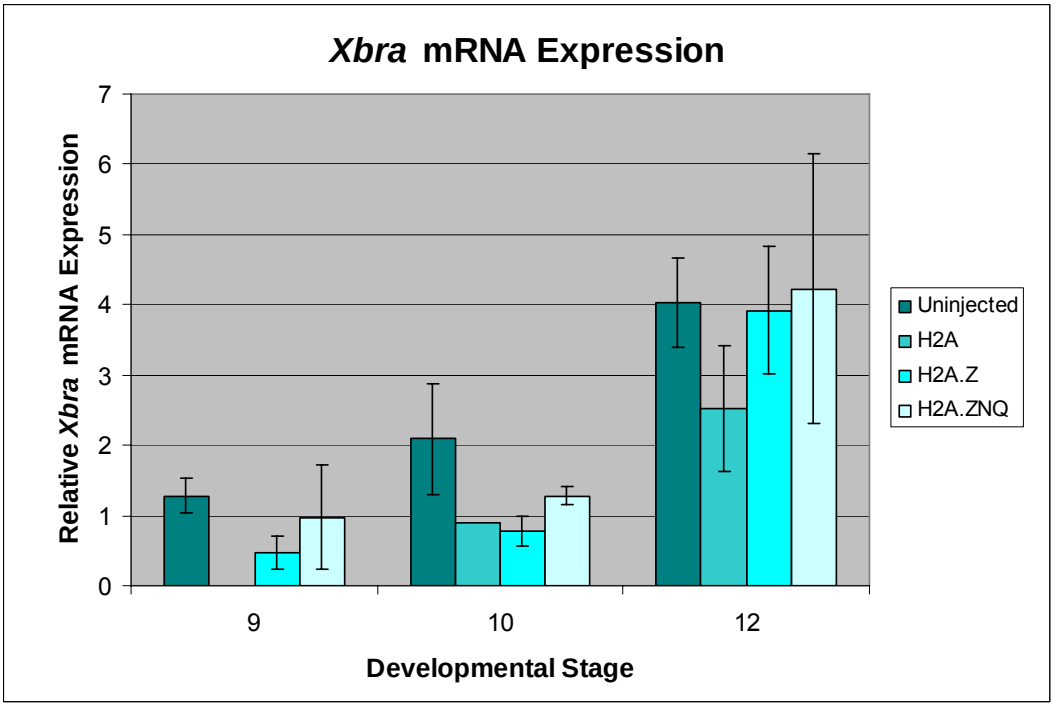

Figure 28 **Levels of *Xbra* mRNA when H2A.Z function is perturbed.** Embryos were injected with mRNA encoding H2A, H2A.Z or a dominant negative H2A.Z (H2A.ZNQ). Histograms are means of pooled sibling sets. Error bars from the mean indicate SEM. For uninjected sibling sets at stage 9 n = 4, stage 10 n = 3 and stage 12 n = 6. For H2A mRNA injected sibling sets at stage 10 n = 1 and stage 12 n = 4. For H2A.Z mRNA injected sibling sets at stage 9 and 10 n = 3, and for stage 12 n = 5. For H2A.ZNQ mRNA injected sibling sets at stage 9 and 12 n = 3, and for stage 10 n = 2. Data is given as expression relative to *H4* and a reference sample at stage 9 as described in 2.5.4.2.

Figure 29 shows the expression levels of *XMyoDb* a downstream marker of mesoderm tissue. There are two *XMyoD* genes in *X. laevis*, I chose to examine the *XMyoDb* transcript here since it has the advantage of not being present in maternal transcripts (Steinbach et al., 1997) and of being expressed at levels at least 10x higher than *XMyoDa* (Steinbach et al., 1998). In uninjected embryos *XMyoDb* mRNA was detected at all three developmental stages investigated (stages 9, 10, and 12) with the mean relative expression higher at stage 12 than stages 9 and 10. *XMyoD* was previously detected by Northern Blot from stage 10 onward with maximal expression at stages 11-19. In these experiments stages 11, 13, and 19 had very similar expression levels, however, the blot was over exposed and may not accurately reflect slight differences in quantity (Hopwood et al., 1989). The other treatments all followed the same trend; there

was minimal or undetectable expression of *XMyoD* mRNA before stage 12. *XMyoD* mRNA levels rose sharply in all treatments at stage 12. These results are given in Figure 29. The highest mean *XMyoD* mRNA levels were from H2A injected embryos (15.4) with uninjected and *H2A.Z* mRNA injected embryos having similar mean measurements (11.4 and 11.8) and NQdn the lowest mean *XMyoD* mRNA level (9.7). However, as with *Gsc* mRNA the differences in *XMyoD* mRNA levels were not significant ($p \geq 0.11$ see Table 7) between the various treatments. *XMyoD* was chosen for investigation because it was a later downstream mesodermal gene and therefore likely to be perturbed if cell fate was affected. These results find no significant difference from normal in NQdn embryos and therefore no evidence for H2A.Z function being essential for cell fate.

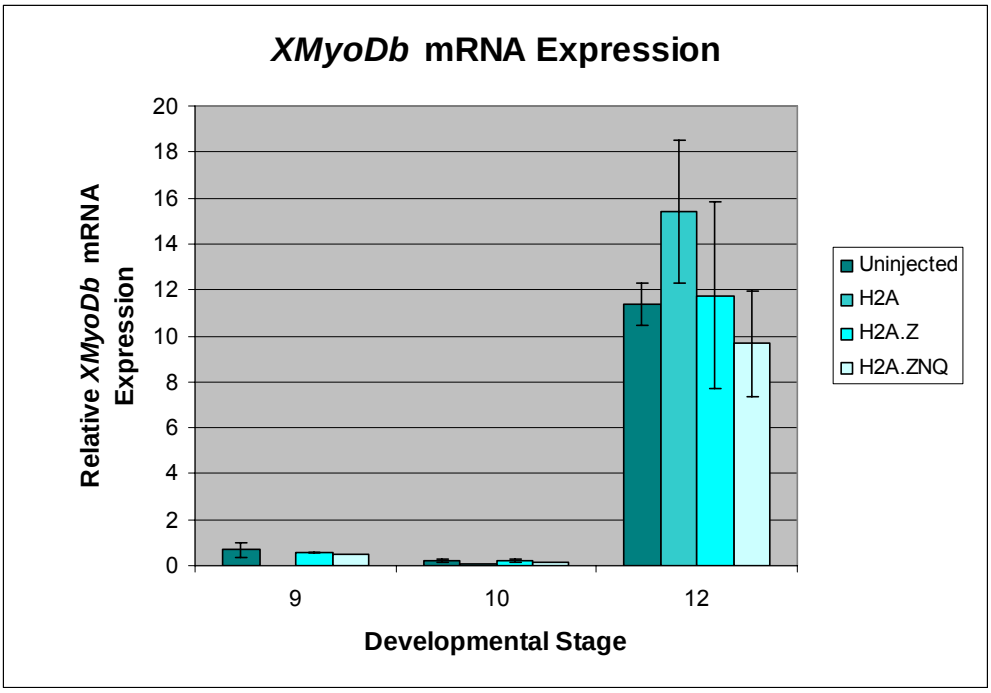

Figure 29 ***XMyoDb* mRNA when H2A.Z function is perturbed**. Embryos were injected with mRNA encoding H2A, H2A.Z or a dominant negative H2A.Z (H2A.ZNQ). Histograms are means of data from pooled sibling sets. Error bars indicate SEM. For uninjected sibling sets at stage 9 n = 3, stage 10 n = 4 and stage 12 n = 8. For H2A mRNA injected sibling sets at stage 10 n = 1 and stage 12 n = 3. For H2A.Z mRNA injected sibling sets at stage 9 n = 3, and for stages 10 and 12 n = 3. For H2A.ZNQ mRNA injected sibling sets at stage 9 and 10 n = 1, and for stage 10 n = 3. Data is given as expression relative to *H4* and a reference sample at stage 9 as described in 2.5.4.2.

Table 7 provides the p values for all the results from injected embryos (Figure 27-Figure 29) for which sufficient repeats were performed before abandoning the RT-PCR technique. The mRNA expression of the investigated marker genes in the injected embryos was never significantly different for uninjected siblings, the lowest p value was 0.07 for *Xbra* mRNA expression in *H2A.Z* mRNA injected embryos, the highest 0.94 for *Gsc* mRNA expression in NQdn embryos. These p values where not unexpected considering the variability in the data for these results (as indicated by the SEM error bars Figure 27 to Figure 28, and p values Table 7). Certainly the differences between the various treatments used in these experiments are small (less than three-fold) compared to the more than ten-fold decrease in *XMyoD* mRNA expression at stage 12 with TSA treatment (see 3.2.2.1, Figure 14). The RT real-time PCR technique is capable of producing lower p values as is demonstrated by analysis of the data for endogenous *H2A.Z* mRNA expression from section 3.2.2.2, Figure 15. The p values of endogenous *H2A.Z* mRNA expression in wild type embryos at stages 10, 12 and 20 is compared to stage 9 endogenous *H2A.Z* mRNA expression (Table 7). It is assumed that the higher p value for stage 10 is due to similarities in H2A.Z levels in stage 10 and late stage 9 embryos. From these results I conclude that when H2A.Z function is perturbed the expression levels of early (*Gsc, Xbra*) and downstream (*XMyoD*) markers for mesodermal cell fate are not perturbed. If perturbing H2A.Z function does not alter the mRNA expression levels of mesodermal marker genes this is likely to be because H2A.Z does not play a major role in cell fate determination. However, on the basis of these results the expression of mesodermal genes in inappropriate locations cannot be excluded. Therefore, localisation of marker gene mRNA by whole mount *in-situ* hybridisation was examined.

		cDNA amplified			
		Gsc	***XMyoD***	***Xbra***	***H2A.Z***
mRNA injected	**Uninj.**	NA	NA	NA	Stage 10: 0.1589 Stage 12: 0.0002 Stage 20: 0.0162
	H2A	Stage 9: 0.3134 Stage 10: 0.5744 Stage 12: 0.1582	Stage 9: NA Stage 10: NA Stage 12: 0.1144	Stage 9: NA Stage 10: NA Stage 12: 0.1963	NA
	H2A.Z	Stage 9: 0.3118 Stage 10: 0.6485 Stage 12: 0.2195	Stage 9: 0.8206 Stage 10: 0.9772 Stage 12: 0.8911	Stage 9: 0.0653 Stage 10: 0.1808 Stage 12: 0.9254	NA
	H2A.Z NQ	Stage 9: 0.2009 Stage 10: 0.9398 Stage 12: 0.2989	Stage 9: NA Stage 10: NA Stage 12: 0.4147	Stage 9: 0.6705 Stage 10: 0.4849 Stage 12: 0.9207	NA

Table 7 **P values for differences in mRNA levels for different treatments.** P values for treatments compared to uninjected controls at the same stage of development for the results given in figures 27, 28, and 29. *H2A, H2A.Z,* and *H2A.ZNQ* mRNA was injected into the embryos at the two cell stage and Uninj. is uninjected wild type control embryos. NA indicates not applicable or insufficient repeat to calculate P value.

4.2.2 Impaired H2A.Z function and the localisation of mesodermal mRNA

Though mRNA levels of the mesodermal marker genes in whole embryo extracts were not abnormal in the investigated stages when H2A.Z function was perturbed, the morphology of the embryos indicates that there is a defect in mesoderm formation. One possible explanation is that where H2A.Z function is perturbed there is aberrant localisation of differentiated cells without measurable changes in overall mRNA levels for mesodermal marker genes from the whole embryo extracts. To investigate this possibility whole mount *in situ* hybridisation was used to localise mRNA expression from selected mesodermal marker genes at developmental stages during (10 and 12), and just prior to (stage 9), gastrulation, the period when mesodermal cell fates emerge (Figure 30). In these experiments I compared localisation of key mesodermal genes in normal and H2A.Zdn embryos.

At stage 10 *Xbra* mRNA is detected in the marginal zone of both the uninjected (Figure 30, A) and H2A.Zdn (Figure 30, B) embryos. At stage 12 in control embryos (Figure 30, C) *Xbra* mRNA is detected in the marginal zone except for a gap on the dorsal side.

At the same stage the uninjected embryos (Figure 30, D) have a comparable staining pattern for *Xbra* mRNA except that the dorsal gap in staining is wider. At stage 12 injected embryos have the morphological features of stage 11½ embryos. In stage 12 defective embryos the dorsal gap in surface *Xbra* mRNA appears wider in the injected embryos than in the controls (Figure 30). Localisation of *Xbra* mRNA is also an indicator for expression of its repressor Gsc. Expanded expression of Gsc would also result in a wider dorsal gap in *Xbra* expression. However, this explanation is inconsistent with the morphology of the defective embryos since anterior head structures reliant on Gsc are not perturbed.

Similarly, at stage 12 stain for *XMyoD* mRNA is detected in two dorsal-lateral regions in both injected (F) and uninjected (E) embryos. By stage 19/20 stain for *XMyoD* mRNA is restricted to the somites in injected (H) and uninjected (G) embryos though in injected embryos the open blastopore has displaced the stain laterally. This is consistent with developmentally lagging appearance of the embryos. In summary, localisation of *Xbra* and *XMyoD* mRNA in the H2A.Z dominant negative treated embryos appears to be displaced by gross changes in morphology, though the embryo is otherwise normal.

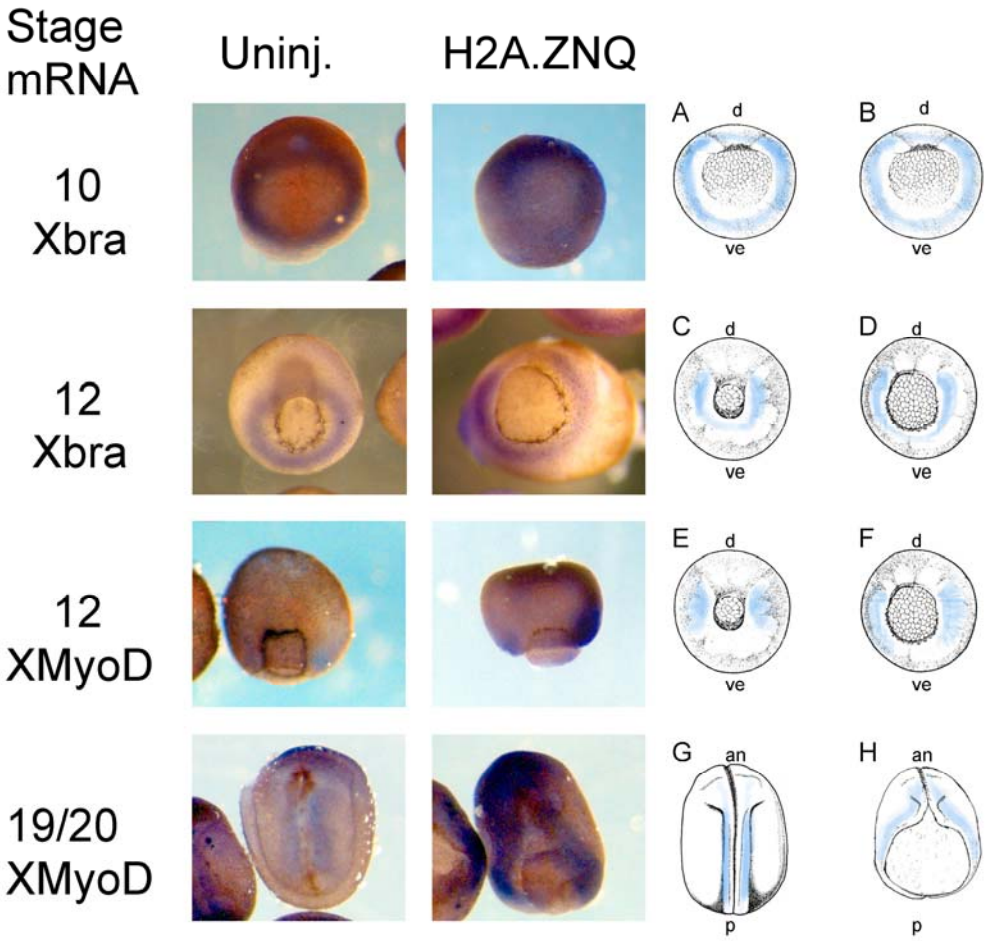

Figure 30: ***Xbra* and *XMyoD* mRNA localisation displaced by abnormal morphology are otherwise normal.** Embryos were uninjected or injected with mRNA encoding a dominant negative H2A.Z (H2A.ZNQ). mRNA detected by BM Purple stain (deep blue to violet). For diagrams A – H: d = dorsal, ve = ventral, an = anterior, and p = posterior. Stained tissues are coloured blue. Drawings for diagrams modified from (Nieuwkoop and Faber, 1994).

4.3 Discussion

This chapter has investigated the level and localisation of transcripts of marker genes for the mesodermal lineage when the function of H2A.Z is perturbed in order to investigate the possibility that H2A.Z is important for correct mesodermal cell fate. That this might be the case was suggested by the morphology of embryos when H2A.Z function was perturbed (see section 1.4.5). H2A.Z could affect mesoderm fate genes by acting to de-repress promoter regions of early dorsal genes such as *Siamois* into a 'poised' state receptive to β-catenin/Tcf-3 or other transcription factors (Fan and Sokol,

1997; Kessler, 1997; Laurent et al., 1997). These could then affect the expression of mesodermal genes downstream, for example Siamois is a transcriptional activator of *Gsc* (Fan and Sokol, 1997; Kessler, 1997; Laurent et al., 1997), eventually producing proper mesoderm formation and morphology which in H2A.Z dominant negative expressing embryos is perturbed (see 1.4.5). The pathways that determine mesodermal cell fate are conserved (Rocheleau et al., 1997) and applied in numerous contexts throughout an organism's life (Ishikawa et al., 2001; Kuhnert et al., 2004; Pinto et al., 2003; Shackleton et al., 2006; Wright et al., 1999). Understanding these pathways is important for advancing biological knowledge and developing new medical treatments. For example, throughout the life of an organism the Wnt pathway acts in numerous contexts. Wnts are known to have numerous functions including cell fate, axis determination, proliferation, cell polarity and migration (Bocchinfuso et al., 1999; Ishikawa et al., 2001; Pinto et al., 2003; van de Wetering et al., 2002; Wright et al., 1999). More specifically, Wnt signalling is implicated in maintenance of adult stem cell niches (Kuhnert et al., 2004; Shackleton et al., 2006) and the ontogeny of cancers of the colon, prostate and melanoma (Hwang et al., 2007; Polakis, 2000; Rubinfeld et al., 1996; van de Wetering et al., 2002; van Es et al., 2003). During early development the canonical Wnt pathway functions in the blastula and gastrula to specify the dorsal-ventral then anterior-posterior axis respectively, and to differentiate mesoderm (Kieker and Niehrs, 2001; Kimelman et al., 1992; Larabell et al., 1997). If H2A.Z is implicated in one or more key developmental signalling pathways for cell fate this would be an important addition to biological knowledge and have medical relevance.

To determine whether H2A.Z has a role in regulating cell fate determination the function of H2A.Z was perturbed by introducing exogenous dominant negative *H2A.Z* mRNA to *X. laevis* embryos at the two-cell stage and comparing the levels and

localisation of marker genes for specific mesodermal tissues at later stages of development, particularly during gastrulation. When the dominant negative H2A.Z (H2A.ZNQ) was introduced the levels of the selected marker genes during gastrulation were not altered (i.e. differences from control embryos were not statistically significant) (Figure 27 to Figure 28, Table 7). Similarly, the localisation of two key transcripts, *Xbra* and *XMyoD*, determined by *in situ* hybridisation at gastrulation and tailbud stages were not perturbed beyond the displacement caused by the gross distortions in morphology (Figure 30). These results demonstrate that cell fate determination is not affected when H2A.Z function is perturbed.

Several mesodermal marker genes were investigated; *Gsc, Xbra, Xvent2,* and *XMyoD. Gooscoid* transcription is a very early zygotic response to maternal canonical Wnt (Wnt11) signalling (Tao et al., 2005). Unlike the other genes *Xvent2* was only investigated with RT-PCR. *Gsc* mRNA levels are not altered when H2A.Z function is perturbed. This is not completely unexpected since maternal Wnt signalling components are most concentrated in dorsal equatorial vegetal blastomeres (blastomeres C1 at stage 6 see section 3.4, Figure 18) (Bauer et al., 1994; Larabell et al., 1997; Wylie et al., 1996), whereas *H2A.Z* transcripts are concentrated animally (section 3.2.3.1, Figure 16). The mesodermal tissues of the trunk form from cells that differentiate and involute through the blastopore later than the prospective head mesoderm. Unlike the head, the trunk morphology is highly perturbed when H2A.Z function was disrupted. The majority of the genes used in this analysis were markers for trunk mesoderm. The levels of markers for dorsal, dorsal-lateral, and ventral-lateral mesoderm, *Xbra, XMyoD,* and *Xvent2* mRNA respectively, are not measurably altered. *Xbra* mRNA levels are normal, supporting the normal (though displaced) localisation of *Xbra* mRNA. The explanation for the wider dorsal gap in *Xbra* mRNA expression when H2A.Z function is perturbed

is not due to repression of transcription by Gsc, as *Gsc* mRNA levels are normal and the delayed appearance of the morphology of the defective embryos during gastrulation adequately explains the localisation of the *Xbra* transcripts. Interestingly, treatment of embryos with the histone deacetylase TSA produces similar defects in morphology (failure of the blastopore to close and shortened trunk) to perturbing H2A.Z function and reduces the mRNA levels of at least one of these marker genes, *XMyoD* (see 3.2.2.1, Figure 14, and also (Steinbach et al., 2000)). This difference between the two treatments indicates that despite similar changes in the morphological appearance of embryos from each treatment the processes that produce these morphologies are different.

Together the selection of genes chosen for RT-PCR, RT real-time PCR, and *in situ* hybridisation investigate the cell fate determinations for numerous mesodermal tissues at several stages of development when normal H2A.Z function is perturbed. No evidence for changes in cell fate determinations was discovered. From these results I conclude that normal H2A.Z function does not have a major role in mesodermal cell fate determinations at gastrulation.

5 H2A.Z has a role in regulating cell movement during early development

5.1 Introduction

This chapter investigates the possibility that H2A.Z affects cell movement by regulating expression of key genes through alterations in chromatin structure (as outlined in 1.1.3 and 4.1). As discussed in Chapter 4 two crucial processes are required for gastrulation and mesoderm formation: cell fate and cell movement. Chapter 4 investigated whether H2A.Z has a role in mesodermal cell fate by determination of the levels and localisation of mRNA for several mesodermal cell fate marker genes in NQdn embryos. No disruption of cell fate was detected in these embryos (see 4.2.1 and 4.2.2). The exclusion of cell fate perturbation led to an alternative explanation for the gross changes in morphology when H2A.Z's developmental function is perturbed; alterations to cell movement.

When H2A.Z function is perturbed larger dorsal gaps are seen in *Xbra* mRNA localisation in gastrula stage embryos (see Figure 30, section 4.2.2). This difference in *Xbra* mRNA localisation compared to normal embryos is not due to lower levels of *Xbra* mRNA (4.2.1.2, Figure 28); rather it is consistent with improper cell movement during convergent extension of marginal zone cells. A disruption to convergent extension would also explain the apparent delay in gastrulation and defective blastopore closure in NQdn embryos (Ridgway et al., 2004a) (Sive et al., 2000). Therefore this chapter will investigate the possibility that H2A.Z has a role in cell movement.

5.1.1 Cell movement during early development

Cell movements during development are of several types including involution, convergent extension, epiboly, and migration. Involution is the folding in of one layer of cells to move beneath another layer. Convergent extension is a process where cells slide over and between each other toward a midline or mid-point reducing surface area and creating a thicker tissue. Epiboly is a similar movement of cells sliding over each other, this time away from a central point or centre-line creating a thinning sheet of tissue with a greater surface area, and migration is the movement of cells relative to an underlying surface. Cells conduct coordinated cell movements in specific directions at particular times during development to produce embryonic patterning.One context where coordinated cell movements are both important and well described is gastrulation in *X. laevis* embryos (Figure 31 and Figure 32). During cleavage divisions there is no cell movement, it is shortly after the MBT that movements begin. By stage 10 bottle cells (dark green cells Figure 31 and Figure 32) deform to begin an involution that creates the lip of the forming blastopore (Figure 31, B; Figure 32, B and F). At the same time a layer of tissue originating at the animal cap is undergoing epiboly, partially driven by outward osmotic forces generated in the blastocoel (Bauer et al., 1994). Forces generated by this epiboly displace marginal zone cells vegetally. A subset of marginal zone cells undergo convergent extension toward the dorsal midline (purple and dark blue cells Figure 31, A and B) driving more vegetal cells towards the blastopore lip and involution thus creating a mesodermal layer (purple and orange cells Figure 31, B and C; Figure 32, F, G, J and K). Formation of further involuting bottle cells laterally extends the lip until it encircles the yolky vegetal cells (stage 11) and epiboly away from the animal pole pushes more marginal zone cells down and around the blastopore lip (Figure 32, G and K). The leading edge of the dorsal mesoderm, the endomesoderm (orange cells Figure 31 and Figure 32), migrates across the roof of the

blastocoel guided by fibronectin adhesion (orange cells, Figure 31, C; Figure 32, F, G; and J, K) (Tada and Smith, 2000) while the trailing mesodermal tissue continues to undergo convergent extension progressively lengthening the embryo (purple cells, Figure 32, G, and H). By stage 14 the anterior-posterior (A-P) axis has been lengthened by combination of forces including a convergent extension and a push from epiboly of ectoderm descended from animal cap cells. These same forces close the blastopore thereby ending gastrulation (Figure 32, D, H, and L) (Keller, 2002). Clearly this program of cell movement is essential for correct morphological development.

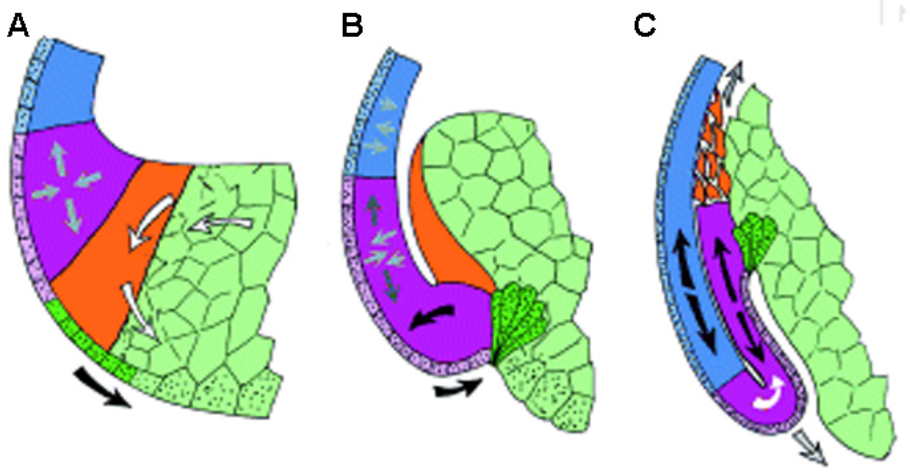

Figure 31 **Initial cell movements in gastrulation**. Diagrams illustrate initial movement of cells and tissues during gastrulation. The presumptive bottle cells (green) undergo apical constriction and apical-basal elongation (A-C). Bottle cell apical constriction (black arrow, A) and Winklbauer vegetal endodermal rotation movements (white arrows, A) form the blastopore lip and place mesendoderm (orange) against the blastocoel roof (A-B), initiating the involution of the IMZ (black arrows, B). This is followed by convergence and extension of the neural and mesodermal tissue (black arrows, C). Mesendoderm migrates over the blastocoel roof (grey arrow, C). Adapted from (Keller et al., 2003).

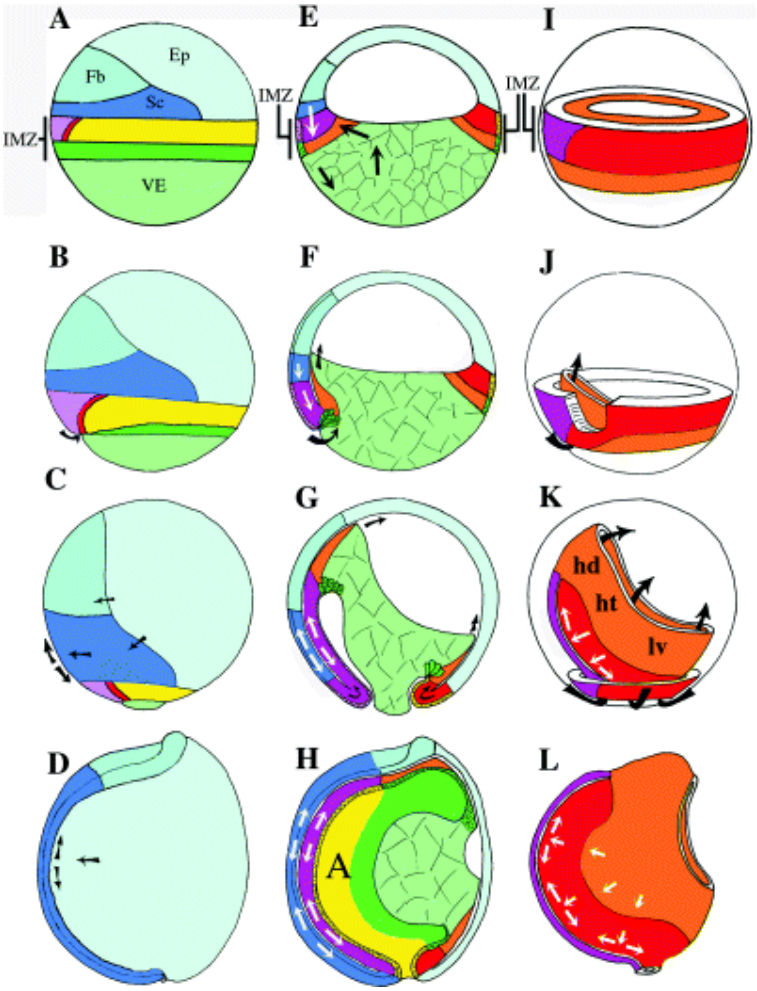

Figure 32 **Cell and tissue movement during gastrulation**. Cell movements given as arrows. Views in diagrams are: (A-D) right lateral, (E-H) midsagittal plane, and (I-L) perspective diagram of the involuting marginal zone (IMZ) tissues. Cell fates colour coded: dark green, bottle cells; orange, dorsal IMZ/endomesoderm; purple, prospective notochord/notochord; light blue, prospective epidermis (Ep); aqua, prospective forebrain (Fb); dark blue, prospective spinal cord (Sc); yellow, superficial endoderm; light green, vegetal endoderm (VE); purple, notochord; red, somitic mesoderm; orange, endomesoderm of the head (hd), heart (ht), and lateral ventral body (lv). (H) 'A' indicates archenteron. Taken from (Keller et al., 2003).

A principle tissue for A-P lengthening of embryos is the notochord (purple cells, Figure 32, H and L), a rod of cells formed by convergent extension of a subset of mesodermal cells toward the dorsal midline (purple cells, Figure 31 and Figure 32). Convergent extension of the mesodermal cells is illustrated in Figure 33. Intercalcation of cells produces tissue lengthening in the A-P axis while reducing its dimensions in both the D-V and sagittal axes. The formation of the resulting rod of tissue applies force, stretching the entire trunk along the A-P axis. The notochord also forms a physical support for

folding of the neural plate (dark blue cells, Figure 32) that eventually closes to form the neural tube (Montcouquiol et al., 2006). The morphology of H2A.Zdn embryos (see 1.4.5) includes failure of neural tube closure, therefore investigation of convergent extension may shed light on the role of H2A.Z in vertebrate development.

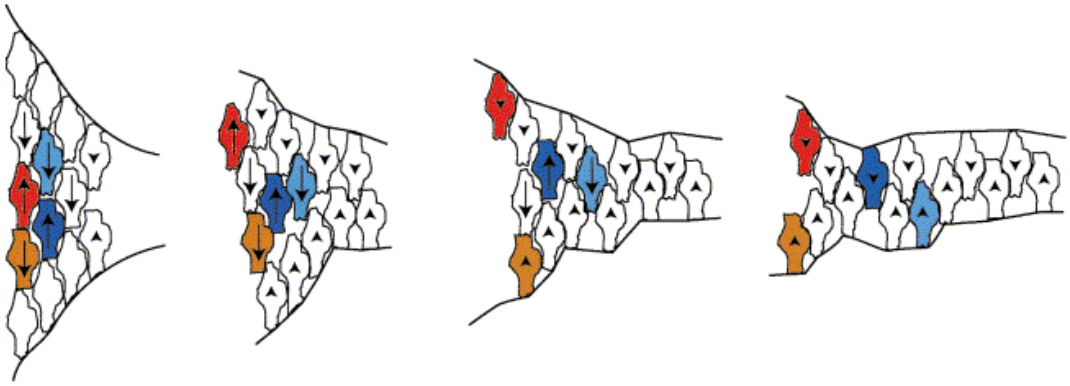

Figure 33 **Convergent extension in *X. laevis* mesoderm**. Diagram showing how convergent extension of mesoderm toward the A-P midline produces an elongation of tissue along the A-P axis. Adapted from (Wallingford et al., 2002).

5.1.2 H2A.Z expression has a role in convergent extension?

Cell movements are regulated by intracellular signalling pathways. Figure 34 is a schematic showing three cell signalling pathways important for development; the canonical Wnt pathway (green), the planar cell polarity (PCP) pathway (purple) and the calcium mediated pathway (blue). Different Wnt proteins signal each pathway, eg. Wnt8 signals the canonical pathway (Fagotto et al., 1997), whereas Wnt11 can initiate both PCP and canonical Wnt responses and Wnt5a calcium mediated signalling (Figure 34) (Tao et al., 2005; Wallingford et al., 2002; Wallingford et al., 2001). The canonical Wnt pathway (green labelled portions of Figure 34) is distinguished from other Wnt pathways by its disrupting β-catenin stabilisation via GSK-3 to produce dorsal cell fates (Larabell et al., 1997; Tao et al., 2005; Weaver and Kimelman, 2004), inducing markers such as *MyoD* (Hoppler et al., 1996). Since in Chapter 4 we demonstrated H2A.Z does not influence cell fate, the canonical Wnt pathway will not be discussed at length.

The PCP pathway (purple labelled portions of Figure 34) was discovered when Xwnt11 was found to signal gastrulation movements using Wnt pathway components such as Frizzled (Fz) and Dishevelled (Dsh), without key components of the canonical Wnt pathway such as β-catenin and GSK-3 (Cadigan and Nusse, 1997). Instead the signal is transduced through other molecules including Prickle (Gubb et al., 1999; Wallingford et al., 2002), Strabismus (Stbm) (Torban et al., 2004) and Knypek (Topczewski et al., 2001). The PCP pathway is also important for convergent extension of mesoderm and notochord (Keller, 2002; Wallingford et al., 2000). Given that cell fate is not affected, the PCP signalling pathway that regulates convergent extension becomes an obvious target for further investigation.

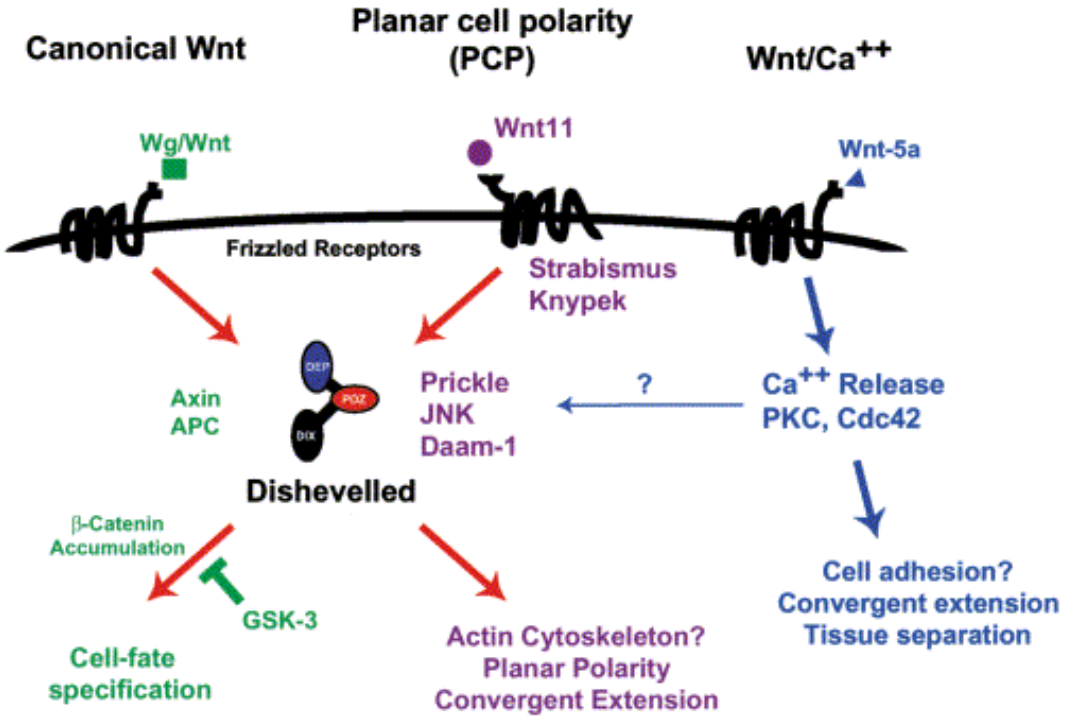

Figure 34 **Canonical Wnt, PCP and Ca^{2+} mediated signalling pathways**. PCP pathway components are shown in purple, canonical Wnt components in green and components of the calcium mediated Wnt pathway in blue. Conserved domains of Dsh are shown schematically DEP (blue), PDZ (red), DIX (black). Adapted from (Wallingford et al., 2002).

The final pathway is the calcium mediated pathway (blue components of Figure 34) (Kuhl et al., 2001; Kuhl et al., 2000; Wallingford et al., 2001) where a Wnt signal

invokes an intracellular calcium release as part of a signalling pathway that inhibits cell adhesion. Whether the calcium mediated pathway inhibits convergent extension is uncertain, with experiments blocking the Ca^{2+} mediated pathway producing conflicting results (Torres et al., 1996; Wallingford et al., 2002; Winklbauer et al., 2001). To explain the discrepancies it has also been proposed that this pathway modulates both the PCP and canonical Wnt pathways (Kuhl et al., 2001).

Previous results indicate that H2A.Z may have a role in convergent extension. If this is the case then it may be through perturbing expression of signalling genes. Interestingly, perturbed expression of PCP pathway components, including Wnt11, Fz-7, Stbm, Dsh, and Daam-1, disrupts convergent extension resulting in *X. laevis* embryos with a similar phenotype to the H2A.Zdn embryos (open blastopore, failure of the neural tube to close properly and shortened trunk) (Djiane et al., 2000; Habas et al., 2001; Itoh et al., 2005; Tada and Smith, 2000; Torban et al., 2004; Wallingford et al., 2000). For example, overexpression of Fz7 and/or Wnt11 produces the above defect (Djiane et al., 2000). Expression levels of markers for cell fate, *Gsc* and *Xbra,* are unaffected when Fz7 is overexpressed. However, overexpression of Fz7 and/or Wnt11, does perturb the localisation of these markers and convergent extension is disrupted (Djiane et al., 2000). Like H2A.Zdn embryos, disruption of PCP components does not perturb cell fate (Djiane et al., 2005; Wallingford et al., 2000; Wallingford et al., 2001). It is thought that in the example above over-stimulation of PCP signalling perturbs cell polarity by increasing motility of cytoskeletal elements (Axelrod et al., 1998; Wallingford et al., 2002).

A key protein in Wnt signalling is dishevelled (Dsh). Lowering Dsh expression resulted in a defect strikingly similar to H2A.Zdn embryos (see Figure 35 compare to Figure 6 section 1.4.5) (Itoh et al., 2005; Wallingford et al., 2000). Convergent extension is

disrupted when Dsh levels are lowered (Tada and Smith, 2000; Wallingford and Harland, 2001; Wallingford et al., 2000). Since the H2A.Zdn defect is consistent with disrupted convergent extension by perturbation of the PCP pathway, and Dsh plays a central role in that pathway, I investigated whether convergent extension is disrupted in H2A.Zdn embryos and whether *Dsh* expression is perturbed.

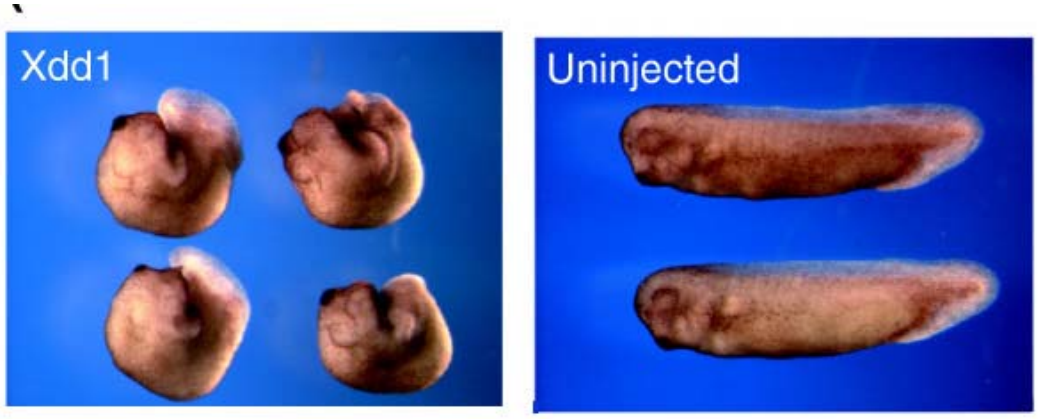

Figure 35 **Morphology of embryos when Dsh function is disrupted**. (Xdd1) Four-cell embryos were injected with 0.6 ng Xdd1 RNA into two vegetal dorsal blastomeres. The injected embryos were allowed to develop until the sibling embryos reached stage 32. (Uninjected) uninjected stage 32 siblings to the embryos shown in the Xdd1 panel. Adapted from (Itoh et al., 2005).

5.2 Results

5.2.1 Is H2A.Z affecting morphology by disrupting cell movements?

5.2.1.1 Localisation of notochord tissue is altered when H2A.Z function is perturbed.

If H2A.Z has a role in determining proper cell movements during development, and not cell fate, then we would expect that cells for various tissues would be present though spatially displaced. Normal notochord is a sharply defined tissue that requires proper convergent extension to form. Xbra is a transcription factor its expression is pan-mesodermal in the early embryo then becomes restricted to the notochord in neurula and tailbud embryos (Artinger et al., 1997; Gont et al., 1993; Herrmann et al., 1990; Latinkic and Smith, 1999; Latinkic et al., 1997; Panitz et al., 1998; Smith et al., 1991;

Xu et al., 2000). In *X. laevis* a combination of *Xbra* co-expressed with another transcription factor *Pintallavis* induces notochord formation (O'Reilly et al., 1995). Since *Xbra* mRNA levels are unchanged when H2A.Z function is perturbed (see 4.2.1.2, Figure 28) it is likely that a normal number of notochord cells are present. However, morphology and *Xbra* mRNA localisation indicate these embryos may not undergo sufficient convergent extension to properly form a notochord and thus elongate the embryo. To determine if this is the case a molecular marker for notochord cells, *Xbcan* mRNA (Sander et al., 2001), was used to detect the presence and localisation of notochord cells in uninjected and NQdn embryos.

Embryos were collected at two stages when the notochord is present and well developed, stages 20 and 33/34 (Nieuwkoop and Faber, 1994). As shown in Figure 36, at stage 20 the uninjected embryos show a well defined notochord at the midline below fused neural folds (Figure 36, A-C). In embryos where H2A.Z function is perturbed the notochord is bifurcated and improperly organised (Figure 36, D-F) indicating that gastrulation is incomplete and that the increased distance between the neural folds prevents closure of the neural tube. This morphology is consistent with previous experiments to disrupt H2A.Z function (compare to Figure 6 section 1.4.5, (Itoh et al., 2005)) and those that disrupt Dsh's function in convergent extension (Figure 35, (Ridgway et al., 2004a)). At stage 33/34 uninjected embryos are normally developed (Figure 36, G and H) (the bowing of the uninjected embryos is due to dehydration during the procedure) and a well defined notochord was stained for *Xbcan* mRNA. In the stage 33/34 NQdn embryos initial experiments failed to detect any staining, perhaps because of more dispersed nature of *Xbcan* mRNA-expressing cells in these embryos. Allowing stain to further develop resulted in specifically stained tissues near the edge of the open blastopore, though not until non-specific staining made this observation

difficult. The image provided (Figure 36, I) is therefore somewhat understained. When H2A.Z function is perturbed the notochord remains bifurcated at stage 33/34 and is shortened and diffuse compared to uninjected embryos. The neural folds also continue to fail to fuse resulting in the persistence of the dorsal opening and two short 'tails' of tissue posteriorly (Figure 36, J). Despite these deformities anterior head structures including the eye and cement gland appear normal. In the NQdn embryos a molecular marker for notochord, *Xbcan* mRNA, is present (Figure 36, I and J) indicating that cells are still being induced into the notochord cell fate and it is the movements necessary for proper convergent extension during notochord formation that are disrupted.

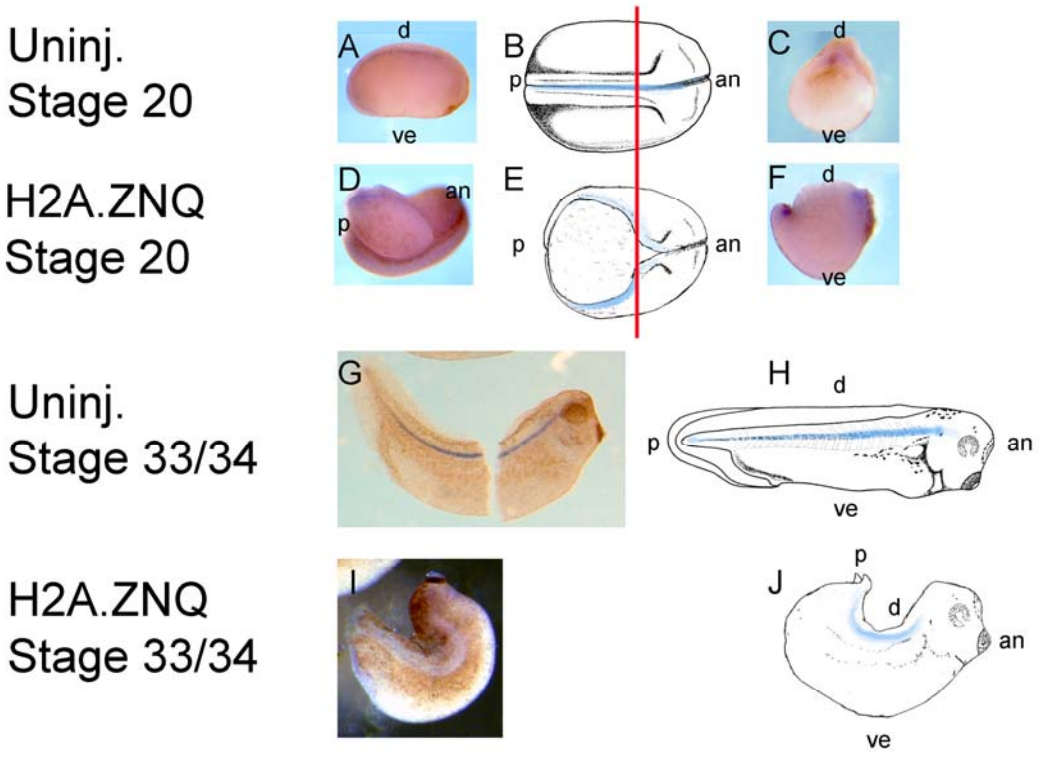

Figure 36: **Notochord development is disrupted when H2A.Z function is perturbed.** Embryos were either injected with H2A.ZNQ mRNA (D, F and I) or uninjected (A, C and G). Embryos were collected for *in situ* hybridisation staining of *Xbcan* a marker for notochord at stages 20 (A-F) and 33/34 (G-J). Schematics showing morphology and staining (B,E,H and J) are adapted from standard tables (Nieuwkoop and Faber, 1994). Orientation is shown thus: d, dorsal; ve, ventral; p, posterior; an, anterior.

5.2.1.2 Perturbing H2A.Z function does not alter the expression levels of *Dishevelled.*

Dsh is a key signalling protein for initiating convergent extension (Djiane et al., 2005; Wallingford et al., 2000; Wallingford et al., 2001) (Figure 34). That Daam-1 links Dsh to actin of the cytoskeleton and depletion of Daam-1 prevents convergent extension provides hints at a mechanism of Dsh in convergent extension (Habas et al., 2001). If Dsh levels are lowered or raised this affects cell movement without perturbing cell fate (Djiane et al., 2005; Wallingford et al., 2000; Wallingford et al., 2001). Therefore I next determined whether H2A.Z's developmental function was related to *Dsh* expression.

To determine the levels of *Dsh* mRNA RT real-time PCR was used to compare normal embryos to those injected with RNA encoding H2A, H2A.Z, or the dominant negative H2A.ZNQ. The reasoning behind selecting these various mRNAs for injection was to determine if any changes seen in *Dsh* mRNA level were specific to those embryos injected with the dominant negative (NQdn), and therefore a result of H2A.Z's developmental function as discussed in section 4.1.4.

The relative levels of *Dsh* mRNA are given in Figure 37. Results are relative to a selected stage 9 uninjected reference sample, all marker gene mRNAs were expected to be present at a low level at this stage. *Dsh* mRNA levels were determined at two gastrulation stages, 10 and 12; a period when convergent extension and other cell movements are crucial for proper development (Wallingford et al., 2000). *Dsh* mRNA was detected at both developmental stages for all of the treatments. Similarly, in all stages and treatments *Dsh* mRNA levels were lower in stage 12 than stage 10, this general decrease in *Dsh* mRNA level is consistent with earlier reports (Sokol et al., 1995). There was no correlation between H2A.Zdn morphology and *Dsh* mRNA levels. At both stages of development the *Dsh* mRNA level in H2A.Zdn embryos was less than uninjected embryos (never more than 0.6 less) and within 0.09 of *H2A* mRNA injected

embryos. This indicates that differences in *Dsh* mRNA between H2A.Zdn embryos and uninjected controls are not specific to H2A.Z's developmental function. Rather the differences may be due to the generalized repressive effect of histone overexpression (Clark-Adams et al., 1988). Interestingly, the highest *Dsh* mRNA levels in both stages were recorded in H2A.Z injected embryos. These embryos appear normal except for a delay in development (Ridgway et al., 2004a). Given that *Dsh* mRNA levels fall during development (Sokol et al., 1995) the higher levels in *H2A.Z* mRNA injected embryos is consistent with the observed developmental delay. To further test my conclusion that H2A.Z does not play a specific role in *Dsh* expression I next determined the significance of these results.

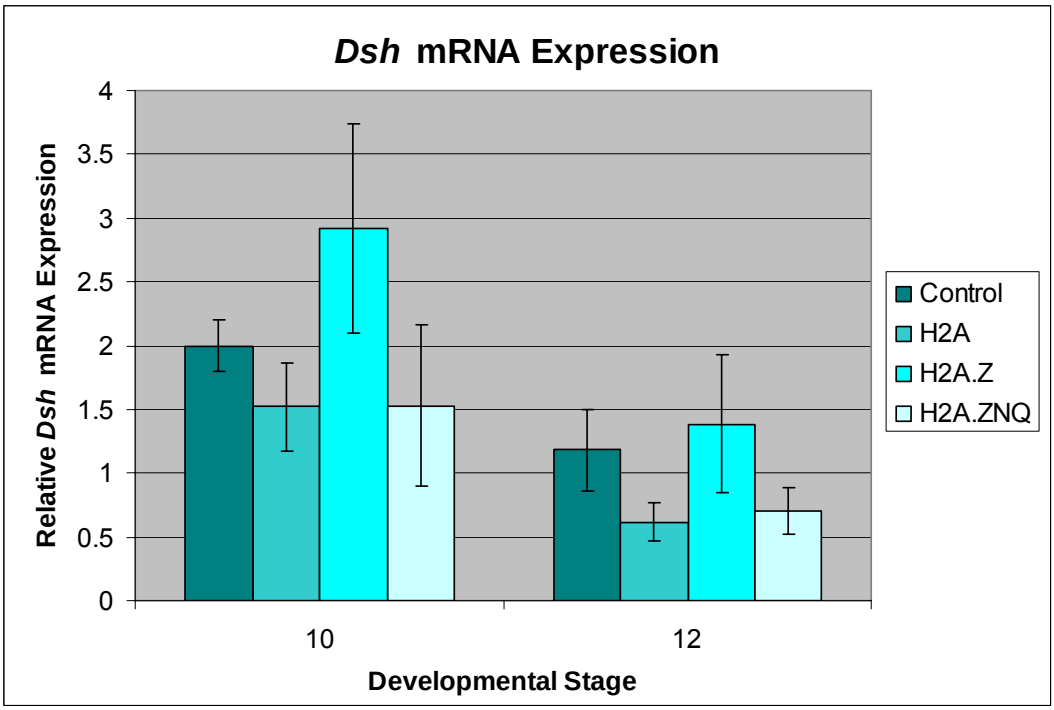

Figure 37 **Levels of *Dsh* mRNA when H2A.Z function is perturbed**. Embryos were injected with mRNA encoding H2A, H2A.Z or a dominant negative H2A.Z (H2A.ZNQ). Histograms are means of results from pooled sibling sets. Error bars indicate SEM. For uninjected sibling sets at stage 10 n = 4 and stage 12 n = 5. For all injected sibling sets n = 3 Data is given as expression relative to *H4* and a reference sample at stage 9 as described in 2.5.4.2.

Final evaluation of the RT real-time PCR results required determination of whether these differences are significant (Table 8), because the variability of the results obtained

was high (as indicated by the size of the SEM error bars relative to the means (Figure 37) and the differences between the mean results for each treatment so small (the largest fold difference was *H2A.Z* mRNA injected embryos compared to NQdn embryos at stage 12, 2.24 fold)). Interpretation of p values was as previously discussed (section 2.5.5). None of the p values were low enough ($p \leq 0.05$) for any treatment mean *Dsh* mRNA level to be considered significantly different to the mean result for uninjected embryos at the same stage. Taken together with the high variability for each *Dsh* mRNA level result and low fold difference between mean *Dsh* mRNA levels of the injected treatments with those from uninjected embryos of the same developmental stage I concluded that there was no significant difference in *Dsh* mRNA levels (Figure 37). Since *Dsh* mRNA is not significantly changed when the developmental function of H2A.Z is perturbed I conclude that H2A.Z does not affect *Dsh* mRNA expression. Therefore, perturbing H2A.Z's developmental function affects cell movement (see 5.2.1.1) and the mechanism is not through regulation of *Dsh* mRNA expression levels.

mRNA injected	**P value**
H2A	Stage 10: 0.258 Stage 12: 0.245
H2A.Z	Stage 10: 0.259 Stage 12: 0.736
H2A.ZNQ	Stage 10: 0.459 Stage 12: 0.324

Table 8 **P values for differences in *Dsh* mRNA levels for different treatments.** P values for injected embryos compared to uninjected embryos at the same stage of development for the results given in Figure 37. *H2A*, *H2A.Z*, and *H2A.ZNQ* indicate the mRNA injected into the embryos at the two cell stage and Uninj. indicates uninjected wild type embryos.

5.3 Discussion

Previously, a developmental function has been proposed for H2A.Z in metazoans that is linked to a conserved histidine motif (Ridgway et al., 2004a). The results presented here support a role for H2A.Z in convergent extension cell movement during development. Firstly, in embryos with H2A.Z perturbed, though notochord cells are present the notochord is not properly formed, producing embryos with shortened trunks indicating H2A.Z is necessary for proper cell movement rather than cell fate. Secondly, head structures including the cement gland and the eye appear normal suggesting migration of the endomesoderm is unaffected. Taken together these morphological observations are consistent with convergent extension being affected when H2A.Z's function is perturbed. As with disruption to H2A.Z's function, perturbations of PCP pathway molecules have been shown to disrupt convergent extension and not cell fate (Wallingford et al., 2002). The embryos resulting from perturbations of PCP pathway components including Wnt11, Stbm, and Fz-7 also have morphology similar to embryos where H2A.Z's function is perturbed (see section 5.1.2 including Figure 34 Figure 35) (Djiane et al., 2000; Tada and Smith, 2000; Torban et al., 2004). Given these similarities, I investigated whether H2A.Z's role in convergent extension was due to disruption of the PCP pathway. Dsh is a key molecule for PCP signalling. A combination of altered Dsh levels and preferential cellular localisation of the Dsh could explain the observed disruption of convergent extension. My investigation revealed that H2A.Z's normal developmental function is not regulating *Dsh* transcription directly or indirectly. Future work will investigate the mechanism of H2A.Z's role in convergent extension.

There are many possible ways H2A.Z function could impact on cell movement. H2A.Z could affect transcription of other signaling components upstream or downstream of

Dsh (such as Frizzled-7 (Djiane et al., 2000), or JNK (Yamanaka et al., 2002)) or molecules affecting translation, or cellular localization of Dsh protein. Wnt11 (upstream of Dsh in the PCP pathway) is a downstream target of Xbra (Tada and Smith, 2000) and I have shown *Xbra* expression is unaffected by perturbing H2A.Z function (4.2.1). This indicates the perturbation could be after Wnt11 in the PCP pathway, such as a block of signal transduction because of Fz over- or under-expression (Tada and Smith, 2000) (Figure 34 section 5.1.2). More work is needed to test this idea.

Alternatively, since both correct Dsh levels and proper cellular localisation are required for regulation of Dsh's functions (Djiane et al., 2000), H2A.Z could be affecting one or more molecules required for correct Dsh localisation. The importance of Dsh localisation begins shortly after fertilisation when small vesicles containing the Dsh protein are transported to the dorsal side of the egg. This initial localisation establishes the dorsal-ventral axis by specifying dorsal cell fates (Miller et al., 1999; Rowning et al., 1997; Weaver et al., 2003; Weaver and Kimelman, 2004). The cells that do not inherit maternal Dsh follow the default ventral cell fate (Miller et al., 1999; Rowning et al., 1997; Weaver et al., 2003; Weaver and Kimelman, 2004). At later stages of development, including the period of gastrulation, the localisation of Dsh is generally cytoplasmic, except Dsh translocates to the cell membrane in cells undergoing convergent extension (Wallingford et al., 2000). The protein Stabismus (Stbm) has been shown to be crucial for the localisation of Dsh to the cell membrane and an agonist of canonical Wnt signalling (Park and Moon, 2002) (in human and mouse there are two homologues, *Vangl1* and *Vangl2* (Kibar et al., 2001; Torban et al., 2004). Stbm is one of the PCP pathway components that when perturbed produces a H2A.Zdn-like phenotype (Park and Moon, 2002) (section 5.1.2). Conversely, transient nuclear localisation is required for Dsh's function in the canonical Wnt pathway (Itoh et al.,

2005). Given the central role localization has in Dsh function future work will investigate whether localization of Dsh to the cell membrane or transduction out of the nucleus to the cytoplasm is disrupted when H2A.Z function is perturbed. The ability to manipulate Dsh localization by mutating the DIX and DEP domains (Tada and Smith, 2000) provides a crucial tool for these further investigations.

6 General discussion

This project investigated the developmental role of H2A.Z during gastrulation and mesoderm formation in *X. laevis*. It was determined that H2A.Z is required for mesoderm cell movement including convergent extension. The evidence for this is threefold. Firstly, *H2A.Z* mRNA localises to mesodermal lineages that undergo cell movement from the early blastula (3.2.3.1) through to tailbud (3.3) and the expression levels of *H2A.Z* mRNA peak during gastrulation, a period of intensive cell movement (3.2.2.2). Secondly, there is no evidence to implicate H2A.Z in mesodermal cell fate determination, the other major process of development at this stage (4.2). Finally, the disruption of H2A.Z perturbs movement of specific tissues in a manner consistent with convergent extension (5.2.1.1).

This chapter clarifies how H2A.Z, a nuclear protein, could effect cell movement during development and may be involved in specifying cell lineages in the early blastula that will later undergo cell movement. The significance of this work is discussed, including its contribution toward understanding the aetiologies of congenital defects and wider implications beyond embryonic development. Finally, directions for future investigations of H2A.Z's developmental role are given.

6.1 H2A.Z incorporation in chromatin structure and gene expression

As discussed in section 1.1 chromatin structure can alter the transcription of genes in a global and targeted manner. Global changes to expression occur through the establishment of large structural domains, whereas targeted changes are produced by localised changes to chromatin structure. H2A.Z occurs in large chromatin domains (1.2.3) (Greaves et al., 2006; Greaves et al., 2007; Meneghini et al., 2003), for example

it is located in the centromere (Greaves et al., 2007). H2A.Z's function in chromosome segregation and genome stability are due to it's presence in this structural domain (Greaves et al., 2007). This role of H2A.Z has been suggested to be dependent on an extended acidic patch on the H2A.Z-containing nucleosome's surface that alters interactions with the H4 tail of the adjacent nucleosome (Suto et al., 2000), thus favouring 30nm fibre formation promoting a 'poised' chromatin state that can be further modified (Fan et al., 2002). H2A.Z is known to bind to INCENP (Greaves et al., 2006). The M6 region was essential for this binding (Greaves et al., 2006). The M7 region containing the histidine motif was not (Greaves et al., 2006). This indicates that H2A.Z's localisation to the centromere and potential role in genome stability (discussed in section 1.2.3) may be initiated in early zygotic cells of mammals. This evidence also indicates that H2A.Z may have a separate role in development, relying distinct features of the H2A.Z containing nucleosome. This project has shown that the role of H2A.Z in vertebrate gastrulation is not likely to be due to the effect of the H2A.Z extended acidic patch on chromatin structure. A histidine motif, separate from the extended acidic patch, is required for H2A.Z's developmental function (Ridgway et al., 2004a). This motif is a putative protein-protein interaction site (Suto et al., 2000), suggesting that H2A.Z may specifically alter the transcription of genes encoded by DNA associated with H2A.Z-containing nucleosomes through interactions with as yet unidentified proteins. H2A.Z is incorporated into nucleosomes by targeted chromatin remodelling (1.2.3) (Jin et al., 2005; Kobor et al., 2004; Mizuguchi et al., 2004; Redon et al., 2002), providing a mechanism whereby specific genes can be affected and H2A.Z non-randomly distributed (Jin et al., 2005; Krogan et al., 2003; Mizuguchi et al., 2004; Ruhl et al., 2006). In *C. elegans* targeting of H2A.Z to specific foregut genes requires PHA-4 (Updike and Mango, 2006), a homologue of transcription factor human FoxA, however

the mechanism has yet to be elucidated. The authors were careful to point out that their experiments do not preclude H2A.Z's interaction with other transcription factors (Updike and Mango, 2006). The relationship between this histidine motif and the transcription factor dependent targeting of H2A.Z seen in *C. elegans* remains unknown. It is tantalising to speculate that the targeting of H2A.Z to developmentally important genes by context specific transcription factors in metazoans is as widespread and conserved as the SWR1 incorporation of H2A.Z into nucleosomes (see 1.2.3).

In this thesis I have shown that H2A.Z may be targeted to genes within signalling pathways for cell movement (or target genes of these pathways) required for proper development (5.2.1, 5.3) not to gene expression pathways for cell fate (4.2.1). With the information now at hand we can propose a preliminary model for H2A.Z's action during development. H2A.Z is incorporated into chromatin at specific sites targeted by the SRCAP complex (Ruhl et al., 2006). Once incorporated, the presence of H2A.Z favours a 'poised' chromatin structure due to interactions between the extended acidic patch and H4 tail of an adjacent nucleosome (Fan et al., 2002; Suto et al., 2000). Interactions between the histidine motif and unidentified proteins could then target the chromatin for further modifications to produce open or closed structures, or binding sites, resulting in repression or enhancement of transcription (there is a wealth of evidence for H2A.Z's involvement in transcriptional regulation (1.2.4) (Albert et al., 2007; Farris et al., 2005). The altered transcription of the targeted genes could then, through their products, regulate signalling pathways for cell movement such as the PCP pathway.

6.2 H2A.Z and cell movement specification from the early blastula

That early maternal *H2A.Z* mRNA expression is asymmetrically restricted in the early blastula, (stage 5) before the mid-blastula transition, to lineages that later undergo cell movement indicates H2A.Z may contribute to specification of cell movement. Asymmetrical localization of maternal mRNA is not unprecedented, some other maternal mRNAs are localized to the future dorsal region of the cytoplasm of the fertilized egg by cortical cytoplasm rotation and cytoskeletal movement of organelles (Elinson and Rowning, 1988; Tao et al., 2005; Vincent et al., 1986; White and Heasman, 2007). It seems likely that the same mechanisms localize maternal *H2A.Z* transcripts.

Two signals later implicated in cell movement are present as maternal transcripts in pre-MBT *X. laevis* embryos; *Wnt5a* and *Wnt11*. Wnt5a can signal convergent extension through the Calcium (Ca^{2+}) mediated pathway, however maternal mRNA is not localized to the dorsal side (Moon et al., 1993) and therefore cannot specify which cells undergo convergent extension. Wnt11 from maternal mRNA is the axis determinant found to act through the canonical Wnt pathway and cell fate after the MBT (Tao et al., 2005). The PCP pathway does not activate until gastrulation and Wnt11 can signal though both pathways at this point (Djiane et al., 2000; Tada and Smith, 2000; Tao et al., 2005). Something more is needed to specify PCP signaling through Wnt11 in gastrula mesoderm. Since neither of these maternally expressed cell movement signaling molecules are cell movement determinants the identity of the molecule that first specifies cell movement is unknown.

This thesis research places H2A.Z as a candidate for the cell movement determinant. The increased presence of maternally transcribed H2A.Z in specific dorsal lineages may facilitate the completion of signaling pathways for cell movement, such as the PCP and

calcium mediated pathways, by regulating the expression of key genes. One hypothesis worth testing is that the enrichment of maternal H2A.Z enables Wnt11 signaling through the PCP pathway. If true, cells without maternal H2A.Z enrichment only respond to Wnt11 via the canonical pathway. In this way maternal H2A.Z would specify lineages to undergo cell movement post MBT.

6.2.1 H2A.Z is co-localized to PCP pathway components in mesoderm

Beyond the initial presence of H2A.Z within the blastula, the variant continues to be enriched in mesodermal tissues that undergo cell movements in gastrulae, specifically the dorsal and lateral regions of the marginal zone. In neurulae and tailbud embryos H2A.Z becomes enriched in notochord, a tissue undergoing convergent extension movements. This pattern of localization overlaps with key genes for cell movement. *Xbra* while not part of a pathway for cell movement has a spatial expression pattern that matches regions of H2A.Z enrichment (i.e. Xbra is expressed in the marginal zone and mesodermal tissues of the gastrula and is enriched in notochord) (4.1.3) (Artinger et al., 1997; Gont et al., 1993; Herrmann et al., 1990; Latinkic and Smith, 1999; Latinkic et al., 1997; Panitz et al., 1998; Smith et al., 1991; Xu et al., 2000). This similarity in expression patterns was a reason for determining whether H2A.Z had a role in cell fate determination. While Xbra expression determines mesoderm cell fate not cell movement, Xbra expression induces expression of Wnt11 and Dsh, key proteins for both PCP and canonical Wnt signaling (Sokol, 1996; Tada and Smith, 2000). In mesoderm tissues H2A.Z enrichment matches the localization of gene expression involved in signaling cell movement, supporting a role for H2A.Z in regulating these signaling pathways in mesodermal tissues throughout development.

6.3 H2A.Z and developmental processes

This work is important because it advances our understanding of the role chromatin, and specifically H2A.Z, play in regulation of developmental gene expression and developmental signalling pathways such as the canonical Wnt pathway. Greater understanding of developmental processes will provide foundations for the solutions to problems relating to early developmental processes, such as the detection and treatment of congenital defects and strategies to prevent reproduction in genetically modified or feral animals harmful to the environment.

It may be that the aetiologies of many developmental defects that are inadequately understood may involve chromatin's role in gene regulation. Genetic networks for developmental signalling genes within *C. elegans* found a selection of genes with a large number of connections (hub genes) (Lehner et al., 2006). All hub genes identified are chromatin remodelling components, indicating a central role for chromatin in developmental signalling pathways. Though this study was performed in *C. elegans* these genes have orthologues in other metazoans suggesting that the hub gene characteristic of chromatin remodelling is conserved (Lehner et al., 2006). Interestingly, the expression patterns of remodelling genes are enriched in a stage and tissue specific manner during *X. laevis* development indicating an important role development (Linder et al., 2004). Hub genes are likely to cause susceptibility to genetic diseases for two reasons. Firstly, they are important to diverse functions including signalling, DNA repair, extracellular matrix, and cytoskeletal functions (Lehner et al., 2006). Secondly, it is proposed that the hub genes modulate gene expression to ensure proper biological outcomes despite mutations in signalling molecules or other problems in signalling pathways such as the Wnt or PCP pathways (Lehner et al., 2006). Incorporation of H2A.Z is reliant on one of these chromatin remodelling complexes, SRCAP, and

therefore could be essential to proper regulation of numerous genes and resilience against congenital defects (Ruhl et al., 2006).

6.3.1 Gastrulation, neurulation, and neural tube defects

Neural tube defects (NTDs) are the second most common congenital defects in humans, after heart defects (Frey and Hauser, 2003), affecting approximately 1 in 1000 live births (Padmanabhan, 2006). NTDs are a significant cause of mortality in the first year of human life (Padmanabhan, 2006). Care of NTD patients also has financial and quality of life costs (Padmanabhan, 2006). Neural tube defects in humans have their root in cell movement and cell fate determinations very early in development, however exact aetiologies remain unknown (Keller, 2002; Padmanabhan, 2006) though the role of dietary folic acid in preventing NTDs is well established (Berry et al., 1999). Better understanding of the events that lead to NTDs should improve prevention, detection, and perhaps treatment.

Work already performed in *X. laevis* indicates that perturbing H2A.Z's function during early development leads to improper gastrulation, defective mesoderm development, and neural tube defects (Ridgway et al., 2004a). The use of *X. laevis* was critical to the discovery of this link between H2A.Z and defective neural tube development. The characteristics of other commonly used developmental models would have prevented the discovery. *D. melanogaster* is an invertebrate. In zebrafish the movements of neural tube closure are unlike those of higher vertebrates, zebrafish with a disrupted PCP pathway do not show NTDs (Papan and Campos-Ortega, 1994; Ueno and Greene, 2003). The mouse may be useful in further work, however as a eutherian is technically difficult as an experimental embryonic model.

NTDs occur where there is a failure of neural tube closure, there are two contexts where failure of convergent extension results in these defects (Wallingford and Harland,

2001). Convergent extension is involved during gastrulation for establishing proper mesodermal structures (Keller, 2002). The notochord then induces neural differentiation in overlying ectoderm tissue (Murdoch et al., 2001). In the induced neural plate convergent extension is required for neural tube closure at neurula stages in mice and *X. laevis* (Copp et al., 2003; Kibar et al., 2001; Murdoch et al., 2001; Wallingford et al., 2002). PCP pathway components have been shown to be required for neural tube closure in both organisms (Copp et al., 2003; Kibar et al., 2001; Murdoch et al., 2001; Wallingford et al., 2002).

In embryos where H2A.Z function is perturbed (Ridgway et al., 2004a), improper gastrulation disrupts normal neurulation. *X. laevis* H2A.Zdn embryos phenocopy the most severe human NTD, where the craniorachischisis, cranial neural tube fails to close from the midbrain down the length of the spinal cord (Ueno and Greene, 2003; Wallingford and Harland, 2001). Craniorachischisis accounts for 10-20% of human NTDs (Berry et al., 1999; Murdoch et al., 2001; Seller, 1987). Mesodermal convergent extension failure in *X. laevis* results in neural folds too separated to fuse; therefore defects in mesodermal convergent extension are also causes for some neural tube defects (Keller, 2002). A similar phenotype has been seen in mice when the PCP pathway is disrupted (Kibar et al., 2001; Wang et al., 2006). In mouse, *Dv12* (a Dsh homologue) is required for lengthening and narrowing of the neural plate consistent with convergent extension, and dominant negative *Dvl2s* produce NTDs because the wider gap between the neural folds prevents neural tube closure (Wang et al., 2006). While the blastopore appears to close in these mouse embryos notochord cell localisation is perturbed (Wang et al., 2006), indicating that convergent extension of mesodermal tissues occurs in mammals as observed in *X. laevis*. *X laev*is embryos with neural plate defects similar to those seen in mouse can be obtained by grafting neural

tissue with blocked PCP signalling onto embryos with normal mesoderm (Wallingford and Harland, 2001). However, even when the morphological movements of *X. laevis* models of NTD do not precisely reiterate the human aetiology the differences may be informative regarding the molecular control of the genes and signalling pathways involved. I have shown that *H2A.Z* mRNA is enriched in mesoderm and notochord, not the neural plate. H2A.Z is required for establishing convergent extension at gastrulation and maintaining it in the developing notochord. The developing neural tissue also undergoes convergent extension. H2A.Z may not have a role in neural convergent extension (it is not detectably enriched in this tissue) perhaps due to different details for the same convergent extension pathway(s) in the two tissue types or related to the interplay of the PCP and Ca^{2+} mediated pathways during convergent extension.

6.3.2 Wider Implications

The pathways that determine developmental gene expression in the early embryo are also central to numerous biological processes throughout an organism's life, including wound healing and the progression of cancer (Sato et al., 2004; Sparmann and van Lohuizen, 2006; Ueno and Greene, 2003; van Es et al., 2003). Embryonic development is therefore a model for the basic processes of multicellular life. Interestingly, a macroarray-based analysis identified H2A.Z as up regulated during tail regeneration in *X. laevis* larvae (Tazaki et al., 2005) indicating that the histone variant is utilised in later regulation of differentiation pathways. A better understanding of the regulation of developmental gene expression would improve our understanding of numerous biological processes and illnesses. Applications of this understanding would include new treatments based on the growth of specific differentiated cells to repair damaged tissues, and anti-cancer drugs with greater specificity for cancerous cells.

6.4 Future work

6.4.1 Localization of Dsh

This work found no change in *Dsh* mRNA levels when H2A.Z's developmental function was disrupted. However, in addition to expression levels, cellular localization of Dsh is important to Dsh function. H2A.Z may affect the PCP pathway by perturbing the expression of genes whose products regulate Dsh localization. Three conserved domains within Dsh are involved in the proteins localization and signaling functions. The DIX domain is required for canonical Wnt signaling, the DEP domain for PCP (including translocation of Dsh to the cell membrane and a signaling function to activate Rac GTPase), and the PDZ domain which functions in both (Park et al., 2005). DEP is required for localization of Dsh to the cell membrane necessary for PCP signaling but not for signaling through the canonical Wnt pathway (Wang et al., 2006). The DEP domain and targeting of Dvl to cell membrane are required for mouse neuralation (Torban et al., 2004; Wallingford and Harland, 2001; Wallingford et al., 2000; Wang et al., 2006). DEP and PDZ are required for PCP and interaction of Dsh with Stbm in mouse neural plate and *X. laevis* mesoderm (Park and Moon, 2002). What remains to be determined is if the developmental function of H2A.Z is acting through Dsh/PCP signaling.

Several experiments could investigate whether H2A.Z indirectly affects Dsh cellular localization. After co-injection of *H2A.ZNQ* and *Dsh-EGFP* mRNA the cellular localization of Dsh-EGFP could be compared to embryos with *Dsh-EGFP* alone. Alternatively, immunofluorescence detection of endogenous Dsh protein could be used overcoming the need for introduced *Dsh-EGFP* mRNA. The results could be confirmed by co-injection of H2A.ZNQ and *Dsh-caax* mRNA (Axelrod, 2001; Axelrod et al.,

1998; Park et al., 2005) that localizes to the cell membrane independently of DEP to see if this rescues the convergent extension in defective embryos

6.4.2 Gene expression/rescue experiments

Having shown that H2A.Z's developmental function is important for the regulation of the pathway for cell movement, it remains unclear whether H2A.Z is affecting the Ca^{2+} mediated or PCP pathway, and at what point(s) H2A.Z may be required for expression of the appropriate gene(s). For example if H2A.Z affects the expression of the membrane bound Stbm then this would block the localisation of Dsh to the cell membrane and the PCP pathway. This hypothesis could be tested by determining *Stbm* mRNA levels and confirmed by rescue of NQdn embryos by co-injection of *Stbm* mRNA. More generally, gene expression levels and localisation experiments like those used in this project applied to selected genes could be used to define which pathway(s) are regulated by H2A.Z and where this regulation of expression is occurring. However, a more efficient approach would be to employ microarrays of the *Xenopus* genome (available from Affymetrix) to material from whole embryos or dissected tissues of interest such as the marginal zone of late blastula embryos. Microarray results of interest could then be confirmed by RT real-time PCR and *in situ* hybridisation or immunofluorescence.

6.4.3 Functional studies

In *X. laevis* activin acts in a concentration-dependant manner to induce numerous mesodermal tissues (Fukui and Asashima, 1994). For example, moderate activin concentrations induce *Xbra,* higher concentrations inhibit *Xbra* and induce *Gsc* and *chordin* (Kurth et al., 2005). At appropriate activin concentrations, *X. laevis* animal caps excised at an appropriate stage of development (stage 8 or 8.5) develop mesodermal

characteristics and undergo convergent extension (Sive et al., 2000; Taverner et al., 2005). Therefore, activin assays on excised animal caps can determine competence for both mesodermal fate (Korner et al., 2003) and convergent extension (Leise and Mueller, 2004), the technique may be used to separate the effects of differentiation/gene expression from those of improper convergent extension (Leise and Mueller, 2004). Simple morphology can demonstrate competence for convergent extension, as competent caps become elongated when cultured with activin. Failure of H2A.Zdn caps to undergo convergent extension would support the conclusion of this research that H2A.Z function is required for proper convergent extension of mesodermal tissues. Mesodermal character of the caps can be determined by RT real-time PCR of marker genes as performed for whole embryos in this project (Leise and Mueller, 2004). Microarray comparison of H2A.Zdn and uninjected animal caps (as discussed in 6.4.2) would also provide information on gene expression patterns within the cultured animal caps.

6.5 Conclusion

The control of cell movement remains a major unanswered question of biology. This work provides some inroads into understanding the regulation of cell movements during development. It has shown that the histone variant H2A.Z is enriched in cell lineages where it is required for cell movement including maternal mRNA localised to dorsal blastomeres, the involuting marginal zone, mesoderm and notochord. The developmental function of H2A.Z is not implicated in cell fate determination because markers for cell fate are normally expressed when H2A.Z is disrupted. Alternatively, gastrulation and notochord formation are perturbed indicating a role in convergent extension. Not only does this work contribute towards understanding of a basic process of biology, in doing so it has implications for the aetiologies of congenital defects and

future medical treatments based on growth of specific tissues for a wide range of ailments.

References

Agius, E., Oelgeschlager, M., Wessely, O., Kemp, C. and De Robertis, E.M. (2000) Endodermal Nodal-related signals and mesoderm induction in Xenopus. *Development*, **127**, 1173-1183.

Akey, C.W. and Luger, K. (2003) Histone chaperones and nucleosome assembly. *Curr Opin Struct Biol*, **13**, 6-14.

Akhtar, A. and Gasser, S.M. (2007) The nuclear envelope and transcriptional control. *Nat Rev Genet*, **8**, 507-517.

Albert, I., Mavrich, T.N., Tomsho, L.P., Qi, J., Zanton, S.J., Schuster, S.C. and Pugh, B.F. (2007) Translational and rotational settings of H2A.Z nucleosomes across the Saccharomyces cerevisiae genome. *Nature*, **446**, 572-576.

Allende, C.C., Allende, J.E. and Firtel, R.A. (1974) The degradation of ribonucleic acids injected into Xenopus laevis oocytes. *Cell*, **2**, 189-196.

Allis, C.D., Glover, C.V., Bowen, J.K. and Gorovsky, M.A. (1980) Histone variants specific to the transcriptionally active, amitotically dividing macronucleus of the unicellular eucaryote, Tetrahymena thermophila. *Cell*, **20**, 609-617.

Allis, C.D., Richman, R., Gorovsky, M.A., Ziegler, Y.S., Touchstone, B., Bradley, W.A. and Cook, R.G. (1986) hv1 is an evolutionarily conserved H2A variant that is preferentially associated with active genes. *J Biol Chem*, **261**, 1941-1948.

Almouzni, G., Khochbin, S., Dimitrov, S. and Wolffe, A.P. (1994) Histone acetylation influences both gene expression and development of Xenopus laevis. *Dev Biol*, **165**, 654-669.

Almouzni, G. and Wolffe, A.P. (1995) Constraints on transcriptional activator function contribute to transcriptional quiescence during early Xenopus embryogenesis. *Embo J*, **14**, 1752-1765.

Altmann, C., Bell, E. and Brivanlou, A. (2000) Genomics and embryology in amphibians. *Genome Biology*, **1**, reports4022.4021-4022.4023.

Ang, S.L. and Rossant, J. (1994) HNF-3 beta is essential for node and notochord formation in mouse development. *Cell*, **78**, 561-574.

Applied_Biosystems. (2004) *Guide to Performing Relative Quantitation of Gene Expression Using Real-Time Quantitative PCR*. Applied Biosystems.

Arents, G., Burlingame, R.W., Wang, B.C., Love, W.E. and Moudrianakis, E.N. (1991) The nucleosomal core histone octamer at 3.1 A resolution: a tripartite protein assembly and a left-handed superhelix. *Proc Natl Acad Sci U S A*, **88**, 10148-10152.

Arents, G. and Moudrianakis, E.N. (1993) Topography of the histone octamer surface: repeating structural motifs utilized in the docking of nucleosomal DNA. *Proc Natl Acad Sci U S A*, **90**, 10489-10493.

Arents, G. and Moudrianakis, E.N. (1995) The histone fold: a ubiquitous architectural motif utilized in DNA compaction and protein dimerization. *Proc Natl Acad Sci U S A*, **92**, 11170-11174.

Artinger, M., Blitz, I., Inoue, K., Tran, U. and Cho, K.W. (1997) Interaction of goosecoid and brachyury in Xenopus mesoderm patterning (abstract only). *Mech Dev*, **65**, 187-196.

Aul, R.B. and Oko, R.J. (2001) The major subacrosomal occupant of bull spermatozoa is a novel histone H2B variant associated with the forming acrosome during spermiogenesis. *Dev Biol*, **239**, 376-387.

Axelrod, J.D. (2001) Unipolar membrane association of Dishevelled mediates Frizzled planar cell polarity signaling. *Genes Dev*, **15**, 1182-1187.

Axelrod, J.D., Miller, J.R., Shulman, J.M., Moon, R.T. and Perrimon, N. (1998) Differential recruitment of Dishevelled provides signaling specificity in the planar cell polarity and Wingless signaling pathways. *Genes Dev*, **12**, 2610-2622.

Aybar, M.J., Nieto, M.A. and Mayor, R. (2003) Snail precedes slug in the genetic cascade required for the specification and migration of the Xenopus neural crest. *Development*, **130**, 483-494.

Ayyanathan, K., Lechner, M.S., Bell, P., Maul, G.G., Schultz, D.C., Yamada, Y., Tanaka, K., Torigoe, K. and Rauscher, F.J., 3rd. (2003) Regulated recruitment of HP1 to a euchromatic gene induces mitotically heritable, epigenetic gene silencing: a mammalian cell culture model of gene variegation. *Genes Dev*, **17**, 1855-1869.

Azuara, V., Perry, P., Sauer, S., Spivakov, M., Jorgensen, H.F., John, R.M., Gouti, M., Casanova, M., Warnes, G., Merkenschlager, M. and Fisher, A.G. (2006) Chromatin signatures of pluripotent cell lines. *Nat Cell Biol*, **8**, 532-538.

Bachvarova, R. and Davidson, E.H. (1966) Nuclear Activation at the Onset of Amphibian Gastrulation. *J. Exp. Zool.*, **163**, 285-296.

Bao, Y. and Shen, X. (2007) INO80 subfamily of chromatin remodeling complexes. *Mutat Res*, **618**, 18-29.

Bauer, D.V., Huang, S. and Moody, S.A. (1994) The cleavage stage origin of Spemann's Organizer: analysis of the movements of blastomere clones before and during gastrulation in Xenopus. *Development*, **120**, 1179-1189.

Baxevanis, A.D., Arents, G., Moudrianakis, E.N. and Landsman, D. (1995) A variety of DNA-binding and multimeric proteins contain the histone fold motif. *Nucleic Acids Res*, **23**, 2685-2691.

Becker, J.M., Caldwell, G.A. and Zachgo, E.A. (1996) *Biotechnology: A Laboratory Course*. Academic Press, San Diego.

Becker, P.B. (2006) Gene regulation: a finger on the mark. *Nature*, **442**, 31-32.

Bednar, J., Horowitz, R.A., Grigoryev, S.A., Carruthers, L.M., Hansen, J.C., Koster, A.J. and Woodcock, C.L. (1998) Nucleosomes, linker DNA, and linker histone form a unique structural motif that directs the higher-order folding and compaction of chromatin. *Proc Natl Acad Sci U S A*, **95**, 14173-14178.

Beilharz, T.H. and Preiss, T. (2007) Widespread use of poly(A) tail length control to accentuate expression of the yeast transcriptome (abstract only). *Rna*, **13**, 982-997.

Belmont, A.S. and Bruce, K. (1994) Visualization of G1 chromosomes: a folded, twisted, supercoiled chromonema model of interphase chromatid structure. *J Cell Biol*, **127**, 287-302.

Belotserkovskaya, R., Oh, S., Bondarenko, V.A., Orphanides, G., Studitsky, V.M. and Reinberg, D. (2003) FACT facilitates transcription-dependent nucleosome alteration. *Science*, **301**, 1090-1093.

Berger, S.L. (2007) The complex language of chromatin regulation during transcription. *Nature*, **447**, 407-412.

Bernstein, B.E., Kamal, M., Lindblad-Toh, K., Bekiranov, S., Bailey, D.K., Huebert, D.J., McMahon, S., Karlsson, E.K., Kulbokas, E.J., 3rd, Gingeras, T.R.,

Schreiber, S.L. and Lander, E.S. (2005) Genomic maps and comparative analysis of histone modifications in human and mouse. *Cell*, **120**, 169-181.

Bernstein, E. and Hake, S.B. (2006) The nucleosome: a little variation goes a long way. *Biochem Cell Biol*, **84**, 505-517.

Berry, R.J., Li, Z., Erickson, J.D., Li, S., Moore, C.A., Wang, H., Mulinare, J., Zhao, P., Wong, L.Y., Gindler, J., Hong, S.X. and Correa, A. (1999) Prevention of neural-tube defects with folic acid in China. China-U.S. Collaborative Project for Neural Tube Defect Prevention. *N Engl J Med*, **341**, 1485-1490.

Bestor, T.H. (2000) The DNA methyltransferases of mammals. *Hum Mol Genet*, **9**, 2395-2402.

Blumberg, B., Wright, C.V., De Robertis, E.M. and Cho, K.W. (1991) Organizer-specific homeobox genes in Xenopus laevis embryos. *Science*, **253**, 194-196.

Bocchinfuso, W.P., Hively, W.P., Couse, J.F., Varmus, H.E. and Korach, K.S. (1999) A mouse mammary tumor virus-Wnt-1 transgene induces mammary gland hyperplasia and tumorigenesis in mice lacking estrogen receptor-alpha. *Cancer Res*, **59**, 1869-1876.

Bouazoune, K. and Brehm, A. (2006) ATP-dependent chromatin remodeling complexes in Drosophila. *Chromosome Res*, **14**, 433-449.

Bouvet, P., Dimitrov, S. and Wolffe, A.P. (1994) Specific regulation of Xenopus chromosomal 5S rRNA gene transcription in vivo by histone H1. *Genes Dev*, **8**, 1147-1159.

Brannon, M., Gomperts, M., Sumoy, L., Moon, R.T. and Kimelman, D. (1997) A beta-catenin/XTcf-3 complex binds to the siamois promoter to regulate dorsal axis specification in Xenopus. *Genes Dev*, **11**, 2359-2370.

Cadigan, K.M. and Nusse, R. (1997) Wnt signaling: a common theme in animal development. *Genes Dev*, **11**, 3286-3305.

Carr, A.M., Dorrington, S.M., Hindley, J., Phear, G.A., Aves, S.J. and Nurse, P. (1994) Analysis of a histone H2A variant from fission yeast: evidence for a role in chromosome stability (Abstract only). *Mol Gen Genet*, **245**, 628-635.

Chadwick, B.P. and Willard, H.F. (2001) A novel chromatin protein, distantly related to histone H2A, is largely excluded from the inactive X chromosome. *J Cell Biol*, **152**, 375-384.

Chalmers, A. (2003) Oriented cell divisions asymetrically segregate aPKC and generate cell fate diversity in the early *Xenopus* embryo. *Development*, **130**, 2657-2668.

Clark-Adams, C.D., Norris, D., Osley, M.A., Fassler, J.S. and Winston, F. (1988) Changes in histone gene dosage alter transcription in yeast. *Genes Dev*, **2**, 150-159.

Clarkson, M.J., Wells, J.R.E., Gibson, F., Saint, R. and Tremethick, D.J. (1999) Regions of variant histone HisAvD required for *Drosophila* development. *Nature*, **399**, 694-697.

Conlon, F.L., Sedgwick, S.G., Weston, K.M. and Smith, J.C. (1996) Inhibition of Xbra transcription activation causes defects in mesodermal patterning and reveals autoregulation of Xbra in dorsal mesoderm. *Development*, **122**, 2427-2435.

Copp, A.J., Greene, N.D. and Murdoch, J.N. (2003) The genetic basis of mammalian neurulation. *Nat Rev Genet*, **4**, 784-793.

Costanzi, C., Stein, P., Worrad, D.M., Schultz, R.M. and Pehrson, J.R. (2000) Histone macroH2A1 is concentrated in the inactive X chromosome of female preimplantation mouse embryos. *Development*, **127**, 2283-2289.

Cunliffe, V. and Smith, J.C. (1992) Ectopic mesoderm formation in Xenopus embryos caused by widespread expression of a Brachyury homologue. *Nature*, **358**, 427-430.

Cunliffe, V. and Smith, J.C. (1994) Specification of mesodermal pattern in Xenopus laevis by interactions between Brachyury, noggin and Xwnt-8. *Embo J*, **13**, 349-359.

Cuthbert, G.L., Daujat, S., Snowden, A.W., Erdjument-Bromage, H., Hagiwara, T., Yamada, M., Schneider, R., Gregory, P.D., Tempst, P., Bannister, A.J. and Kouzarides, T. (2004) Histone deimination antagonizes arginine methylation. *Cell*, **118**, 545-553.

Dai, J. and Higgins, J.M. (2005) Haspin: a mitotic histone kinase required for metaphase chromosome alignment. *Cell Cycle*, **4**, 665-668.

Dale, L. and Slack, J.M. (1987a) Fate map for the 32-cell stage of Xenopus laevis. *Development*, **99**, 527-551.

Dale, L. and Slack, J.M. (1987b) Regional specification within the mesoderm of early embryos of Xenopus laevis. *Development*, **100**, 279-295.

de Napoles, M., Mermoud, J.E., Wakao, R., Tang, Y.A., Endoh, M., Appanah, R., Nesterova, T.B., Silva, J., Otte, A.P., Vidal, M., Koseki, H. and Brockdorff, N. (2004) Polycomb group proteins Ring1A/B link ubiquitylation of histone H2A to heritable gene silencing and X inactivation. *Dev Cell*, **7**, 663-676.

Denslow, S.A. and Wade, P.A. (2007) The human Mi-2/NuRD complex and gene regulation. *Oncogene*, **26**, 5433-5438.

Dhillon, N. and Kamakaka, R.T. (2000) A histone variant, Htz1p, and a Sir1p-like protein, Esc2p, mediate silencing at HMR. *Mol Cell*, **6**, 769-780.

Dimitrov, S., Almouzni, G., Dasso, M. and Wolffe, A.P. (1993) Chromatin transitions during early *Xenopus* embryogenesis: changes in histone H4 acetylation and in linker histone type. *Developmental Biology*, **160**, 214-227.

Dimitrov, S., Dasso, M.C. and Wolffe, A.P. (1994) Remodeling sperm chromatin in Xenopus laevis egg extracts: the role of core histone phosphorylation and linker histone B4 in chromatin assembly. *J Cell Biol*, **126**, 591-601.

Djiane, A., Riou, J., Umbhauer, M., Boucaut, J. and Shi, D. (2000) Role of frizzled 7 in the regulation of convergent extension movements during gastrulation in Xenopus laevis. *Development*, **127**, 3091-3100.

Djiane, A., Yogev, S. and Mlodzik, M. (2005) The apical determinants aPKC and dPatj regulate Frizzled-dependent planar cell polarity in the Drosophila eye. *Cell*, **121**, 621-631.

Doenecke, D., Albig, W., Bode, C., Drabent, B., Franke, K., Gavenis, K. and Witt, O. (1997) Histones: genetic diversity and tissue-specific gene expression. *Histochem Cell Biol*, **107**, 1-10.

Doerfler, W. (1981) DNA methylation--a regulatory signal in eukaryotic gene expression. *J Gen Virol*, **57**, 1-20.

Donahue, P.R., Palmer, D.K., Conie, J.M., Sabatini, L.M. and Blumfield, M. (1986) *Drosophila* histone H2A.2 is associated with the interbands of polytene chromosomes. *Proc Natl Acad Sci*, **83**, 4744-4748.

Dorigo, B., Schalch, T., Kulangara, A., Duda, S., Schroeder, R.R. and Richmond, T.J. (2004) Nucleosome arrays reveal the two-start organization of the chromatin fiber. *Science*, **306**, 1571-1573.

Dosch, R., Gawantka, V., Delius, H., Blumenstock, C. and Niehrs, C. (1997) Bmp-4 acts as a morphogen in dorsoventral mesoderm patterning in Xenopus. *Development*, **124**, 2325-2334.

Driscoll, R., Hudson, A. and Jackson, S.P. (2007) Yeast Rtt109 promotes genome stability by acetylating histone H3 on lysine 56. *Science*, **315**, 649-652.

Earnshaw, W.C., Honda, B.M., Laskey, R.A. and Thomas, J.O. (1980) Assembly of nucleosomes: the reaction involving X. laevis nucleoplasmin. *Cell*, **21**, 373-383.

Ehrenhofer-Murray, A.E. (2004) Chromatin dynamics at DNA replication, transcription and repair. *Eur J Biochem*, **271**, 2335-2349.

Eickbush, T.H. and Moudrianakis, E.N. (1978) The histone core complex: an octamer assembled by two sets of protein-protein interactions (abstract only). *Biochemistry*, **17**, 4955-4964.

Eimon, P.M. and Harland, R.M. (2002) Effects of heterodimerization and proteolytic processing on Derriere and Nodal activity: implications for mesoderm induction in Xenopus. *Development*, **129**, 3089-3103.

Elinson, R.P. and Rowning, B. (1988) A transient array of parallel microtubules in frog eggs: potential tracks for a cytoplasmic rotation that specifies the dorso-ventral axis (abstract only). *Dev Biol*, **128**, 185-197.

Ernst, S.G., Miller, H., Brenner, C.A., Nocente-McGrath, C., Francis, S. and McIsaac, R. (1987) Characterization of a cDNA clone coding for a sea urchin histone H2A variant related to the H2A.F/Z histone protein in vertebrates. *Nucleic Acids Res*, **15**, 4629-4644.

Faast, R., Thonglairoam, V., Schulz, T.C., Beall, J., Wells, J.R.E., Taylor, H., Matthaei, K., Rathjen, P.D., Tremethick, D.J. and Lyons, I. (2001) Histone Variant H2A.Z is required for early mammalian development. *Current Biology*, **11**, 1183-1187.

Fagotto, F., Guger, K. and Gumbiner, B.M. (1997) Induction of the primary dorsalizing center in Xenopus by the Wnt/GSK/beta-catenin signaling pathway, but not by Vg1, Activin or Noggin. *Development*, **124**, 453-460.

Fan, J.Y., Gordon, F., Luger, K., Hansen, J.C. and Tremethick, D.J. (2002) The essential histone variant H2A.Z regulates the equilibrium between different chromatin conformational states. *Nat Struct Biol*, **9**, 172-176.

Fan, M.J. and Sokol, S.Y. (1997) A role for Siamois in Spemann organizer formation. *Development*, **124**, 2581-2589.

Farris, S.D., Rubio, E.D., Moon, J.J., Gombert, W.M., Nelson, B.H. and Krumm, A. (2005) Transcription-induced chromatin remodeling at the c-myc gene involves the local exchange of histone H2A.Z. *J Biol Chem*, **280**, 25298-25303.

Felsenfeld, G. and Groudine, M. (2003) Controlling the double helix. *Nature*, **421**, 448-453.

Finch, J.T. and Klug, A. (1976) Solenoidal model for superstructure in chromatin. *Proc Natl Acad Sci U S A*, **73**, 1897-1901.

Fischle, W., Tseng, B.S., Dormann, H.L., Ueberheide, B.M., Garcia, B.A., Shabanowitz, J., Hunt, D.F., Funabiki, H. and Allis, C.D. (2005) Regulation of HP1-chromatin binding by histone H3 methylation and phosphorylation. *Nature*, **438**, 1116-1122.

Frey, L. and Hauser, W.A. (2003) Epidemiology of neural tube defects. *Epilepsia*, **44**, 4-13.

Fukui, A. and Asashima, M. (1994) Control of cell differentiation and morphogenesis in amphibian development (abstract only). *Int. J. Dev. Biol.*, **38**, 257-266.

Gawantka, V., Delius, H., Hirschfeld, K., Blumenstock, C. and Niehrs, C. (1995) Antagonizing the Spemann organizer: role of the homeobox gene Xvent-1. *Embo J*, **14**, 6268-6279.

Gawantka, V., Pollet, N., Delius, H., Vingron, M., Pfister, R., Nitsch, R., Blumenstock, C. and Niehrs, C. (1998) Gene expression screening in Xenopus identifies

molecular pathways, predicts gene function and provides a global view of embryonic patterning. *Mech Dev*, **77**, 95-141.

Gerhart, J., Danilchik, M., Doniach, T., Roberts, S., Rowning, B. and Stewart, R. (1989) Cortical rotation of the Xenopus egg: consequences for the anteroposterior pattern of embryonic dorsal development (abstract only). *Development*, **107 Suppl**, 37-51.

Gerhart, J. and Keller, R. (1986) Region-specific cell activities in amphibian gastrulation. *Annu Rev Cell Biol*, **2**, 201-229.

Getzoff, E.D., Tainer, J.A., Weiner, P.K., Kollman, P.A., Richardson, J.S. and Richardson, D.C. (1983) Electrostatic recognition between superoxide and copper, zinc superoxide dismutase (abstract only). *Nature*, **306**, 287-290.

Gimlich, R.L. and Gerhart, J.C. (1984) Early cellular interactions promote embryonic axis formation in Xenopus laevis (abstract only). *Dev Biol*, **104**, 117-130.

Gont, L.K., Steinbeisser, H., Blumberg, B. and de Robertis, E.M. (1993) Tail formation as a continuation of gastrulation: the multiple cell populations of the Xenopus tailbud derive from the late blastopore lip. *Development*, **119**, 991-1004.

Gordon, F., Luger, K. and Hansen, J.C. (2005) The core histone N-terminal tail domains function independently and additively during salt-dependent oligomerization of nucleosomal arrays. *J Biol Chem*, **280**, 33701-33706.

Graham, C.F. (1966) The regulation of DNA synthesis and mitosis in multinucleate frog eggs. *J Cell Sci*, **1**, 363-374.

Grandjean, V., Yaman, R., Cuzin, F. and Rassoulzadegan, M. (2007) Inheritance of an Epigenetic Mark: The CpG DNA Methyltransferase 1 Is Required for De Novo Establishment of a Complex Pattern of Non-CpG Methylation. *PLoS ONE*, **2**, e1136.

Greaves, I.K., Rangasamy, D., Devoy, M., Marshall Graves, J.A. and Tremethick, D.J. (2006) The X and Y chromosomes assemble into H2A.Z-containing [corrected] facultative heterochromatin [corrected] following meiosis. *Mol Cell Biol*, **26**, 5394-5405.

Greaves, I.K., Rangasamy, D., Ridgway, P. and Tremethick, D.J. (2007) H2A.Z contributes to the unique 3D structure of the centromere. *Proc Natl Acad Sci U S A*, **104**, 525-530.

Green, M.R. (2005) Eukaryotic transcription activation: right on target. *Mol Cell*, **18**, 399-402.

Grewal, S.I. and Jia, S. (2007) Heterochromatin revisited. *Nat Rev Genet*, **8**, 35-46.

Gubb, D., Green, C., Huen, D., Coulson, D., Johnson, G., Tree, D., Collier, S. and Roote, J. (1999) The balance between isoforms of the prickle LIM domain protein is critical for planar polarity in Drosophila imaginal discs. *Genes Dev*, **13**, 2315-2327.

Habas, R., Kato, Y. and He, X. (2001) Wnt/Frizzled activation of Rho regulates vertebrate gastrulation and requires a novel Formin homology protein Daam1. *Cell*, **107**, 843-854.

Hahn, S. (2004) Structure and mechanism of the RNA polymerase II transcription machinery. *Nat Struct Mol Biol*, **11**, 394-403.

Harland, R.M. (1991) In situ hybridization: an improved whole-mount method for Xenopus embryos. *Methods Cell Biol*, **36**, 685-695.

Harvey, R.P., Whiting, J.A., Coles, L.S., Krieg, P.A. and Wells, J.R. (1983) H2A.F: an extremely variant histone H2A sequence expressed in the chicken embryo. *Proc Natl Acad Sci U S A*, **80**, 2819-2823.

Hatch, C.L. and Bonner, W.M. (1990) The human histone H2A.Z gene. Sequence and regulation. *J Biol Chem*, **265**, 15211-15218.

Hatch, C.L. and Bonner, W.M. (1996) An upstream region of the H2AZ gene promoter modulates promoter activity in different cell types. *Biochim Biophys Acta*, **1305**, 59-62.

Hayward, D.C., Catmull, J., Reece-Hoyes, J.S., Berghammer, H., Dodd, H., Hann, S.J., Miller, D.J. and Ball, E.E. (2001) Gene structure and larval expression of cnox-2Am from the coral Acropora millepora. *Dev Genes Evol*, **211**, 10-19.

Heard, E. and Bickmore, W. (2007) The ins and outs of gene regulation and chromosome territory organisation. *Curr Opin Cell Biol*, **19**, 311-316.

Hecht, A., Vleminckx, K., Stemmler, M.P., van Roy, F. and Kemler, R. (2000) The p300/CBP acetyltransferases function as transcriptional coactivators of beta-catenin in vertebrates. *Embo J*, **19**, 1839-1850.

Herrmann, B.G., Labeit, S., Poustka, A., King, T.R. and Lehrach, H. (1990) Cloning of the T gene required in mesoderm formation in the mouse. *Nature*, **343**, 617-622.

Hirschhorn, J.N., Brown, S.A., Clark, C.D. and Winston, F. (1992) Evidence that SNF2/SWI2 and SNF5 activate transcription in yeast by altering chromatin structure. *Genes Dev*, **6**, 2288-2298.

Hoppler, S., Brown, J.D. and Moon, R.T. (1996) Expression of a dominant-negative Wnt blocks induction of MyoD in Xenopus embryos. *Genes Dev*, **10**, 2805-2817.

Hopwood, N.D., Pluck, A. and Gurdon, J.B. (1989) MyoD expression in the forming somites is an early response to mesoderm induction in Xenopus embryos (Abstract only). *Embo J*, **8**, 3409-3417.

Hopwood, N.D., Pluck, A., Gurdon, J.B. and Dilworth, S.M. (1992) Expression of XMyoD protein in early Xenopus laevis embryos. *Development*, **114**, 31-38.

Horn, P.J. and Peterson, C.L. (2002) Molecular biology. Chromatin higher order folding--wrapping up transcription. *Science*, **297**, 1824-1827.

Hwang, S.I., Thumar, J., Lundgren, D.H., Rezaul, K., Mayya, V., Wu, L., Eng, J., Wright, M.E. and Han, D.K. (2007) Direct cancer tissue proteomics: a method to identify candidate cancer biomarkers from formalin-fixed paraffin-embedded archival tissues. *Oncogene*, **26**, 65-76.

Iouzalen, N., Moreau, J. and Mechali, M. (1996) H2A.ZI, a new variant histone expressed during Xenopus early development exhibits several distinct features from the core histone H2A. *Nucleic Acids Res*, **24**, 3947-3952.

Ishikawa, T., Tamai, Y., Zorn, A.M., Yoshida, H., Seldin, M.F., Nishikawa, S. and Taketo, M.M. (2001) Mouse Wnt receptor gene Fzd5 is essential for yolk sac and placental angiogenesis. *Development*, **128**, 25-33.

Itoh, K., Brott, B.K., Bae, G.U., Ratcliffe, M.J. and Sokol, S.Y. (2005) Nuclear localization is required for Dishevelled function in Wnt/beta-catenin signaling. *J Biol*, **4**, 3.

Jackson, J.D., Falciano, V.T. and Gorovsky, M.A. (1996) A likely histone H2A.F/Z variant in Saccharomyces cerevisiae. *Trends Biochem Sci*, **21**, 466-467.

Jackson, J.D. and Gorovsky, M.A. (2000) Histone H2A.Z has a conserved function that is distinct from that of the major H2A sequence variants. *Nucleic Acids Res*, **28**, 3811-3816.

Jin, J., Cai, Y., Li, B., Conaway, R.C., Workman, J.L., Conaway, J.W. and Kusch, T. (2005) In and out: histone variant exchange in chromatin. *Trends Biochem Sci*, **30**, 680-687.

Kageura, H. (1997) Activation of dorsal development by contact between the cortical dorsal determinant and the equatorial core cytoplasm in eggs of Xenopus laevis. *Development*, **124**, 1543-1551.

Keller, R. (2002) Shaping the vertebrate body plan by polarized embryonic cell movements. *Science*, **298**, 1950-1954.

Keller, R., Davidson, L.A. and Shook, D.R. (2003) How we are shaped: the biomechanics of gastrulation. *Differentiation*, **71**, 171-205.

Keller, R., Shih, J., Sater, A.K. and Moreno, C. (1992) Planar induction of convergence and extension of the neural plate by the organizer of Xenopus. *Dev Dyn*, **193**, 218-234.

Kessler, D.S. (1997) Siamois is required for formation of Spemann's organizer. *Proc Natl Acad Sci U S A*, **94**, 13017-13022.

Kibar, Z., Vogan, K.J., Groulx, N., Justice, M.J., Underhill, D.A. and Gros, P. (2001) Ltap, a mammalian homolog of Drosophila Strabismus/Van Gogh, is altered in the mouse neural tube mutant Loop-tail. *Nat Genet*, **28**, 251-255.

Kieker, C. and Niehrs, C. (2001) A morphogen gradient of Wnt/β-catenin signalling regulates anteropostior neural patterning in *Xenopus*. *Development*, **128**, 4189-4201.

Kikkawa, M., Takano, K. and Shinagawa, A. (1996) Location and behavior of dorsal determinants during first cell cycle in Xenopus eggs. *Development*, **122**, 3687-3696.

Kikyo, N. and Wolffe, A.P. (2000) Reprogramming nuclei: insights from cloning, nuclear transfer and heterokaryons. *J Cell Sci*, **113 (Pt 1)**, 11-20.

Kimelman, D., Christian, J.L. and Moon, R.T. (1992) Synergistic principles of development: overlapping patterning systems in Xenopus mesoderm induction. *Development*, **116**, 1-9.

Kireeva, M.L., Walter, W., Tchernajenko, V., Bondarenko, V., Kashlev, M. and Studitsky, V.M. (2002) Nucleosome remodeling induced by RNA polymerase II: loss of the H2A/H2B dimer during transcription. *Mol Cell*, **9**, 541-552.

Kispert, A., Koschorz, B. and Herrmann, B.G. (1995) The T protein encoded by Brachyury is a tissue-specific transcription factor. *Embo J*, **14**, 4763-4772.

Klein, D. (2002) Quantification using real-time PCR technology: applications and limitations. *Trends Mol Med*, **8**, 257-260.

Kobor, M.S., Venkatasubrahmanyam, S., Meneghini, M.D., Gin, J.W., Jennings, J.L., Link, A.J., Madhani, H.D. and Rine, J. (2004) A protein complex containing the conserved Swi2/Snf2-related ATPase Swr1p deposits histone variant H2A.Z into euchromatin. *PLoS Biol*, **2**, E131.

Korner, U., Bustin, M., Scheer, U. and Hock, R. (2003) Developmental role of HMGN proteins in Xenopus laevis. *Mech Dev*, **120**, 1177-1192.

Kouzarides, T. (2007) Chromatin modifications and their function. *Cell*, **128**, 693-705.

Krieg, P.A. and Melton, D.A. (1984) Functional messenger RNAs are produced by SP6 in vitro transcription of cloned cDNAs. *Nucleic Acids Res*, **12**, 7057-7070.

Krishnamoorthy, T., Chen, X., Govin, J., Cheung, W.L., Dorsey, J., Schindler, K., Winter, E., Allis, C.D., Guacci, V., Khochbin, S., Fuller, M.T. and Berger, S.L. (2006) Phosphorylation of histone H4 Ser1 regulates sporulation in yeast and is conserved in fly and mouse spermatogenesis. *Genes Dev*, **20**, 2580-2592.

Krogan, N.J., Baetz, K., Keogh, M.C., Datta, N., Sawa, C., Kwok, T.C., Thompson, N.J., Davey, M.G., Pootoolal, J., Hughes, T.R., Emili, A., Buratowski, S., Hieter, P. and Greenblatt, J.F. (2004) Regulation of chromosome stability by the

histone H2A variant Htz1, the Swr1 chromatin remodeling complex, and the histone acetyltransferase NuA4. *Proc Natl Acad Sci U S A*, **101**, 13513-13518.

Krogan, N.J., Keogh, M.C., Datta, N., Sawa, C., Ryan, O.W., Ding, H., Haw, R.A., Pootoolal, J., Tong, A., Canadien, V., Richards, D.P., Wu, X., Emili, A., Hughes, T.R., Buratowski, S. and Greenblatt, J.F. (2003) A Snf2 family ATPase complex required for recruitment of the histone H2A variant Htz1. *Mol Cell*, **12**, 1565-1576.

Kuhl, M., Geis, K., Sheldahl, L.C., Pukrop, T., Moon, R.T. and Wedlich, D. (2001) Antagonistic regulation of convergent extension movements in Xenopus by Wnt/beta-catenin and Wnt/Ca2+ signaling. *Mech Dev*, **106**, 61-76.

Kuhl, M., Sheldahl, L.C., Malbon, C.C. and Moon, R.T. (2000) Ca(2+)/calmodulin-dependent protein kinase II is stimulated by Wnt and Frizzled homologs and promotes ventral cell fates in Xenopus. *J Biol Chem*, **275**, 12701-12711.

Kuhnert, F., Davis, C.R., Wang, H.T., Chu, P., Lee, M., Yuan, J., Nusse, R. and Kuo, C.J. (2004) Essential requirement for Wnt signaling in proliferation of adult small intestine and colon revealed by adenoviral expression of Dickkopf-1. *Proc Natl Acad Sci U S A*, **101**, 266-271.

Kuo, M.H., Zhou, J., Jambeck, P., Churchill, M.E. and Allis, C.D. (1998) Histone acetyltransferase activity of yeast Gcn5p is required for the activation of target genes in vivo. *Genes Dev*, **12**, 627-639.

Kurth, T., Meissner, S., Schackel, S. and Steinbeisser, H. (2005) Establishment of mesodermal gene expression patterns in early Xenopus embryos: the role of repression. *Dev Dyn*, **233**, 418-429.

Larabell, C.A., Torres, M., Rowning, B.A., Yost, C., Miller, J.R., Wu, M., Kimelman, D. and Moon, R.T. (1997) Establishment of the dorso-ventral axis in Xenopus embryos is presaged by early asymmetries in beta-catenin that are modulated by the Wnt signaling pathway. *J Cell Biol*, **136**, 1123-1136.

Larochelle, M. and Gaudreau, L. (2003) H2A.Z has a function reminiscent of an activator required for preferential binding to intergenic DNA. *Embo J*, **22**, 4512-4522.

Latinkic, B.V. and Smith, J.C. (1999) Goosecoid and mix.1 repress Brachyury expression and are required for head formation in Xenopus. *Development*, **126**, 1769-1779.

Latinkic, B.V., Umbhauer, M., Neal, K.A., Lerchner, W., Smith, J.C. and Cunliffe, V. (1997) The Xenopus Brachyury promoter is activated by FGF and low concentrations of activin and suppressed by high concentrations of activin and by paired-type homeodomain proteins. *Genes Dev*, **11**, 3265-3276.

Laurenson, P. and Rine, J. (1992) Silencers, silencing, and heritable transcriptional states. *Microbiol Rev*, **56**, 543-560.

Laurent, M.N., Blitz, I.L., Hashimoto, C., Rothbacher, U. and Cho, K.W. (1997) The Xenopus homeobox gene twin mediates Wnt induction of goosecoid in establishment of Spemann's organizer. *Development*, **124**, 4905-4916.

Leach, T.J., Mazzeo, M., Chotkowski, H.L., Madigan, J.P., Wotring, M.G. and Glaser, R.L. (2000) Histone H2A.Z is widely but nonrandomly distributed in chromosomes of Drosophila melanogaster. *J Biol Chem*, **275**, 23267-23272.

Lee, H., Habas, R. and Abate-Shen, C. (2004) MSX1 cooperates with histone H1b for inhibition of transcription and myogenesis. *Science*, **304**, 1675-1678.

Lehner, B., Crombie, C., Tischler, J., Fortunato, A. and Fraser, A.G. (2006) Systematic mapping of genetic interactions in Caenorhabditis elegans identifies common modifiers of diverse signaling pathways. *Nat Genet*, **38**, 896-903.

Leise, W.F., 3rd and Mueller, P.R. (2004) Inhibition of the cell cycle is required for convergent extension of the paraxial mesoderm during Xenopus neurulation. *Development*, **131**, 1703-1715.

Lerchner, W., Latinkic, B.V., Remacle, J.E., Huylebroeck, D. and Smith, J.C. (2000) Region-specific activation of the Xenopus brachyury promoter involves active repression in ectoderm and endoderm: a study using transgenic frog embryos. *Development*, **127**, 2729-2739.

Li, B., Carey, M. and Workman, J.L. (2007) The role of chromatin during transcription. *Cell*, **128**, 707-719.

Li, Q., Herrler, M., Landsberger, N., Kaludov, N., Ogryzko, V.V., Nakatani, Y. and Wolffe, A.P. (1998) Xenopus NF-Y pre-sets chromatin to potentiate p300 and acetylation-responsive transcription from the Xenopus hsp70 promoter in vivo. *Embo J*, **17**, 6300-6315.

Linder, B., Cabot, R.A., Schwickert, T. and Rupp, R.A. (2004) The SNF2 domain protein family in higher vertebrates displays dynamic expression patterns in Xenopus laevis embryos. *Gene*, **326**, 59-66.

Linder, B., Mentele, E., Mansperger, K., Straub, T., Kremmer, E. and Rupp, R.A. (2007) CHD4/Mi-2beta activity is required for the positioning of the mesoderm/neuroectoderm boundary in Xenopus. *Genes Dev*, **21**, 973-983.

Lo, W.S., Trievel, R.C., Rojas, J.R., Duggan, L., Hsu, J.Y., Allis, C.D., Marmorstein, R. and Berger, S.L. (2000) Phosphorylation of serine 10 in histone H3 is functionally linked in vitro and in vivo to Gcn5-mediated acetylation at lysine 14. *Mol Cell*, **5**, 917-926.

Luger, K., Mader, A.W., Richmond, R.K., Sargent, D.F. and Richmond, T.J. (1997) Crystal structure of the nucleosome core particle at 2.8 A resolution. *Nature*, **389**, 251-260.

Luk, E., Vu, N.D., Patteson, K., Mizuguchi, G., Wu, W.H., Ranjan, A., Backus, J., Sen, S., Lewis, M., Bai, Y. and Wu, C. (2007) Chz1, a nuclear chaperone for histone H2AZ. *Mol Cell*, **25**, 357-368.

Madigan, J.P., Chotkowski, H.L. and Glaser, R.L. (2002) DNA double-strand break-induced phosphorylation of Drosophila histone variant H2Av helps prevent radiation-induced apoptosis. *Nucleic Acids Res*, **30**, 3698-3705.

McClelland, M. and Ivarie, R. (1982) Asymmetrical distribution of CpG in an 'average' mammalian gene. *Nucleic Acids Res*, **10**, 7865-7877.

Meneghini, M.D., Wu, M. and Madhani, H.D. (2003) Conserved histone variant H2A.Z protects euchromatin from the ectopic spread of silent heterochromatin. *Cell*, **112**, 725-736.

Millar, C.B., Xu, F., Zhang, K. and Grunstein, M. (2006) Acetylation of H2AZ Lys 14 is associated with genome-wide gene activity in yeast. *Genes Dev*, **20**, 711-722.

Miller, J.R., Cartwright, E.M., Brownlee, G.G., Fedoroff, N.V. and Brown, D.D. (1978) The nucleotide sequence of oocyte 5S DNA in Xenopus laevis. II. The GC-rich region (abstract only). *Cell*, **13**, 717-725.

Miller, J.R., Rowning, B.A., Larabell, C.A., Yang-Snyder, J.A., Bates, R.L. and Moon, R.T. (1999) Establishment of the dorsal-ventral axis in Xenopus embryos coincides with the dorsal enrichment of dishevelled that is dependent on cortical rotation. *J Cell Biol*, **146**, 427-437.

Misteli, T. (2007) Beyond the sequence: cellular organization of genome function. *Cell*, **128**, 787-800.

Mizuguchi, G., Shen, X., Landry, J., Wu, W.H., Sen, S. and Wu, C. (2004) ATP-driven exchange of histone H2AZ variant catalyzed by SWR1 chromatin remodeling complex. *Science*, **303**, 343-348.

Mohrmann, L. and Verrijzer, C.P. (2005) Composition and functional specificity of SWI2/SNF2 class chromatin remodeling complexes. *Biochim Biophys Acta*, **1681**, 59-73.

Montcouquiol, M., Crenshaw, E.B., 3rd and Kelley, M.W. (2006) Noncanonical Wnt signaling and neural polarity. *Annu Rev Neurosci*, **29**, 363-386.

Moon, R.T., DeMarais, A.A. and Olson, D.J. (1993) Responses to Wnt signals in vertebrate embryos may involve changes to cell adhesion and cell movement. *J Cell Sci Suppl.*, **17**, 183-188.

Mueller, R.D., Yasuda, H., Hatch, C.L., Bonner, W.M. and Bradbury, E.M. (1985) Identification of ubiquitinated histones 2A and 2B in Physarum polycephalum. Disappearance of these proteins at metaphase and reappearance at anaphase. *J Biol Chem*, **260**, 5147-5153.

Murdoch, J.N., Doudney, K., Paternotte, C., Copp, A.J. and Stanier, P. (2001) Severe neural tube defects in the loop-tail mouse result from mutation of Lpp1, a novel gene involved in floor plate specification. *Hum Mol Genet*, **10**, 2593-2601.

Nagy, L., Kao, H.Y., Chakravarti, D., Lin, R.J., Hassig, C.A., Ayer, D.E., Schreiber, S.L. and Evans, R.M. (1997) Nuclear receptor repression mediated by a complex containing SMRT, mSin3A, and histone deacetylase. *Cell*, **89**, 373-380.

Nakano, H., Amemiya, S., Shiokawa, K. and Taira, M. (2000) RNA interference for the organizer-specific gene Xlim-1 in Xenopus embryos. *Biochem Biophys Res Commun*, **274**, 434-439.

Nathan, D., Ingvarsdottir, K., Sterner, D.E., Bylebyl, G.R., Dokmanovic, M., Dorsey, J.A., Whelan, K.A., Krsmanovic, M., Lane, W.S., Meluh, P.B., Johnson, E.S. and Berger, S.L. (2006) Histone sumoylation is a negative regulator in Saccharomyces cerevisiae and shows dynamic interplay with positive-acting histone modifications. *Genes Dev*, **20**, 966-976.

Naveh-Many, T. and Cedar, H. (1981) Active gene sequences are undermethylated. *Proc Natl Acad Sci U S A*, **78**, 4246-4250.

Nelson, C.J., Santos-Rosa, H. and Kouzarides, T. (2006) Proline isomerization of histone H3 regulates lysine methylation and gene expression. *Cell*, **126**, 905-916.

Newport, J. and Kirschner, M. (1982) A major developmental transition in early Xenopus embryos: I. characterization and timing of cellular changes at the midblastula stage. *Cell*, **30**, 675-686.

Ng, H.H., Robert, F., Young, R.A. and Struhl, K. (2003) Targeted recruitment of Set1 histone methylase by elongating Pol II provides a localized mark and memory of recent transcriptional activity. *Mol Cell*, **11**, 709-719.

Nickel, B.E., Roth, S.Y., Cook, R.G., Allis, C.D. and Davie, J.R. (1987) Changes in the histone H2A variant H2A.Z and polyubiquitinated histone species in developing trout testis (abstract only). *Biochemistry*, **26**, 4417-4421.

Niehrs, C., Steinbeisser, H. and De Robertis, E.M. (1994) Mesodermal patterning by a gradient of the vertebrate homeobox gene goosecoid. *Science*, **263**, 817-820.

Nieuwkoop, P.D. and Faber, J. (1994) *Normal Table of Xenopus laevis (Daudin)*. Garland Publishing, Inc., New York and London.

Nusse, R. and Varmus, H.E. (1982) Many tumors induced by the mouse mammary tumor virus contain a provirus integrated in the same region of the host genome (abstract only). *Cell*, **31**, 99-109.

Nusslein-Volhard, C. and Wieschaus, E. (1980) Mutations affecting segment number and polarity in Drosophila (abstract only). *Nature*, **287**, 795-801.

O'Reilly, M.A., Smith, J.C. and Cunliffe, V. (1995) Patterning of the mesoderm in Xenopus: dose-dependent and synergistic effects of Brachyury and Pintallavis. *Development*, **121**, 1351-1359.

Ohsumi, K. and Katagiri, C. (1991) Occurrence of H1 subtypes specific to pronuclei and cleavage-stage cell nuclei of anuran amphibians (abstract only). *Dev Biol*, **147**, 110-120.

Onichtchouk, D., Gawantka, V., Dosch, R., Delius, H., Hirschfeld, K., Blumenstock, C. and Niehrs, C. (1996) The Xvent-2 homeobox gene is part of the BMP-4 signalling pathway controlling [correction of controling] dorsoventral patterning of Xenopus mesoderm. *Development*, **122**, 3045-3053.

Owen-Hughes, T. and Engeholm, M. (2007) Pyrosequencing positions nucleosomes precisely. *Genome Biol*, **8**, 217.

Padmanabhan, R. (2006) Etiology, pathogenesis and prevention of neural tube defects. *Congenit Anom (Kyoto)*, **46**, 55-67.

Panitz, F., Krain, B., Hollemann, T., Nordheim, A. and Pieler, T. (1998) The Spemann organizer-expressed zinc finger gene Xegr-1 responds to the MAP kinase/Ets-SRF signal transduction pathway. *Embo J*, **17**, 4414-4425.

Papan, C. and Campos-Ortega, J.A. (1994) On the formation of the neural keel and neural tube in the zebrafish *Danio (Brachydanio) rerio*. *Dev Genes Evol*, **203**, 178-186.

Park, M. and Moon, R.T. (2002) The planar cell-polarity gene stbm regulates cell behaviour and cell fate in vertebrate embryos. *Nat Cell Biol*, **4**, 20-25.

Park, T.J., Gray, R.S., Sato, A., Habas, R. and Wallingford, J.B. (2005) Subcellular localization and signaling properties of dishevelled in developing vertebrate embryos. *Curr Biol*, **15**, 1039-1044.

Park, Y.J., Dyer, P.N., Tremethick, D.J. and Luger, K. (2004) A new fluorescence resonance energy transfer approach demonstrates that the histone variant H2AZ stabilizes the histone octamer within the nucleosome. *J Biol Chem*, **279**, 24274-24282.

Paull, T.T., Rogakou, E.P., Yamazaki, V., Kirchgessner, C.U., Gellert, M. and Bonner, W.M. (2000) A critical role for histone H2AX in recruitment of repair factors to nuclear foci after DNA damage. *Curr Biol*, **10**, 886-895.

Pepin, D., Vanderhyden, B.C., Picketts, D.J. and Murphy, B.D. (2007) ISWI chromatin remodeling in ovarian somatic and germ cells: revenge of the NURFs. *Trends Endocrinol Metab*, **18**, 215-224.

Peterson, C.L. and Laniel, M.A. (2004) Histones and histone modifications. *Curr Biol*, **14**, R546-551.

Pinto, D., Gregorieff, A., Begthel, H. and Clevers, H. (2003) Canonical Wnt signals are essential for homeostasis of the intestinal epithelium. *Genes Dev*, **17**, 1709-1713.

Polakis, P. (2000) Wnt signaling and cancer. *Genes Dev*, **14**, 1837-1851.

Prioleau, M.N., Huet, J., Sentenac, A. and Mechali, M. (1994) Competition between chromatin and transcription complex assembly regulates gene expression during early development. *Cell*, **77**, 439-449.

Raisner, R.M., Hartley, P.D., Meneghini, M.D., Bao, M.Z., Liu, C.L., Schreiber, S.L., Rando, O.J. and Madhani, H.D. (2005) Histone variant H2A.Z marks the 5' ends of both active and inactive genes in euchromatin. *Cell*, **123**, 233-248.

Rangasamy, D., Berven, L., Ridgway, P. and Tremethick, D.J. (2003) Pericentric heterochromatin becomes enriched with H2A.Z during early mammalian development. *Embo J*, **22**, 1599-1607.

Rangasamy, D., Greaves, I. and Tremethick, D.J. (2004) RNA interference demonstrates a novel role for H2A.Z in chromosome segregation. *Nat Struct Mol Biol*, **11**, 650-655.

Redon, C., Pilch, D., Rogakou, E., Sedelnikova, O., Newrock, K. and Bonner, W. (2002) Histone H2A variants H2AX and H2AZ. *Curr Opin Genet Dev*, **12**, 162-169.

Ridgway, P., Brown, K.D., Rangasamy, D., Svensson, U. and Tremethick, D.J. (2004a) Unique residues on the H2A.Z containing nucleosome surface are important for Xenopus laevis development. *J Biol Chem*, **279**, 43815-43820.

Ridgway, P., Rangasamy, D., Berven, L., Svensson, U. and Tremethick, D.J. (2004b) Analysis of histone variant H2A.Z localization and expression during early development. *Methods Enzymol*, **375**, 239-252.

Robinson, P.J. and Rhodes, D. (2006) Structure of the '30 nm' chromatin fibre: a key role for the linker histone. *Curr Opin Struct Biol*, **16**, 336-343.

Rocheleau, C.E., Downs, W.D., Lin, R., Wittmann, C., Bei, Y., Cha, Y.H., Ali, M., Priess, J.R. and Mello, C.C. (1997) Wnt signaling and an APC-related gene specify endoderm in early C. elegans embryos. *Cell*, **90**, 707-716.

Rogakou, E.P., Pilch, D.R., Orr, A.H., Ivanova, V.S. and Bonner, W.M. (1998) DNA double-stranded breaks induce histone H2AX phosphorylation on serine 139. *J Biol Chem*, **273**, 5858-5868.

Roizes, G. (1976) A possible structure for calf satellite DNA I. *Nucleic Acids Res*, **3**, 2677-2696.

Rosen, B. and Beddington, R.S. (1993) Whole-mount in situ hybridization in the mouse embryo: gene expression in three dimensions. *Trends Genet*, **9**, 162-167.

Rowning, B.A., Wells, J., Wu, M., Gerhart, J.C., Moon, R.T. and Larabell, C.A. (1997) Microtubule-mediated transport of organelles and localization of beta-catenin to the future dorsal side of Xenopus eggs. *Proc Natl Acad Sci U S A*, **94**, 1224-1229.

Rozen, S. and Skaletsky, H.J. (2000) Primer3 on the WWW for general users and for biologist programmers. In Krawetz, S. and Misener, S. (eds.), *Bioinformatics Methods and Protocols: Methods in Molecular Biology*. Humana Press, Totowa, pp. 365-386.

Rubinfeld, B., Albert, I., Porfiri, E., Fiol, C., Munemitsu, S. and Polakis, P. (1996) Binding of GSK3beta to the APC-beta-catenin complex and regulation of complex assembly. *Science*, **272**, 1023-1026.

Ruhl, D.D., Jin, J., Cai, Y., Swanson, S., Florens, L., Washburn, M.P., Conaway, R.C., Conaway, J.W. and Chrivia, J.C. (2006) Purification of a human SRCAP complex that remodels chromatin by incorporating the histone variant H2A.Z into nucleosomes. *Biochemistry*, **45**, 5671-5677.

Ruiz-Carrillo, A., Jorcano, J.L., Eder, G. and Lurz, R. (1979) In vitro core particle and nucleosome assembly at physiological ionic strength. *Proc Natl Acad Sci U S A*, **76**, 3284-3288.

Rupp, R.A. and Weintraub, H. (1991) Ubiquitous MyoD transcription at the midblastula transition precedes induction-dependent MyoD expression in presumptive mesoderm of X. laevis. *Cell*, **65**, 927-937.

Saha, A., Wittmeyer, J. and Cairns, B.R. (2006) Chromatin remodelling: the industrial revolution of DNA around histones. *Nat Rev Mol Cell Biol*, **7**, 437-447.

Saka, Y., Tada, M. and Smith, J.C. (2000) A screen for targets of the Xenopus T-box gene Xbra. *Mech Dev*, **93**, 27-39.

Sambrook, J., Fritch, E.F. and Maniatis, T. (1989) *Molecular Cloning: Laboratory Manual*. Cold Spring Harbour Laboratory Press.

Sander, V., Mullegger, J. and Lepperdinger, G. (2001) Xenopus brevican is expressed in the notochord and the brain during early embryogenesis. *Mech Dev*, **102**, 251-253.

Sanner, M., Olsen, A. and Spehner, J.-C. (1996) Reduced Surface: An efficient way to compute molecular surfaces (abstract only). *Biopolymers*, **38**, 305-320.

Santisteban, M.S., Kalashnikova, T. and Smith, M.M. (2000) Histone H2A.Z regulates transcription and is partially redundant with nucleosome remodeling complexes. *Cell*, **103**, 411-422.

Sato, N., Meijer, L., Skaltsounis, L., Greengard, P. and Brivanlou, A.H. (2004) Maintenance of pluripotency in human and mouse embryonic stem cells through activation of Wnt signaling by a pharmacological GSK-3-specific inhibitor. *Nat Med*, **10**, 55-63.

Schalch, T., Duda, S., Sargent, D.F. and Richmond, T.J. (2005) X-ray structure of a tetranucleosome and its implications for the chromatin fibre. *Nature*, **436**, 138-141.

Schotta, G., Lachner, M., Sarma, K., Ebert, A., Sengupta, R., Reuter, G., Reinberg, D. and Jenuwein, T. (2004) A silencing pathway to induce H3-K9 and H4-K20 trimethylation at constitutive heterochromatin. *Genes Dev*, **18**, 1251-1262.

Seller, M.J. (1987) Neural tube defects and sex ratios. *Am J Med Genet*, **26**, 699-707.

Sexton, T., Schober, H., Fraser, P. and Gasser, S.M. (2007) Gene regulation through nuclear organization. *Nat Struct Mol Biol*, **14**, 1049-1055.

Shackleton, M., Vaillant, F., Simpson, K.J., Stingl, J., Smyth, G.K., Asselin-Labat, M.L., Wu, L., Lindeman, G.J. and Visvader, J.E. (2006) Generation of a functional mammary gland from a single stem cell. *Nature*, **439**, 84-88.

Shogren-Knaak, M., Ishii, H., Sun, J.M., Pazin, M.J., Davie, J.R. and Peterson, C.L. (2006) Histone H4-K16 acetylation controls chromatin structure and protein interactions. *Science*, **311**, 844-847.

Shukla, A. and Bhaumik, S.R. (2007) H2B-K123 ubiquitination stimulates RNAPII elongation independent of H3-K4 methylation. *Biochem Biophys Res Commun*, **359**, 214-220.

Sive, H.L., Grainger, R.M. and Harland, R.M. (2000) *Early Development of Xenopus laevis: A Laboratory Manual*. Cold Spring Harbour Laboratory Press, New York.

Smith, J.C. (2001) Making mesoderm--upstream and downstream of Xbra. *Int J Dev Biol*, **45**, 219-224.

Smith, J.C., Price, B.M., Green, J.B., Weigel, D. and Herrmann, B.G. (1991) Expression of a Xenopus homolog of Brachyury (T) is an immediate-early response to mesoderm induction. *Cell*, **67**, 79-87.

Sobel, R.E., Cook, R.G., Perry, C.A., Annunziato, A.T. and Allis, C.D. (1995) Conservation of deposition-related acetylation sites in newly synthesized histones H3 and H4. *Proc Natl Acad Sci U S A*, **92**, 1237-1241.

Sokol, S.Y. (1996) Analysis of Dishevelled signalling pathways during Xenopus development. *Curr Biol*, **6**, 1456-1467.

Sokol, S.Y., Klingensmith, J., Perrimon, N. and Itoh, K. (1995) Dorsalizing and neuralizing properties of Xdsh, a maternally expressed Xenopus homolog of dishevelled. *Development*, **121**, 3487.

Sparmann, A. and van Lohuizen, M. (2006) Polycomb silencers control cell fate, development and cancer. *Nat Rev Cancer*, **6**, 846-856.

Stancheva, I., El-Maarri, O., Walter, J., Niveleau, A. and Meehan, R.R. (2002) DNA methylation at promoter regions regulates the timing of gene activation in Xenopus laevis embryos. *Dev Biol*, **243**, 155-165.

Stargell, L.A., Bowen, J., Dadd, C.A., Dedon, P.C., Davis, M., Cook, R.C. and al., e. (1993) Temporal and spatial association of histone H2A varient hv1 with transcriptionally competent chromatin during nuclear development in *Tetrahymena thermophila*. *Genes Dev*, **7**, 2641-2651.

Steinbach, O.C., Ulshofer, A., Authaler, A. and Rupp, R.A. (1998) Temporal restriction of MyoD induction and autocatalysis during Xenopus mesoderm formation. *Dev Biol*, **202**, 280-292.

Steinbach, O.C., Wolffe, A.P. and Rupp, R.A. (1997) Somatic linker histones cause loss of mesodermal competence in Xenopus. *Nature*, **389**, 395-399.

Steinbach, O.C., Wolffe, A.P. and Rupp, R.A.W. (2000) Histone deacetylase activity is required for the induction of the MyoD muscle cell lineage in *Xenopus*. *Biological Chemistry*, **381**, 1013-1016.

Stewart, M.D., Sommerville, J. and Wong, J. (2006) Dynamic regulation of histone modifications in Xenopus oocytes through histone exchange. *Mol Cell Biol*, **26**, 6890-6901.

Student. (1908) Probable error of a mean. *Biometrika*, **6**, 1-25.

Sullivan, B. and Karpen, G. (2001) Centromere identity in Drosophila is not determined in vivo by replication timing. *J Cell Biol*, **154**, 683-690.

Sullivan, K.F. (2001) A solid foundation: functional specialization of centromeric chromatin. *Curr Opin Genet Dev*, **11**, 182-188.

Suto, R.K., Clarkson, M.J., Tremethick, D.J. and Luger, K. (2000) Crystal structure of a nucleosome core particle containing the variant histone H2A.Z. *Nat Struct Biol*, **7**, 1121-1124.

Swaminathan, J., Baxter, E.M. and Corces, V.G. (2005) The role of histone H2Av variant replacement and histone H4 acetylation in the establishment of Drosophila heterochromatin. *Genes Dev*, **19**, 65-76.

Tada, M., Casey, E.S., Fairclough, L. and Smith, J.C. (1998) Bix1, a direct target of Xenopus T-box genes, causes formation of ventral mesoderm and endoderm. *Development*, **125**, 3997-4006.

Tada, M., O'Reilly, M.A. and Smith, J.C. (1997) Analysis of competence and of Brachyury autoinduction by use of hormone-inducible Xbra. *Development*, **124**, 2225-2234.

Tada, M. and Smith, J.C. (2000) Xwnt11 is a target of Xenopus Brachyury: regulation of gastrulation movements via Dishevelled, but not through the canonical Wnt pathway. *Development*, **127**, 2227-2238.

Tao, Q., Yokota, C., Puck, H., Kofron, M., Birsoy, B., Yan, D., Asashima, M., Wylie, C.C., Lin, X. and Heasman, J. (2005) Maternal wnt11 activates the canonical wnt signaling pathway required for axis formation in Xenopus embryos. *Cell*, **120**, 857-871.

Taverner, N.V., Kofron, M., Shin, Y., Kabitschke, C., Gilchrist, M.J., Wylie, C., Cho, K.W., Heasman, J. and Smith, J.C. (2005) Microarray-based identification of VegT targets in Xenopus. *Mech Dev*, **122**, 333-354.

Tazaki, A., Kitayama, A., Terasaka, C., Watanabe, K., Ueno, N. and Mochii, M. (2005) Macroarray-based analysis of tail regeneration in Xenopus laevis larvae. *Dev Dyn*, **233**, 1394-1404.

Thatcher, T.H. and Gorovsky, M.A. (1994) Phylogenetic analysis of the core histones H2A,H2B, H3, and H4. *Nucleic Acids Res.*, **22**, 174-179.

Thomas, M.C. and Chiang, C.M. (2006) The general transcription machinery and general cofactors (abstract only). *Crit Rev Biochem Mol Biol*, **41**, 105-178.

Tintignac, L.A., Sirri, V., Leibovitch, M.P., Lecluse, Y., Castedo, M., Metivier, D., Kroemer, G. and Leibovitch, S.A. (2004) Mutant MyoD lacking Cdc2 phosphorylation sites delays M-phase entry. *Mol Cell Biol*, **24**, 1809-1821.

Topczewski, J., Sepich, D.S., Myers, D.C., Walker, C., Amores, A., Lele, Z., Hammerschmidt, M., Postlethwait, J. and Solnica-Krezel, L. (2001) The zebrafish glypican knypek controls cell polarity during gastrulation movements of convergent extension. *Dev Cell*, **1**, 251-264.

Torban, E., Kor, C. and Gros, P. (2004) Van Gogh-like2 (Strabismus) and its role in planar cell polarity and convergent extension in vertebrates. *Trends Genet*, **20**, 570-577.

Torres, M.A., Yang-Snyder, J.A., Purcell, S.M., DeMarais, A.A., McGrew, L.L. and Moon, R.T. (1996) Activities of the Wnt-1 class of secreted signaling factors are antagonized by the Wnt-5A class and by a dominant negative cadherin in early Xenopus development. *J Cell Biol*, **133**, 1123-1137.

Tremethick, D.J. (2007) Higher-order structures of chromatin: the elusive 30 nm fiber. *Cell*, **128**, 651-654.

Turner, P.C., Bagenal, E.B., Vlad, M.T. and Woodland, H.R. (1988) The organisation and expression of histone genes from Xenopus borealis. *Nucleic Acids Res*, **16**, 3471-3485.

Ueno, N. and Greene, N.D. (2003) Planar cell polarity genes and neural tube closure. *Birth Defects Res C Embryo Today*, **69**, 318-324.

Updike, D.L. and Mango, S.E. (2006) Temporal regulation of foregut development by HTZ-1/H2A.Z and PHA-4/FoxA. *PLoS Genet*, **2**, e161.

Vakoc, C.R., Mandat, S.A., Olenchock, B.A. and Blobel, G.A. (2005) Histone H3 lysine 9 methylation and HP1gamma are associated with transcription elongation through mammalian chromatin. *Mol Cell*, **19**, 381-391.

van Daal, A. and Elgin, S.C.R. (1992) A histone variant, H2AvD, is essential in *Drosophila melanogaster*. *Mol. Biol. Cell*, **3**, 593-602.

van de Wetering, M., Sancho, E., Verweij, C., de Lau, W., Oving, I., Hurlstone, A., van der Horn, K., Batlle, E., Coudreuse, D., Haramis, A.P., Tjon-Pon-Fong, M., Moerer, P., van den Born, M., Soete, G., Pals, S., Eilers, M., Medema, R. and Clevers, H. (2002) The beta-catenin/TCF-4 complex imposes a crypt progenitor phenotype on colorectal cancer cells. *Cell*, **111**, 241-250.

van Es, J.H., Barker, N. and Clevers, H. (2003) You Wnt some, you lose some: oncogenes in the Wnt signaling pathway. *Curr Opin Genet Dev*, **13**, 28-33.

Varga-Weisz, P.D., Blank, T.A. and Becker, P.B. (1995) Energy-dependent chromatin accessibility and nucleosome mobility in a cell-free system. *Embo J*, **14**, 2209-2216.

Veenstra, G.J., Weeks, D.L. and Wolffe, A.P. (2000) Distinct roles for TBP and TBP-like factor in early embryonic gene transcription in Xenopus. *Science*, **290**, 2312-2315.

Vermaak, D. and Wolffe, A.P. (1998) Chromatin and chromosomal controls in development. *Dev Genet*, **22**, 1-6.

Vincent, J.P., Oster, G.F. and Gerhart, J.C. (1986) Kinematics of gray crescent formation in Xenopus eggs: the displacement of subcortical cytoplasm relative to the egg surface (abstract only). *Dev Biol*, **113**, 484-500.

Vize, P. (2003) Xenbase: a *Xenopus* web resource. Vol. 2004.

Wallingford, J.B., Fraser, S.E. and Harland, R.M. (2002) Convergent extension: the molecular control of polarized cell movement during embryonic development. *Dev Cell*, **2**, 695-706.

Wallingford, J.B. and Harland, R.M. (2001) Xenopus Dishevelled signaling regulates both neural and mesodermal convergent extension: parallel forces elongating the body axis. *Development*, **128**, 2581-2592.

Wallingford, J.B., Rowning, B.A., Vogeli, K.M., Rothbacher, U., Fraser, S.E. and Harland, R.M. (2000) Dishevelled controls cell polarity during Xenopus gastrulation. *Nature*, **405**, 81-85.

Wallingford, J.B., Vogeli, K.M. and Harland, R.M. (2001) Regulation of convergent extension in Xenopus by Wnt5a and Frizzled-8 is independent of the canonical Wnt pathway. *Int J Dev Biol*, **45**, 225-227.

Walsh, C.P., Chaillet, J.R. and Bestor, T.H. (1998) Transcription of IAP endogenous retroviruses is constrained by cytosine methylation. *Nat Genet*, **20**, 116-117.

Wang, J., Hamblet, N.S., Mark, S., Dickinson, M.E., Brinkman, B.C., Segil, N., Fraser, S.E., Chen, P., Wallingford, J.B. and Wynshaw-Boris, A. (2006) Dishevelled genes mediate a conserved mammalian PCP pathway to regulate convergent extension during neurulation. *Development*, **133**, 1767-1778.

Wang, Y., Wysocka, J., Sayegh, J., Lee, Y.H., Perlin, J.R., Leonelli, L., Sonbuchner, L.S., McDonald, C.H., Cook, R.G., Dou, Y., Roeder, R.G., Clarke, S., Stallcup, M.R., Allis, C.D. and Coonrod, S.A. (2004) Human PAD4 regulates histone arginine methylation levels via demethylimination. *Science*, **306**, 279-283.

Weaver, C., Farr, G.H., 3rd, Pan, W., Rowning, B.A., Wang, J., Mao, J., Wu, D., Li, L., Larabell, C.A. and Kimelman, D. (2003) GBP binds kinesin light chain and translocates during cortical rotation in Xenopus eggs. *Development*, **130**, 5425-5436.

Weaver, C. and Kimelman, D. (2004) Move it or lose it: axis specification in Xenopus. *Development*, **131**, 3491-3499.

White, E.M., Shapiro, D.L., Allis, C.D. and Gorovsky, M.A. (1988) Sequence and properties of the message encoding Tetrahymena hv1, a highly evolutionarily conserved histone H2A variant that is associated with active genes. *Nucleic Acids Res*, **16**, 179-198.

White, J.A. and Heasman, J. (2007) Maternal control of pattern formation in Xenopus laevis. *J Exp Zoolog B Mol Dev Evol*.

Whitehouse, I., Flaus, A., Cairns, B.R., White, M.F., Workman, J.L. and Owen-Hughes, T. (1999) Nucleosome mobilization catalysed by the yeast SWI/SNF complex. *Nature*, **400**, 784-787.

Winklbauer, R. (1990) Mesodermal cell migration during Xenopus gastrulation. *Dev Biol*, **142**, 155-168.

Winklbauer, R., Medina, A., Swain, R.K. and Steinbeisser, H. (2001) Frizzled-7 signalling controls tissue separation during Xenopus gastrulation. *Nature*, **413**, 856-860.

Wolffe, A.P. and Hayes, J.J. (1999) Chromatin disruption and modification. *Nucleic Acids Res.*, **27**, 711- 720.

Woodcock, C.L. and Dimitrov, S. (2001) Higher-order structure of chromatin and chromosomes. *Curr Opin Genet Dev*, **11**, 130-135.

Wright, M., Aikawa, M., Szeto, W. and Papkoff, J. (1999) Identification of a Wnt-responsive signal transduction pathway in primary endothelial cells. *Biochem Biophys Res Commun*, **263**, 384-388.

Wu, W.H., Alami, S., Luk, E., Wu, C.H., Sen, S., Mizuguchi, G., Wei, D. and Wu, C. (2005) Swc2 is a widely conserved H2AZ-binding module essential for ATP-dependent histone exchange. *Nat Struct Mol Biol*, **12**, 1064-1071.

Wyatt, G.R. (1951) Recognition and estimation of 5-methylcytosine in nucleic acids. *Biochem J*, **48**, 581-584.

Wylie, C., Kofron, M., Payne, C., Anderson, R., Hosobuchi, M., Joseph, E. and Heasman, J. (1996) Maternal beta-catenin establishes a 'dorsal signal' in early Xenopus embryos. *Development*, **122**, 2987-2996.

Xu, F., Zhang, K. and Grunstein, M. (2005) Acetylation in histone H3 globular domain regulates gene expression in yeast. *Cell*, **121**, 375-385.

Xu, R.H., Peng, Y., Fan, J., Yan, D., Yamagoe, S., Princler, G., Sredni, D., Ozato, K. and Kung, H.F. (2000) Histone acetylation is a checkpoint in FGF-stimulated mesoderm induction. *Dev Dyn*, **218**, 628-635.

Yamanaka, H., Moriguchi, T., Masuyama, N., Kusakabe, M., Hanafusa, H., Takada, R., Takada, S. and Nishida, E. (2002) JNK functions in the non-canonical Wnt pathway to regulate convergent extension movements in vertebrates. *EMBO Rep*, **3**, 69-75.

Yokotal, C., Mukasa, T., Higashi, M., Odaka, A., Muroya, K., Uchiyama, H., Eto, Y., Asashima, M. and Momoi, T. (1995) Activin induces the expression of the Xenopus homologue of sonic hedgehog during mesoderm formation in Xenopus explants. *Biochem Biophys Res Commun*, **207**, 1-7.

Zernicka-Goetz, M., Pines, J., Ryan, K., Siemering, K.R., Haseloff, J., Evans, M.J. and Gurdon, J.B. (1996) An indelible lineage marker for Xenopus using a mutated green fluorescent protein. *Development*, **122**, 3719-3724.

Zhang, L., Eugeni, E.E., Parthun, M.R. and Freitas, M.A. (2003) Identification of novel histone post-translational modifications by peptide mass fingerprinting. *Chromosoma*, **112**, 77-86.